Department of Mechanical Engineering
The Hong Kong Polytechnic University

Suppression of Structural Vibration with a New Type of Vibration Absorber

by

Tang Shun Leung

A thesis submitted in partial fulfillment of the
requirements for the Degree of Master of Philosophy

September 2003

Acknowledgements

I would like to express my heartfelt thanks and appreciation to my chief supervisor, Dr. W. O. Wong, for his patient guidance and encouragement at various crucial stages of this project. I would like to express my appreciation to him for his valuable suggestions. Without his supervision, this thesis could not be completed.

I am grateful to my co-supervisor, Prof L. Cheng, for giving me inspiration and sharing his knowledge of his insight into research.

I am indebted to the fellows of research group for their encouragement, technical supports and friendship. Finally, I would like to thanks for The Hong Kong Polytechnic University for the financial support.

Declaration

I declare that this thesis contains no material which has previously been presented for the award of any other degree or diploma in any university or institute, and to the best of my knowledge the material is original except where due reference is made in the text of the thesis.

Shun Leung TANG

Abstract of thesis entitled 'SUPPRESSION OF STRUCTURAL VIBRATION WITH A NEW TYPE OF VIBRATION ABSORBER'
submitted by TANG Shun Leung
for the degree of Master of Philosophy
at the Hong Kong Polytechnic University in September 2003

Abstract

A new type of dynamic vibration absorber (DVA) has been designed to be the combination of different types of vibration absorbers attaching at a single point, which, was proposed and evaluated for vibration suppression. The effects of a number of absorber parameters and locations of attachment have been compared. Holographic full-field vibration visualization techniques have been tried for finding a suitable location of absorber on the controlled structure.

Basic theories of the new dynamic absorber in suppression of vibration have been established. The suppression of harmonic vibrations of a single-degree-of-freedom (SDOF), multi-degree-of-freedom (MDOF) discrete system and continuous systems such as beams and plates by the proposed dynamic vibration absorbers have been evaluated by both computer simulations and experimental tests. The results obtained in both parts are presented and discussed.

For suppression of rigid body vibration, the performance of the commonly used translational absorber was compared to those of a rotational absorber and the proposed absorber. From the numerical analysis, it was found that the translational one has the poorest performance in terms of the range of the absorption frequency; rotational absorber is better while the proposed absorber can completely absorb all the rigid body vibrations.

For flexural vibration of continuous structures such as beams and plates, the performance of the commonly used translational absorber was compared to those of the rotational absorber and the proposed absorber by finite element analysis and experimental tests. It was found that the proposed type of absorber provides excellent performance and simpler implementation than those of the standard sprung mass absorbers as reported in textbooks and other published literature. Even though there are many techniques for the optimization of tuning and location of vibration absorbers as reported in the literature, most of them require highly computational intensive analysis before the user can determine the tuning values and the best location of the absorber. The proposed absorber is a combination of translational and rotational absorbers to be attached onto the vibrating structure at a single point. With the knowledge of the modal parameters of the structures, it is straightforward to determine an effective attachment point for suppression of vibration. The numerical predictions are verified by experimental tests.

Nomenclature

A	Cross-section area of a structure
a_r	Scaling constant of the r^{th} natural modes
D	Coefficient matrix of the equation of motion
F_0	Amplitude of the excitation force
I	Moment of inertia of the structure
I_r	Moment of inertia of the rotational vibration absorber
I_t	Moment of inertia of the translational vibration absorber
k	Stiffness of the primary SDOF structure
k_1	Stiffness of the 1^{st} spring of the structure
k_2	Stiffness of the 2^{nd} spring of the structure
k_a	Stiffness of the dynamic vibration absorber
k_{ij}	The i^{th} column and j^{th} row element of the stiffness matrix
$\tilde{k}$	Dimensionless stiffness ratio
$\tilde{k}_t$	Dimensionless stiffness ratio of the translational absorber
$\tilde{k}_r$	Dimensionless stiffness ratio of the rotational absorber
L	Total Length of the structure
l_1	Distance of the Cg of the structure from one end
l_2	Distance of the Cg of the structure from the other end
$\tilde{l}$	Dimensionless length ratio between l_1 and l_2
m	Primary mass of a single degree of freedom structure
m_a	Mass of the dynamic vibration absorber
m_{ij}	The i^{th} column and j^{th} row element of the mass matrix
m_r	Mass of the rotational absorber
m_t	Mass of the translational absorber
$\tilde{m}_t$	Dimensionless mass ratio of the translational absorber
$\tilde{m}_r$	Dimensionless mass ratio of the rotational absorber
q_1	Generalized translational force at the left end of an element
q_2	Generalized rotational force at the left end of an element
q_3	Generalized translational force at the right end of an element
q_4	Generalized rotational force at the right end of an element
t	Dimensional time
V	Potential energy of the structure
w_1	Transverse displacement of the left end of an element
w_2	Transverse displacement of the right end of an element
w_3	Displacement slope at the left end of an element
w_4	Displacement slope at the right end of an element
x	Displacement of the primary SDOF structure
X	Translational amplitude of the structure
x_1	Displacement of the primary structure

x_2	Displacement of the dynamic vibration absorber
x_a	Displacement of the dynamic vibration absorber
$\ddot{x}$	Acceleration of the primary SDOF structure
$\ddot{x}_a$	Acceleration of the dynamic vibration absorber
$\ddot{x}_1$	Acceleration of the primary the structure
$\ddot{x}_2$	Acceleration of the dynamic vibration absorber
y_a	Distance between the Cg and the excitation force
$\tilde{y}$	Dimensionless length ratio between the Cg and the excitation force
z	Inertia ratio
$\tilde{z}$	Dimensionless inertia ratio

Greek Symbols

Θ	Rotational amplitude of the of the structure
θ	Rotational amplitude of the structure
$\ddot{\theta}$	Rotational velocity of the structure
ϕ	Rotational amplitude of the rotational absorber
$\ddot{\phi}$	Rotational acceleration of the rotational absorber
ϕ_{jr}	The j^{th} element of the mode shape vector at the r^{th} mode
ω_1	Natural frequency of the 1^{st} mode
ω_2	Natural frequency of the 2^{nd} mode
ω_{dr}	Driving frequency of the force
ω_{r1}	Natural frequency of the 1^{st} mode of the rotational absorber
ω_{r2}	Natural frequency of the 2^{nd} mode of the rotational absorber
ω_{r3}	Natural frequency of the 3^{rd} mode of the rotational absorber
ω_{t1}	Natural frequency of the 1^{st} mode of the translational absorber
ω_{t2}	Natural frequency of the 2^{nd} mode of absorber
ω_{t3}	Natural frequency of the 3^{rd} mode of the translational absorber
$\tilde{\omega}$	Dimensionless frequency ratio of vibration
$\tilde{\omega}_1$	Dimensionless natural frequency ratio of the 1^{st} mode
$\tilde{\omega}_2$	Dimensionless natural frequency ratio of the 2^{nd} mode
ψ_{ir}	The i^{th} element of the mode shape vector at the r^{th} mode
ξ	Displacement of the element
ρ	Density of a material

Contents

Page

List of figures

1. Introduction

Machine or product casings are usually in the form of thin plates or shells which may act like loudspeakers when they are vibrating due to internal excitation. The vibration and sound radiation of machine casings excited at one or a few discrete frequencies may be suppressed in an economic way by attaching one or more vibration absorbers on to the casings.

A dynamic vibration absorber is an auxiliary mass-spring system, which, when correctly tuned and attached to a vibrating plate or shell subject to a harmonic excitation, causes the steady-state motion of the point to which it is attached to cease. Such devices have been invented for more than one hundred years but they are still not commonly used. One reason is the lack of a systematic way to find a good attachment point for the absorber such that the vibration amplitude and the sound radiation of the whole structure can be reduced. Optimization of the tuning parameters and location of the attachment is highly computationally intensive. An improper selection of attachment point for the absorber may lead to an amplification of vibration and sound radiation in other parts of the structure. This motivates the present research study of finding a more systematic way of using dynamic absorbers for vibration suppression. The performances of several types of dynamic absorbers of simple design were compared and a new type of dynamic absorber was analyzed and proposed for vibration suppression. The new dynamic absorber is able to absorb both the rotational and translational motions of the structure at the attachment point.

It provides superior vibration suppression performance to the standard sprung mass absorber in beam and plate vibration if it is properly located on to the vibrating structure.

The performance of different types of vibration absorber including the translational type, which is commonly used, the rotational type and the proposed type are compared by numerical analysis and experimental tests.

There are several articles in the literature [1][2] reporting the use of simple vibration absorbers for vibration suppression and they show the importance of the attachment point of the absorber on to the primary structure. Some researchers [3][4] studied the free and deterministically forced vibration of systems that were composed of combinations of simpler assemblies such as beams, plates, spring-mass systems, etc.. However, very few of them reported the effect of changing the positions of the absorber on the vibrating system. In this study, the importance of the position of the attached absorber was studied and a guideline is proposed for choosing a suitable location of the vibrating structure for attaching the dynamic vibration absorber. Also, researchers proposed the use of a number of absorbers of different tuning values and attachment points for good absorption results. In contrast, the proposed absorber is a simple combination of translational and rotational absorbers to be attached on to the vibrating structure at a single point. It was hoped that an economical and practical way of using absorbers in vibroacoustic control could be devised for the engineers working in the field.

In order to determine a suitable location for attaching a dynamic absorber on to the vibrating structure, modal analysis of the structure is required. A whole field optical measurement technique called ESPI [5][6] was used for the measurement of modal frequencies and modeshapes as it is more convenient than the traditional point-wise technique.

In this project, the suppression of rigid body motion, flexural vibration of beams and plates by the standard translational-type, the rotational-type and the proposed combined type of dynamic vibration absorbers were analyzed and compared via theoretical models, computer simulations and experiments.

1.1. Objectives

In this project, an easy, economical, and practical solution in vibration suppression is proposed by means of using dynamic vibration absorbers.

To make the vibration suppression economical, a new type of vibration absorber for structural vibration suppression was developed. We combined different kinds of dynamic vibration absorbers to be a single vibration absorber, which gives superior performance in vibration suppression.

To control vibration easily, guideline for determining a good location for attaching different kinds of vibration absorber was investigated. Different kinds of absorber need different methods in determining the location of installation. For example, in this project, it was found to be effective to attach the rotational vibration absorber at the nodal location of a structure, a visualization technique called Electronic Speckle Pattern Interferometry (ESPI) was used for finding a good location for installing the absorber.

To ensure the newly developed vibration absorber and the technique suggested to be practical, they are all tested by simulations and experiments for validation.

1.2. Review of dynamic vibration absorber designed for vibration suppression

A dynamic vibration absorber (DVA) is an auxiliary mass, which is frequently attached to vibrating systems by springs and damping devices to assist in controlling the vibration and sound radiation of structures. The theory of the standard translational-type dynamic vibration absorbers was firstly reported by Den Hartog in 1909 [7].

Harris and Crede [8] provided a description of a number of different DVA arrangements, including pendulum and linear sprung mass arrangements. A description is also given a device in tube form, in which a fluid rolls from one tank to another, often used for antiroll in ships. Absorber systems can include rotational or linear motion, or both.

Traditional passive dynamic absorbers can be effective only at a single resonant frequency, and may not be effective at other resonant frequencies or for modes where a node is present at the location of the absorber. An active dynamic absorber with a force generator acting as the absorber mass was reported by Rockwell [9] for the control of beam vibrations. A sensor mounted on the other side of the beam detected the motion of the beam and sent a feedback signal to the generator, which, in turn, reacts against the motion of the vibration.

Besides those DVAs with self-tuning capabilities [10], another strategy is to search for a set of optimal parameters so as to guarantee that the vibration level is minimized over

a frequency band, taking into account their design constraints. Design Curves are presented by Den Hartog [7] for the case of undamped single-degree-of-freedom primary systems subjected to harmonic and white noise random excitation. Warburton [11] presents expressions for optimum absorber parameters derived for undamped single-degree-of-freedom primary systems, considering harmonic and white noise random excitations. Warburton also reported the effect of damping in the primary system on optimum absorber parameters in another article [12]. Frequency domain-based performance indices are also used for investigating single-degree-of-freedom primary systems in different applications. Wang and Cheng compare four optimization methods [13], as applied to single-degree-of-freedom system with primary damping.

In reference [14], Nishimura *et al.* address the optimization of a DVA for multi-degree-of-freedom systems subjected to random input with a dominant frequency, using an optimization method based on optimal control theory. Kitis *et al.* [15] proposed an efficient optimal design algorithm for minimizing the response of a multi-degree-of-freedom system under sinusoidal loading. More recently, a modal theory for viscoelastic dynamic neutralizers was developed [16,17] and different optimization techniques for the optimal design of neutralizers over a finite frequency band. However, most of the studies of optimization of the tuning parameters and location of the attachment of vibration absorbers in the literature are very computationally intensive and they are only sound for structures of some particular configurations.

1.3. Review of structural-borne noise attenuation using dynamic vibration absorbers

A dynamic vibration absorber may be used for suppression of structural vibration and sound radiation from the structure. Fuller *et al.* [18,19] presented a technique for tuning absorbers applied to a cylindrical shell to minimize radiated sound. To suppress the vibration amplitudes involving high modes, Nagaya and Li [20] presented a method using neural network procedures in solving non-linear equations for predicting tuning parameters of the absorber for higher mode noise absorption.

Many techniques have been developed to reduce the vibration of the cylindrical shell and the resulting interior noise [21, 22]. Passive control has been the traditional technique used to achieve these goals. In a passive control system, the vibration and the coupled sound are reduced by adding appropriate passive elements or by modifying the structure. Fuller has studied the reduction of the interior sound field by changing the parameters of the cylindrical shell [23] or by adding detuned, passive dynamic absorber [19]. For aircraft cabin noise [24, 25], DVA provided a high reduction of noise because the aircraft cabin noise due to propellers had a discrete spectrum with low frequency. Since absorbers can be made small and light and can be installed conveniently, DVAs find widely applications in attenuating this kind of noise [26]. However, there is no general systematic way of determining the attachment point of absorbers reported. In this project, the position of the attachment of the DVA was studied and the proposed DVA was investigated such that vibration amplitude of the whole surface was suppressed and the sound radiation from the controlled structure could be attenuated.

1.4. Review of electronic speckle pattern interferometry for modal analysis

As presented in the later chapters, it was found that an effective attachment point for vibration absorbers could be determined based on a modal analysis of the controlled structure. This process can be simplified by using a full-field optical technique called Electronic Speckle Pattern Interferometry (ESPI) [6, 27]. Because of its simple setup and measurement procedures, it is a convienent tool for the identification of the modal frequencies and vibration shapes of the controlled structures.

Holographic interferometry is a traditional method used to find small deflections and to perform vibration analysis [28]. Techniques used for holographic vibration analysis can be classified as real time interferometry and time-averagedd interferometry. These kinds of holographic techniques provide large amount of practical and theoretical information on vibration analysis. However, the time consuming process of film registration and development limits the effective application of holographic vibration analysis. ESPI, a process using a video system for direct recording and display of interferograms exists for speeding up holographic vibration analysis [29]. Since ESPI uses a video recording and display system, it provides a real time dynamic displacement measurement platform in vibration analysis.

For vibration analysis by the ESPI technique, a reconstructed image is obtained by diffraction and intensity detection (a schematic set-up for time-averagedd ESPI is shown in

Figure 1.3.1). This reconstruction process includes high-pass filtering and full-wave rectification of the obtained video signal.

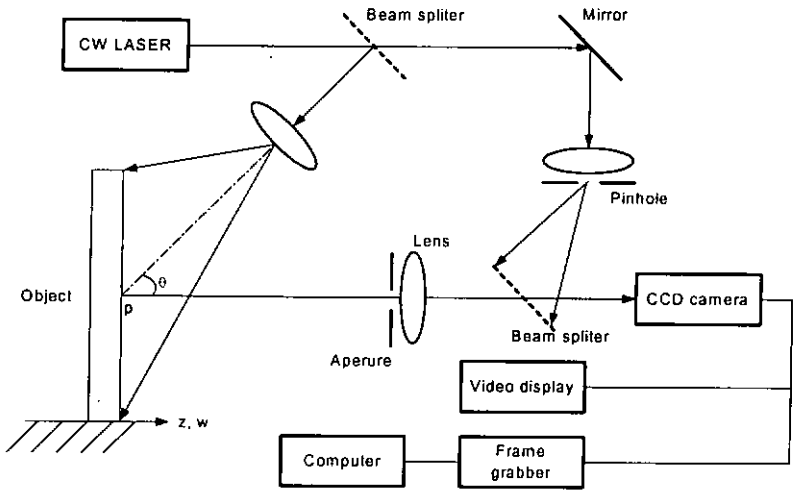

Figure 1.3.1. Schematic set-up of time-averaged ESPI

If the object's movement is greater than the wavelength of the light, dark and bright fringes will be formed due to the interference fringes smearing together during the TV exposure resulting in lower recorded fringe modulation and proportionally lower intensity after demodulation [27]. A time-averaged fringe pattern can be formed when the standing vibration of the object is suitably excited. So, we can obtain pictures for the vibration mode-shapes of the structure in a convenient way by using this technique.

With the aid of this full field measurement method and knowledge of the mode-shape of the contributing modes, a suitable location for attaching the dynamic vibration absorber can be determined.

1.5. Thesis outline and new results

A literature survey of DVA for suppression of vibration and attenuation of sound radiation from vibrating structure and a review of the normal mode theory and ESPI are reported in Chapter 1.

The theories for vibration control of discrete and continuous systems are described in Chapter 2. Based on the governing equations of motion, equations for the dynamic response of the new type of vibration absorber are established. Hence, equations for finding the effect of the vibration absorbers on rigid-body motion and multi-degrees-of-freedom systems are derived. Numerical models for the flexural vibration of continuous structures including beams and plates with vibration absorbers are developed by the finite element method.

In Chapter 3, numerical studies are presented for the absorption of rigid body motions of vibrating platforms with different types of DVA. To investigate the effect of distributed models such as beams and plates, finite element models are developed and approximate solutions obtained by using self-written and commercial programs. The results found are verified by experiments.

Finally, discussions of the results and conclusions are presented in Chapter 4.

2. Theory

2.1. Vibration suppression of discrete systems using dynamic vibration absorber

In this project undamped structures and absorbers were used in all numerical analysis. Comparing to the analysis with the damped systems, it was able to give a clearer picture of the effects of the dynamic absorbers (such as how the natural frequencies shift) in the current investigation.

2.1.1. The traditional dynamic vibration absorber

A traditional approach to protect a device from steady-state harmonic disturbance at a constant frequency is the addition of a vibration absorber. Unlike a vibration isolator, an absorber is a second mass-spring system added to the primary structure to protect it from vibration. The purpose of adding the absorber is to transmit the vibration energy from the primary structure to the second mass-spring system [30]. The new system becomes a two-degree-of-freedom system which has two natural frequencies. If the auxiliary mass-spring system has no damping and is tuned to the forcing frequency, it acts as a dynamic absorber and enforces a node at its point of attachment of the primary system [31].

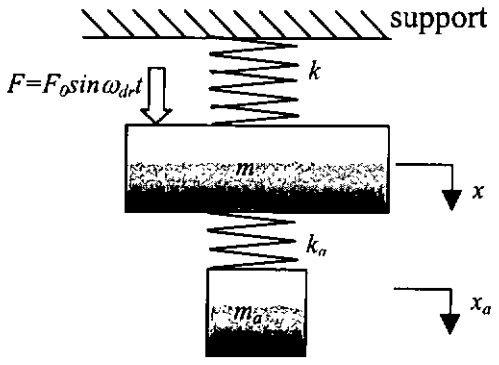

Figure 2.1.1a Model of dynamic vibration absorber attached on a system with a forced vibration

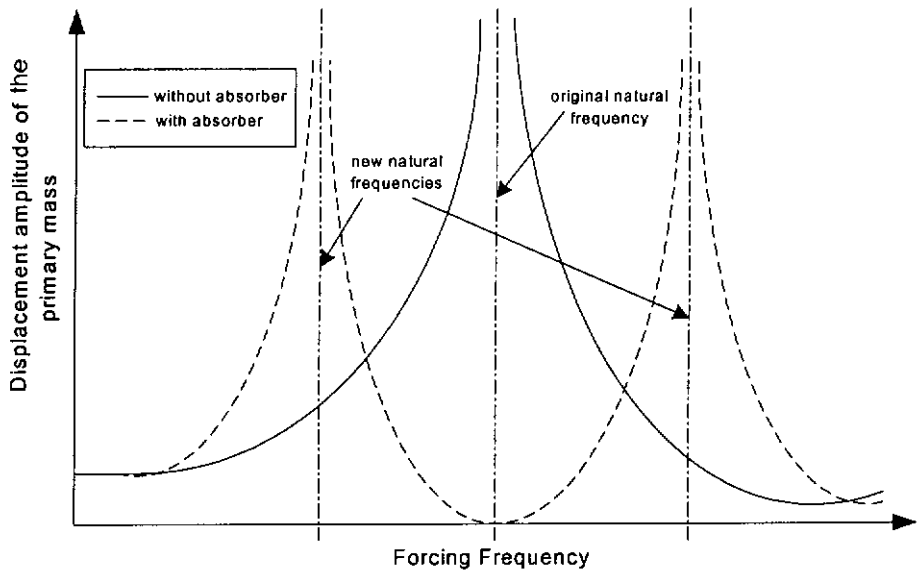

Figure 2.2.1b Vibration amplitude of the primary mass m.

As shown in Figure 2.1.1b, the absorber has split the original natural frequency into two natural frequencies of the combined system: the original structure with the attached absorber. The mass and stiffness of the absorber can be optimized to minimize the vibration of the original device. As x is the displacement of the primary system (with mass m and stiffness k) and x_a is the displacement of the absorber mass (with mass m_a and stiffness k_a), the equation of motion is:

$$\begin{bmatrix} m & 0 \\ 0 & m_a \end{bmatrix} \begin{bmatrix} \ddot{x} \\ \ddot{x}_a \end{bmatrix} + \begin{bmatrix} k + k_a & -k_a \\ -k_a & k_a \end{bmatrix} \begin{bmatrix} x \\ x_a \end{bmatrix} = \begin{bmatrix} F_0 \sin \omega_{dr} t \\ 0 \end{bmatrix} \tag{2.1.1}$$

Let the steady-state solution for x and x_a be

$$x(t) = X \sin \omega_{dr} t$$

$$x_a(t) = X_a \sin\omega_{dr} t \tag{2.1.2}$$

Substituting equations 2.1.2 into 2.1.1, we have:

$$\begin{bmatrix} k + k_a - m & -k_a \\ -k_a & k_a - m_a {\omega_{dr}}^2 \end{bmatrix} \begin{bmatrix} X \\ X_a \end{bmatrix} \sin\omega_{dr} t = \begin{bmatrix} F_0 \\ 0 \end{bmatrix} \sin\omega_{dr} t \tag{2.1.3}$$

$$\text{So, } \begin{bmatrix} X \\ X_a \end{bmatrix} = \begin{bmatrix} k + k_a - m & -k_a \\ -k_a & k_a - m_a {\omega_{dr}}^2 \end{bmatrix}^{-1} \begin{bmatrix} F_0 \\ 0 \end{bmatrix}$$

$$= \frac{1}{(k + k_a - m{\omega_{dr}}^2)(k_a - m_a {\omega_{dr}}^2) - {k_a}^2} \begin{bmatrix} (k_a - m_a {\omega_{dr}}^2) F_0 \\ k_a F_0 \end{bmatrix} \tag{2.1.4}$$

Hence, by choosing suitable k_a and m_a such that $k_a = m_a {\omega_{dr}}^2$, X can be reduced to zero.

In such a case, the amplitude of motion of the absorber is:

$$X_a = F_0 / k_a \tag{2.1.5}$$

2.1.2. Vibration absorber for absorbing rigid body motions

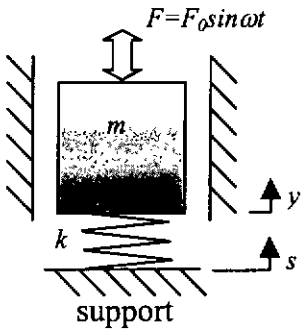

Figure 2.1.2. Ideal single-degree-of-freedom system

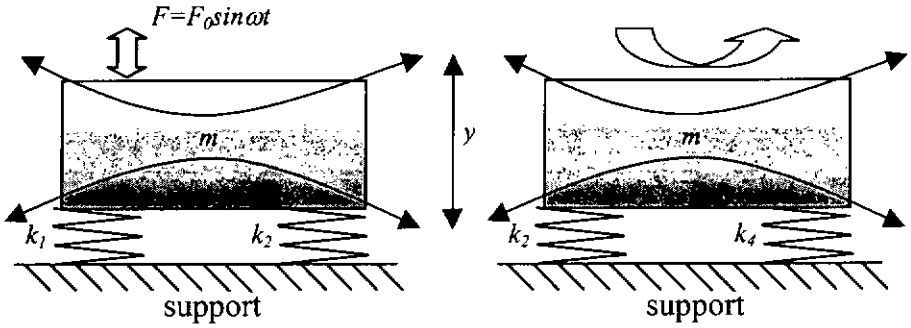

Figure 2.1.3. Model of a vibrating platform have resilient support at each of the four corners

The idealized single-degree-of-freedom system as shown in Figure 2.1.2 consisting of a mass supported by a spring is hard to be realized in practice, since even in the simplest case of a mass suspended by a spring, the mass can not be constrained to move along a straight line. It is important to understand what modification must be made to the simple theory to interpret practical cases.

A rigid resilient supported body exhibits the six natural modes of vibration as shown diagrammatically in Figure 2.1.3. Each of the modes may be excited independently or together with others. The six modes are vertical translation, a rocking mode about a point above or below the center of gravity, and corresponding rocking modes when viewed in the other elevation and the rotational mode. If excitation in a particular direction results in motion of the mounted equipment not only in the same direction as the excitation but also in some other modes of vibration, then the two modes are said to be coupled. Without loss of generality, the vibrating platform can be simplified to a rigid beam with a variable center of gravity. The performance of vibration absorption by a standard translational vibration absorber, a rotational vibration absorber, and a combined type of absorber is presented in the followings.

Consider a rigid beam of mass m with it's center of mass at l_1, supported by two springs with stiffness k_1 and k_2 as shown in Figure 2.1.4. Let the length of the beam be L. The model is set up as mentioned above so that the computation can be simplified.

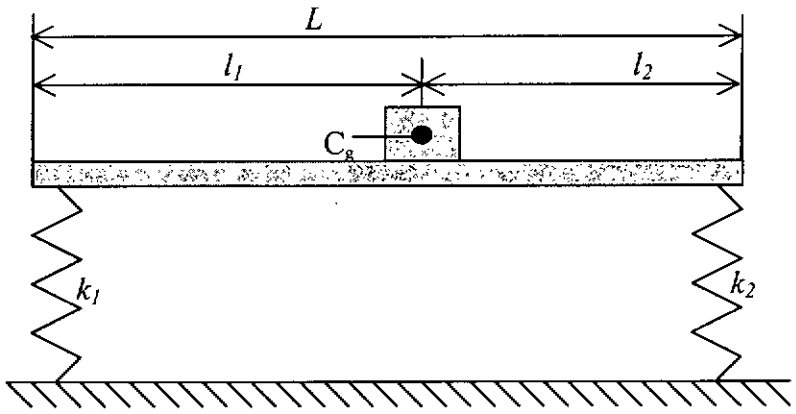

Figure 2.1.4. Model of a rigid beam without any vibration absorber

The differential equations governing the behavior of free vibration of the system in Figure 2.1.4 can be described by the following matrix equations:

$$\begin{bmatrix} m & 0 \\ 0 & I \end{bmatrix}\begin{bmatrix} \ddot{x} \\ \ddot{\theta} \end{bmatrix}+\begin{bmatrix} k_1+k_2 & k_2l_2-k_1l_1 \\ k_2l_2-k_1l_1 & k_1{l_1}^2+k_2{l_2}^2 \end{bmatrix}\begin{bmatrix} x \\ \theta \end{bmatrix}=0$$

$$\begin{bmatrix} k_1+k_2-m\omega^2 & k_2l_2-k_1l_1 \\ k_2l_2-k_1l_1 & k_1{l_1}^2+k_2{l_2}^2-I\omega^2 \end{bmatrix}\begin{bmatrix} x \\ \theta \end{bmatrix}=0 \qquad (2.1.6)$$

With $\tilde{k}=\frac{k_2}{k_1}$, $\tilde{z}=\frac{I}{mL^2}$, $\tilde{l}=\frac{l_1}{L}$, $\tilde{\omega}=\frac{\omega}{\sqrt{k_1/m}}$, $\tilde{y}=\frac{y_a}{L}$

The non-dimensional form of the determinant of the coefficient matrix $D(\omega)$ is shown below:

$$\frac{D}{L^2{k_1}^2}=\left[1+\tilde{k}-\tilde{\omega}^2\right]\left[\tilde{l}^2+\tilde{k}(1-\tilde{l})^2-\tilde{z}\tilde{\omega}^2\right]-\left[\tilde{k}(1-\tilde{l})-\tilde{l}\right]^2 \qquad (2.1.7)$$

The roots (ω_1 and ω_2) of the equation $D(\omega)=0$ are the natural frequencies of the system.

$$\frac{D}{L^2{k_1}^2}=\left[\tilde{\omega}^2-{\omega_1}^2\right]\left[\tilde{\omega}^2-{\omega_2}^2\right]$$

$$So, \qquad \tilde{\omega}_1^{\,2}=\frac{1}{2}\left[1+\tilde{k}+\left(\frac{\tilde{l}^2+\tilde{k}(1-\tilde{l})^2}{\tilde{z}}\right)+\sqrt{\left(1+\tilde{k}+\frac{\tilde{l}^2+\tilde{k}(1-\tilde{l})^2}{\tilde{z}}\right)^2-\frac{4\tilde{k}}{\tilde{z}}}\right]$$

$$\tilde{\omega}_2^{\,2} = \frac{1}{2}\left[1+\tilde{k}+\left(\frac{\tilde{l}^{\,2}+\tilde{k}(1-\tilde{l})^2}{\tilde{z}}\right)-\sqrt{\left(1+\tilde{k}+\frac{\tilde{l}^{\,2}+\tilde{k}(1-\tilde{l})^2}{\tilde{z}}\right)^2-\frac{4\tilde{k}}{\tilde{z}}}\right]$$

If a sinusoidal force F is applied at l_1+y_a. The differential equations of the system become:

$$\begin{bmatrix} k_1+k_2-m\omega^2 & k_2l_2-k_1l_1 \\ k_2l_2-k_1l_1 & k_1l_1^{\,2}+k_2l_2^{\,2}-I\omega^2 \end{bmatrix}\begin{bmatrix} x \\ \theta \end{bmatrix}=\begin{bmatrix} F \\ Fy_a \end{bmatrix}\sin\omega t$$

And, the steady-state amplitude for an arbitrary value of ω are obtained by Cramer's rule:

$$\frac{X}{F/k_1}=\frac{1}{D}\left\{\left[\tilde{l}^{\,2}+\tilde{k}(1-\tilde{l})^2-\tilde{z}\tilde{\omega}^2\right]-\tilde{y}\left[\tilde{k}(1-\tilde{l})-\tilde{l}\right]\right\} \tag{2.1.8}$$

$$\frac{\Theta}{F/k_1L}=\frac{1}{D}\left\{\tilde{y}\left[1+\tilde{k}-\tilde{\omega}^2\right]-\left[\tilde{k}(1-\tilde{l})-\tilde{l}\right]\right\} \tag{2.1.9}$$

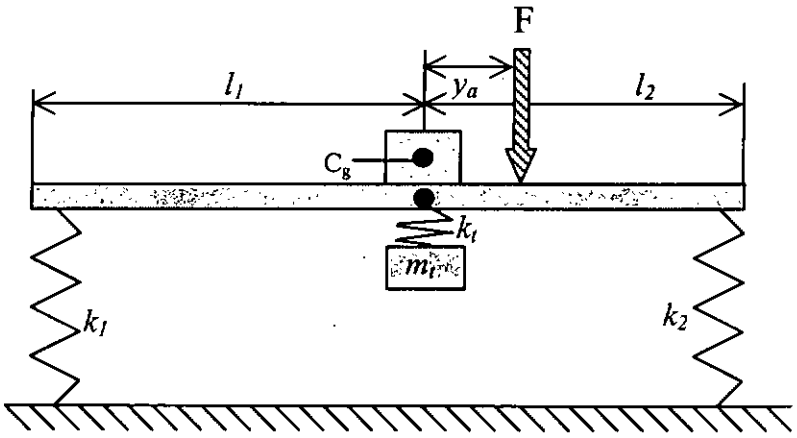

Figure 2.1.5. Model of a rigid beam with a translational absorber

To control the vibration, traditional translational absorber may be added to the system. As shown in Figure 2.1.5, an additional mass m_t and a spring of stiffness k_t are attached to the beam. Let x_2 be the absorber displacement from its original position, the differential equations governing the behavior of the system will be:

$$\begin{bmatrix} m & 0 & 0 \\ 0 & I & 0 \\ 0 & 0 & m_t \end{bmatrix}\begin{bmatrix} \ddot{x}_1 \\ \ddot{\theta} \\ \ddot{x}_2 \end{bmatrix}+\begin{bmatrix} k_1+k_2+k_t & k_2l_2-k_1l_1 & -k_t \\ k_2l_2-k_1l_1 & k_1l_1^{\,2}+k_2l_2^{\,2} & 0 \\ -k_t & 0 & k_t \end{bmatrix}\begin{bmatrix} x_1 \\ \theta \\ x_2 \end{bmatrix}=\begin{bmatrix} F \\ y_aF \\ 0 \end{bmatrix}\sin\omega t$$

$$\begin{bmatrix} k_1+k_2+k_t-m\omega^2 & k_2l_2-k_1l_1 & -k_t \\ k_2l_2-k_1l_1 & k_1l_1^{\,2}+k_2l_2^{\,2}-I\omega^2 & 0 \\ -k_t & 0 & k_t-m_t\omega^2 \end{bmatrix}\begin{bmatrix} x_1 \\ \theta \\ x_2 \end{bmatrix}=\begin{bmatrix} F \\ y_aF \\ 0 \end{bmatrix}\sin\omega t \qquad (2.1.10)$$

With $\tilde{k}=\frac{k_2}{k_1}$, $\tilde{k}_t=\frac{k_t}{k_1}$, $\tilde{z}=\frac{I}{mL^2}$, $\tilde{l}=\frac{l_1}{L}$, $\tilde{\omega}=\frac{\omega}{\sqrt{k_1/m}}$, $\tilde{y}=\frac{y_a}{L}$, $\tilde{m}_t=\frac{m_t}{m}$

$$\frac{D}{L^2k_1^{\,3}}=\left[1+\tilde{k}+\tilde{k}_t-\tilde{\omega}^2\right]\left[\tilde{l}^{\,2}+\tilde{k}(1-\tilde{l})^2-\tilde{z}\tilde{\omega}^2\right]\left[\tilde{k}_t-\tilde{m}_t\tilde{\omega}^2\right]-\left[\tilde{l}^{\,2}+\tilde{k}(1-\tilde{l})^2-\tilde{z}\tilde{\omega}^2\right]\left[-\tilde{k}_t\right]^2$$

$$-\left[\tilde{k}_t-\tilde{m}_t\tilde{\omega}^2\right]\left[\tilde{k}(1-\tilde{l})-\tilde{l}\right]^2 \qquad (2.1.11)$$

$$\frac{D}{L^2k_1^{\,2}}=\left[\tilde{\omega}^2-\omega_{t1}^{\,2}\right]\left[\tilde{\omega}^2-\omega_{t2}^{\,2}\right]\left[\tilde{\omega}^2-\omega_{t3}^{\,2}\right]$$

$$\frac{X}{F/k_1}=\frac{1}{D}\left\{\left[\tilde{l}^{\,2}+\tilde{k}(1-\tilde{l})^2-\tilde{z}\tilde{\omega}^2\right]\left[\tilde{k}_t-\tilde{m}_t\tilde{\omega}^2\right]-\tilde{y}\left[\tilde{k}(1-\tilde{l})-\tilde{l}\right]\left[\tilde{k}_t-\tilde{m}_t\tilde{\omega}^2\right]\right\} \qquad (2.1.12)$$

$$\frac{\Theta}{F/k_1L}=\frac{1}{D}\left\{\tilde{y}\left[1+\tilde{k}+\tilde{k}_t-\tilde{\omega}^2\right]\left[\tilde{k}_t-\tilde{m}_t\tilde{\omega}^2\right]-\tilde{y}\tilde{k}_t^{\,2}-\left[\tilde{k}(1-\tilde{l})-\tilde{l}\right]\left[\tilde{k}_t-\tilde{m}_t\tilde{\omega}^2\right]\right\} \qquad (2.1.13)$$

$$\frac{X_2}{F/k_1}=\frac{1}{D}\left\{\tilde{y}\tilde{k}_t\left[\tilde{k}(1-\tilde{l})-\tilde{l}\right]-\left[-\tilde{k}_t\right]\left[\tilde{l}^2+\tilde{k}(1-\tilde{l})^2-\tilde{z}\tilde{\omega}^2\right]\right\} \tag{2.1.14}$$

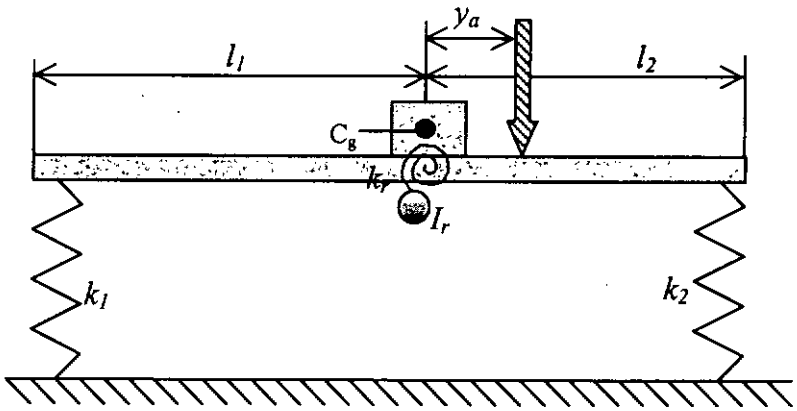

Figure 2.1.6. Model of a rigid beam with a rotational absorber

Instead of attaching a traditional translational absorber, an alternate method to suppress the vibration would be the addition of a rotational absorber and this method is rarely reported in the literature. As shown in Figure 2.1.6, the attached rotational DVA with inertia I_r and rotational spring of stiffness k_r was attached to the rigid beam. Let ϕ be the rotation of the absorber, the differential equations governing the behavior of the system will be:

$$\begin{bmatrix} m & 0 & 0 \\ 0 & I & 0 \\ 0 & 0 & I_r \end{bmatrix}\begin{bmatrix} \ddot{x}_1 \\ \ddot{\theta} \\ \ddot{\phi} \end{bmatrix}+\begin{bmatrix} k_1+k_2 & k_2l_2-k_1l_1 & 0 \\ k_2l_2-k_1l_1 & k_1l_1^{\,2}+k_2l_2^{\,2}+k_r & -k_r \\ 0 & -k_r & k_r \end{bmatrix}\begin{bmatrix} x_1 \\ \theta \\ \phi \end{bmatrix}=\begin{bmatrix} F \\ y_aF \\ 0 \end{bmatrix}\sin\omega t$$

$$\begin{bmatrix} k_1+k_2-m\omega^2 & k_2l_2-k_1l_1 & 0 \\ k_2l_2-k_1l_1 & k_1l_1^{\,2}+k_2l_2^{\,2}+k_r-I\omega^2 & -k_r \\ 0 & -k_r & k_r-I_r\omega^2 \end{bmatrix}\begin{bmatrix} x_1 \\ \theta \\ \phi \end{bmatrix}=\begin{bmatrix} F \\ y_aF \\ 0 \end{bmatrix}\sin\omega t \tag{2.1.15}$$

$$For\ \tilde{k}=\frac{k_2}{k_1},\ \tilde{k}_r=\frac{k_r}{k_1L^2},\ \tilde{z}=\frac{I}{mL^2},\ \tilde{I}_r=\frac{I_r}{mL^2},\ \tilde{l}=\frac{l_1}{L},\ \tilde{\omega}=\frac{\omega}{\sqrt{k_1/m}},\ \tilde{y}=\frac{y_a}{L}$$

$$\frac{D}{L^4k_1^{\,3}}=\left[1+\tilde{k}-\tilde{\omega}^2\right]\left[\tilde{I}^{\,2}+\tilde{k}(1-\tilde{l})^2+\tilde{k}_r-\tilde{z}\tilde{\omega}^2\right]\left[\tilde{k}_r-\tilde{I}_r\tilde{\omega}^2\right]-\left[1+\tilde{k}-\tilde{\omega}^2\right]\left[-\tilde{k}_r\right]^2$$

$$-\left[\tilde{k}_r-\tilde{I}_r\tilde{\omega}^2\right]\left[\tilde{k}(1-\tilde{l})-\tilde{l}\right]^2 \qquad (2.1.16)$$

$$\frac{D}{L^4k_1^{\,2}}=\left[\tilde{\omega}^2-\omega_{r1}^{\,2}\right]\left[\tilde{\omega}^2-\omega_{r2}^{\,2}\right]\left[\tilde{\omega}^2-\omega_{r3}^{\,2}\right]$$

$$\frac{X}{F/k_1}=\frac{1}{D}\left\{\left[\tilde{l}^{\,2}+\tilde{k}(1-\tilde{l})^2+\tilde{k}_r-\tilde{z}\tilde{\omega}^2\right]\left[\tilde{k}_r-\tilde{I}_r\tilde{\omega}^2\right]-\tilde{k}_r^{\,2}-\tilde{y}\left[\tilde{k}(1-\tilde{l})-\tilde{l}\right]\left[\tilde{k}_r-\tilde{I}_r\tilde{\omega}^2\right]\right\} \qquad (2.1.17)$$

$$\frac{\Theta}{F/k_1L}=\frac{1}{D}\left\{\tilde{y}\left[1+\tilde{k}-\tilde{\omega}^2\right]\left[\tilde{k}_r-\tilde{I}_r\tilde{\omega}^2\right]-\left[\tilde{k}(1-\tilde{l})-\tilde{l}\right]\left[\tilde{k}_r-\tilde{I}_r\tilde{\omega}^2\right]\right\} \qquad (2.1.18)$$

$$\frac{\Phi}{F/k_1}=\frac{1}{D}\left\{-\tilde{k}_r\left[\tilde{k}(1-\tilde{l})-\tilde{l}\right]-\tilde{y}\left[-\tilde{k}_r\right]\left[1+\tilde{k}-\tilde{\omega}^2\right]\right\} \qquad (2.1.19)$$

To investigate the response of the structure if both rotational and translational vibration absorbers were attached to the system at the same point of a rigid beam model as illustrated in Figure 2.1.7., the equation of motion of the combined system is expressed in Equation (2.1.20).

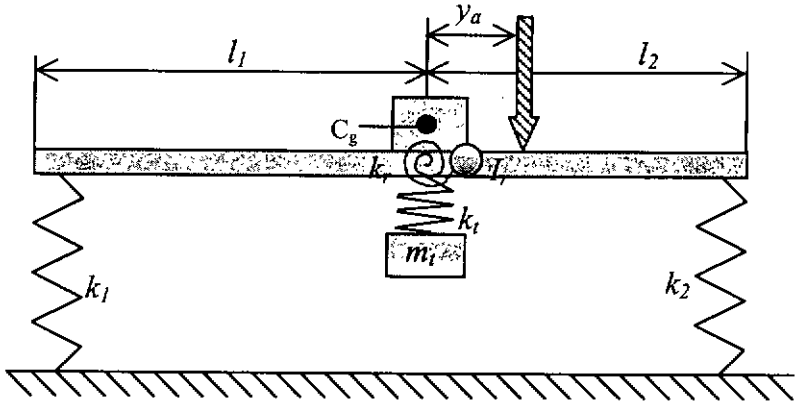

Figure 2.1.7. Vibrating structure with both rotational and translational vibration absorbers.

$$\begin{bmatrix} m & 0 & 0 & 0 \\ 0 & I & 0 & 0 \\ 0 & 0 & m_t & 0 \\ 0 & 0 & 0 & I_r \end{bmatrix} \begin{bmatrix} \ddot{x}_1 \\ \ddot{\theta} \\ \ddot{x}_2 \\ \ddot{\phi} \end{bmatrix} + \begin{bmatrix} k_1+k_2+k_t & k_2l_2-k_1l_1 & -k_t & 0 \\ k_2l_2-k_1l_1 & k_1l_1^{\,2}+k_2l_2^{\,2}+k_r & 0 & -k_r \\ -k_t & 0 & k_t & 0 \\ 0 & -k_r & 0 & k_r \end{bmatrix} \begin{bmatrix} x_1 \\ \theta \\ x_2 \\ \phi \end{bmatrix} = \begin{bmatrix} F \\ y_aF \\ 0 \\ 0 \end{bmatrix} \sin \omega t$$

$$\begin{bmatrix} k_1+k_2+k_t-m\omega^2 & k_2l_2-k_1l_1 & -k_t & 0 \\ k_2l_2-k_1l_1 & k_1l_1^{\,2}+k_2l_2^{\,2}+k_r-I\omega^2 & 0 & -k_r \\ -k_t & 0 & k_t-m_t\omega^2 & 0 \\ 0 & -k_r & 0 & k_r-I_r\omega^2 \end{bmatrix} \begin{bmatrix} x_1 \\ \theta \\ x_2 \\ \phi \end{bmatrix} = \begin{bmatrix} F \\ y_aF \\ 0 \\ 0 \end{bmatrix} \sin \omega t$$

(2.1.20)

Hence, X_1, X_2, Θ and Φ can be found by a similar procedure as the cases of the rigid beam with a pure translational absorber or pure rotational absorber described before.

2.1.3. Effect of a vibration absorber attached on to a multi-degree-of-freedom system

The theory of vibration absorption for a two-degree-of-freedom system as described in the previous section can be extended to an n-degree-of-freedom system. Large-amplitude responses will occur in a n-degree-of-freedom system if a harmonic excitation of frequency close to one of the natural frequencies of the system is applied. Vibration absorbers can be designed to reduce the steady-state amplitudes of the primary structure. Effect of a multi-degree-of-freedom system were commonly mentioned in textbooks [33][34], to give a rough idea on how the vibration absorber(s) affects a multi-degree-of-freedom, related analysis methods and equations were described in this section.

Consider an n-degree-of-freedom system subjected to a harmonic excitation close to one of the system's natural frequencies. Let x_1, x_2, ..., x_n be the chosen generalized coordinates. Let m_{ij} and k_{ij} be the element of the mass and stiffness matrices respectively. A vibration absorber with mass $\tilde{m}$ and stiffness $\tilde{k}$ is attached to the system at a point whose displacement is given by x_1. Based on the equation of motion $M\ddot{x} + Kx = F$

with $x = \begin{bmatrix} x_1 \\ x_2 \\ \vdots \\ x_{n+1} \end{bmatrix}$. The generalized coordinate x_{n+1} is defined as the displacement of the absorber mass. The mass and stiffness matrices for the resulting n+1-degree-of-freedom system are:

$$M=\begin{bmatrix} m_{11} & m_{12} & \cdots & m_{1n} & 0 \\ m_{21} & m_{22} & \cdots & m_{2n} & 0 \\ \vdots & \vdots & \ddots & \vdots & \vdots \\ m_{n1} & m_{n2} & \cdots & m_{nn} & 0 \\ 0 & 0 & \cdots & 0 & \tilde{m} \end{bmatrix} \tag{2.1.21}$$

$$K=\begin{bmatrix} k_{11}+\tilde{k} & k_{12} & \cdots & k_{1n} & -\tilde{k} \\ k_{21} & k_{22} & \cdots & k_{2n} & 0 \\ \vdots & \vdots & \ddots & \vdots & \vdots \\ k_{n1} & k_{n2} & \cdots & k_{nn} & 0 \\ -\tilde{k} & 0 & \cdots & 0 & \tilde{k} \end{bmatrix} \tag{2.1.22}$$

For a single-frequency harmonic excitation, the force vector is:

$$F=\begin{bmatrix} A_1 \\ A_2 \\ \vdots \\ A_n \\ 0 \end{bmatrix} \sin \omega t$$

Hence,

$$D=\begin{bmatrix} A_1 & k_{12}-m_{12}\omega^2 & k_{13}-m_{13}\omega^2 & \cdots & k_{1n}-m_{n2}\omega^2 & -\tilde{k} \\ A_2 & k_{22}-m_{22}\omega^2 & k_{23}-m_{23}\omega^2 & \cdots & k_{2n}-m_{2n}\omega^2 & 0 \\ A_3 & \vdots & \vdots & \cdots & \vdots & 0 \\ \vdots & \vdots & \vdots & \ddots & \vdots & \vdots \\ A_n & k_{n2}-m_{n2}\omega^2 & k_{n3}-m_{n3}\omega^2 & \cdots & k_{nn}-m_{nn}\omega^2 & 0 \\ 0 & 0 & \cdots & \cdots & \cdots & \tilde{k}-\tilde{m}\omega^2 \end{bmatrix} \tag{2.1.23}$$

where $D(\omega) = \det(-\omega^2 M - K)$. If the absorber is tuned with it's natural frequency equal to $\tilde{\omega} = \sqrt{\frac{\tilde{k}}{\tilde{m}}}$, which is equal to the excitation frequency, then, X_1 the vibration amplitude where the absorber attached will become zero.

Using a similar conversion to that shown in Section 2.1.2, the steady-state amplitude of the particle of the primary system to which the absorber attached can be calculated.

In the case when two vibration absorbers are added at the first and second elements of the system, it becomes an n+2 DOF system. By similar calculation, the generalized coordinate x_{n+2} is defined as the displacement of the absorber mass. The mass and stiffness matrices for the resulting n+2-degree-of-freedom system are:

$$M = \begin{bmatrix} m_{11} & m_{12} & \cdots & 0 & 0 \\ m_{21} & m_{22} & \cdots & 0 & 0 \\ \vdots & \vdots & \ddots & \vdots & \vdots \\ 0 & 0 & \cdots & \tilde{m}_1 & 0 \\ 0 & 0 & \cdots & 0 & \tilde{m}_2 \end{bmatrix} \tag{2.1.24}$$

$$K = \begin{bmatrix} k_{11} + \tilde{k}_1 & k_{12} & \cdots & -\tilde{k}_1 & 0 \\ k_{21} & k_{22} + \tilde{k}_2 & \cdots & 0 & -\tilde{k}_2 \\ \vdots & \vdots & \ddots & \vdots & \vdots \\ -\tilde{k}_1 & 0 & \cdots & \tilde{k}_1 & 0 \\ 0 & -\tilde{k}_2 & \cdots & 0 & \tilde{k}_2 \end{bmatrix} \tag{2.1.25}$$

Hence,

$$D=\begin{bmatrix} k_{12}+\tilde{k}_1-m_{12}\omega^2 & k_{12}-m_{12}\omega^2 & k_{13}-m_{13}\omega^2 & \cdots & -\tilde{k}_1 & 0 \\ k_{21}-m_{21}\omega^2 & k_{22}+\tilde{k}_2-m_{22}\omega^2 & k_{23}-m_{23}\omega^2 & \cdots & 0 & -\tilde{k}_2 \\ \vdots & \vdots & \vdots & \ddots & 0 & 0 \\ k_{n11}-m_{n2}\omega^2 & k_{n2}-m_{n2}\omega^2 & k_{n3}-m_{n3}\omega^2 & \cdots & 0 & \vdots \\ -\tilde{k}_1 & 0 & \cdots & \cdots & \tilde{k}_1-\tilde{m}_1\omega^2 & 0 \\ 0 & -\tilde{k}_2 & \cdots & \cdots & 0 & \tilde{k}_2-\tilde{m}\omega^2 \end{bmatrix} \quad (2.1.26)$$

With the M and K matrices, forcing frequency ω and the force function provided, using a similar procedure to that described in Section 2.1.2, the steady-state translational amplitude and rotational amplitude of each element of the system can be derived.

With a similar argument to that the two-degree-of-freedom system, the addition of a vibration absorber tuned to the excitation frequency of a multi-degree-of-freedom system leads to zero steady motion of the system particle at which it is attached.

The vibration absorber attached to a multi-degree-of-freedom system works by shifting the natural frequencies of the system away from the excitation frequency. The natural frequency near the excitation frequency is decreased and a natural frequency is added between the excitation frequency and the next higher natural frequency of the primary system.

The addition of damping to the absorber leads to a more complicated analysis. The steady-state amplitude cannot be eliminated completely for any particle when damping present.

An optimum tuning frequency and optimum damping ratio can be determined for a specific system [13][14]. As the major purpose of the present analysis is to investigate the suppression of vibration and the resulting sound radiated from the structure under a pure harmonic excitation, damping in both the primary and the attached structures are neglected for the simplification of calculations.

2.2. Vibration suppression of continuous systems using vibration absorbers

2.2.1. Modal analysis of forced vibration of undamped structures

The dynamic response of structures under forced vibration may be explained by the well-known mode-simulation method [32]. A DVA may be attached to a node or an anti-node of a vibration mode which have the most significant contribution to the dynamic response to the excitation.

For a system with n degrees-of-freedom, the governing equations of motion are a set of n coupled ordinary differential equations of the second order. The solutions of these equations become more complicated when the number of degrees-of-freedom of the system is large. In such a case, a more convenient method known as modal analysis can be used to predict the dynamic response of the system. The classical theory can be found in textbooks [33, 34] and it is briefly described in the following.

Expansion theory is used and the displacements of the masses are expressed as a linear combination of the normal modes of the system. This linear transformation uncouples the

equations of motion so that we obtain a set of n uncoupled differential equations. Assume the equation of motion of a multi-degree of freedom system under the external force F is:

$$[m]\ddot{x} + [k]x = F, \tag{2.2.1}$$

where F is the vector of arbitrary external forces. To solve this equation by modal analysis, it is necessary to solve the eigenvalue problem.

$$\omega^2[m]X = [k]X$$

or $$(\omega^2[m] - [k])X = 0 \tag{2.2.2}$$

By this equation, the mode shape vectors X_1, X_2, ...,.X_n and the corresponding natural frequencies ω_1, ω_2, ..., ω_n can be found. The solution vector of equation 2.2.2 can be expressed by a linear combination of the normal modes by means of the expansion theorem:

$$x(t) = q_1(t)X_1 + q_2(t)X_2 + ... + q_n(t)X_n \tag{2.2.3}$$

where $q_1(t)$, $q_2(t)$, ..., $q_n(t)$ are time-dependent generalized coordinates, also known as the modal participation coefficients or principle coordinates. By defining a modal matrix $[X]$ in which the j^{th} column is the vector X_j, that is:

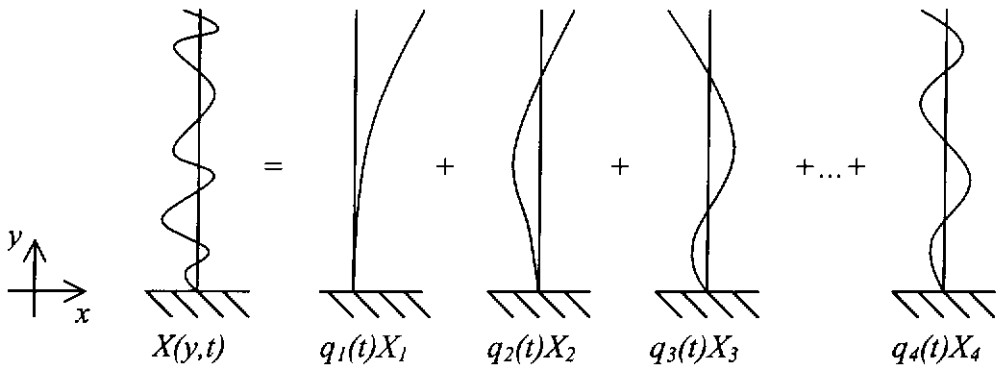

Figure 2.2.1. Combination of the normal modes to be the forced vibration deformation

$$[X] = [X_1\ X_2\ \ldots . X_n] \tag{2.2.4}$$

So, equation 2.2.3 becomes:

$$x(t) = [X]q(t) \tag{2.2.5}$$

where $q(t) = \begin{Bmatrix} q_1(t) \\ q_2(t) \\ \vdots \\ q_n(t) \end{Bmatrix}$

Since $[X]$ is not a function of time, by differentiating equation 2.2.5 twice,

$$\ddot{x}(t) = [X]\ddot{q}(t) \tag{2.2.6}$$

Substitute 2.2.5 and 2.2.6 into 2.2.1, we have:

$$[m][X]\ddot{q} + [k][X]q = F \tag{2.2.7}$$

multiplying by $[X]^T$,the equation becomes:

$$[X]^T[m][X]\ddot{q} + [X]^T[k][X]q = [X]^T F \tag{2.2.8}$$

The normal modes are normalized as:

$$[X]^T[m][X] = [I] \tag{2.2.9}$$

and $$[X]^T[k][X] = [\omega^2] \tag{2.2.10}$$

define the vector of generalized force $Q(t)$ associated with the generalized coordinates $q(t)$ as:

$$Q(t) = [X]^T F(t) \tag{2.2.11}$$

Substituting equations 2.2.9, 2.2.10 and 2.2.11 into 2.2.8, we have:

$$\ddot{q}(t) + [\omega^2]q(t) = Q(t) \tag{2.2.12}$$

where $\ddot{q}_i(t) + \omega_i^2 q_i(t) = Q_i(t)$ for i= 1, 2, 3, …, n (2.2.13)

The solution of the equations 2.2.13 can be expressed as:

$$q_i(t) = q_i(0)\cos\omega_i t + \left(\frac{\dot{q}(0)}{\omega_i}\right)\sin\omega_i t + \frac{1}{\omega}\int_0 Q(\tau)\sin\omega_i(t-\tau)d\tau \qquad (2.2.14)$$

for i= 1, 2, 3, ..., n

Initial conditions $q_i(0)$ and $\dot{q}_i(0)$ can be obtained by the initial value of the physical displacements $x_i(0)$ and velocity $\dot{x}_i(0)$:

$$q(0) = [X]^T[m]x(0) \qquad (2.2.15)$$

$$\dot{q}(0) = [X]^T[m]\dot{x}(0) \qquad (2.2.16)$$

If the generalized displacements $q_i(t)$ are obtained, by equations 2.2.14, 2.2.15 and 2.2.16, the physical displacement $x_i(t)$ can be found by equation 2.2.5.

2.2.2. Suppression of flexural vibration of beams using dynamic vibration absorbers

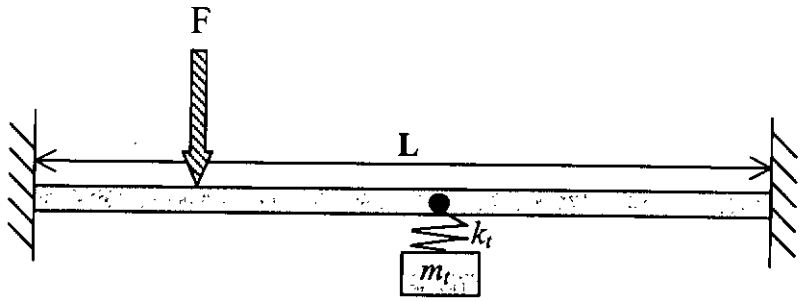

Figure 2.2.2. Illustration of a beam with a translational DVA under an external excitation

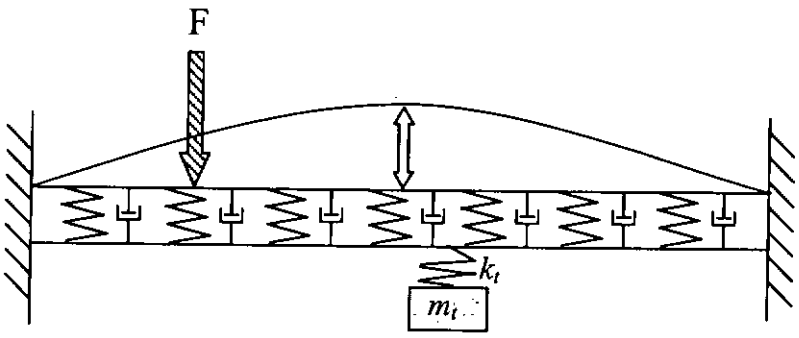

Figure 2.2.3. Illustration of the beam in figure 2.2.2 as a multiple SDOF systems

Vibration suppression of continuous systems with a DVA is described in this section. As shown in Figure 2.2.2, a clamped flexible beam with a DVA at its center of mass is considered. To study this kind of continuous system, finite element modeling is a tool commonly used [35][36]. The methodology of analyzing a model by finite element was briefly described in this section.

In finite element modeling, a continuous system in Figure 2.2.2 is divided into a finite number of discrete elements as illustrated in Figure 2.2.3. Interpolations for the dependent

variables are assumed across each element and are chosen to assure appropriate inter-element continuity. The beam then could be considered as a multi-degree-of-freedom vibrating system.

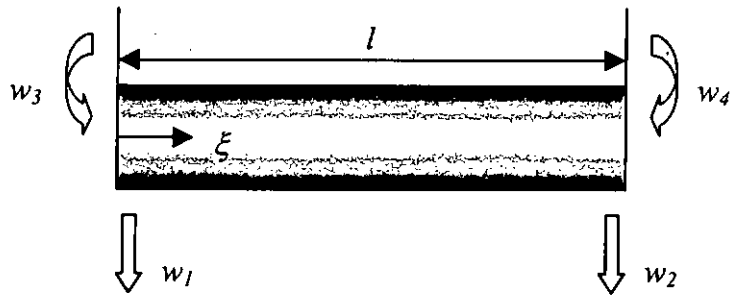

Figure 2.2.4. Beam element has 4 degree-of-freedoms, represented by displacements and rotations at the ends of the element.

The potential energy scalar product for a beam involves the second spatial derivatives of the displacement. Thus a Rayleigh-Ritz [35] or assumed modes approximation [36] must be twice differentiable. When the beam model is developed by the assumed modes method, the requirement that the interpolation to be twice differentiable leads to requiring that displacement and slope to be continuous at element boundaries. In order to enforce this requirement over the entire beam, each beam element has four degree-of-freedoms represented by the displacements and slopes at the end of the element. Let w_1 and w_3 be the transverse displacement of the left end and right end of the element respectively, w_2 and w_4 represents the slope at the left end and the right end of the element as shown in figure 2.2.3. If ξ is the local coordinate over the beam element, the finite element approximation for the displacement $u(\xi, t)$ across the beam must satisfy:

$$u(0,t)=w_1,\ \frac{\partial u}{\partial \xi}(0,t)=w_2,\quad u(l,t)=w_3\ \text{ and }\ \frac{\partial u}{\partial \xi}(l,t)=w_4 \tag{2.2.16}$$

The deflection of a beam element without transverse loading across its span, but with prescribed displacement and slope at its ends is approximated as:

$$u(\xi)=C_1\xi^3+C_2\xi^2+C_3\xi+C_4 \tag{2.2.17}$$

Using equations (2.2.16) and (2.2.17) to determine the constant leads to:

$$C_1=\frac{1}{l^3}(2w_1+lw_2-2w_3+lw_4),$$

$$C_2=\frac{1}{l^2}(-3w_1-2lw_2+3w_3-lw_4),$$

$$C_3=\frac{w_2}{l},\ \text{and}$$

$$C_4=w_1 \tag{2.2.18}$$

Hence, we have:

$$u(\xi,t)=(1-3\frac{\xi^2}{l^2}+2\frac{\xi^3}{l^3})w_1+(\frac{\xi}{l}-2\frac{\xi^2}{l^2}+\frac{\xi^3}{l^3})w_2+(3\frac{\xi^2}{l^2}-2\frac{\xi^3}{l^3})w_3+(-\frac{\xi^2}{l^2}+2\frac{\xi^3}{l^3})w_4 \tag{2.2.19}$$

The kinetic energy of the beam element is:

$$T=\frac{1}{2}\int_0^l \rho A\left(\frac{\partial u}{\partial \xi}\right)^2 \partial\zeta \tag{2.2.20}$$

Use Equation (2.2.19) and (2.2.20), the kinetic energy of the beam element becomes $T = \frac{1}{2}\dot{w}\, M\dot{w}$ where $\dot{w} = [\dot{w}_1 \quad \dot{w}_2 \quad \dot{w}_3 \quad \dot{w}_4]$ and the local element mass matrix for a uniform beam element is:

$$m = \frac{\rho A l}{420}\begin{bmatrix} 156 & 22l & 54 & -13l \\ 22l & 4l^2 & 13l & -3l^2 \\ 54 & 13l & 156 & -22l \\ -13l & -3l^2 & -22l & 4l^2 \end{bmatrix} \tag{2.2.21}$$

The potential energy of the beam element is:

$$V = \frac{1}{2}\int_0^l EI\left(\frac{\partial u}{\partial \xi}\right)^2 \partial\zeta \tag{2.2.22}$$

Substitute equation (2.2.19) into (2.2.22), $V = 1/2 w^T k w$, where the local element stiffness matrix for a uniform beam is:

$$k = \frac{EI}{l^3}\begin{bmatrix} 12 & 6l & -12 & 6l \\ 6l & 4l^2 & -6l & 2l^2 \\ -12 & -6l & 12 & -6l \\ 6l & 2l^2 & -6l & 4l^2 \end{bmatrix} \tag{2.2.23}$$

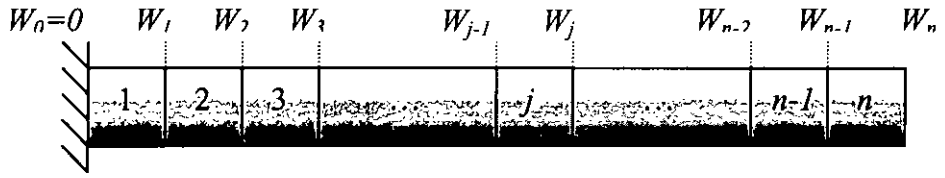

Figure 2.2.5. An n-element model of a fixed-free beam which is fixed at x=0, W_0=0

A beam element has four degree of freedom. The local generalized coordinates are the displacements at the ends of the elements. An n-element finite element model of a beam, as shown in figure 2.2.5., has at most $2n+2$ degrees of freedom. The global generalized coordinates are the displacements of the boundaries between elements and the end of the bar. Each geometric boundary condition reduces one of the global degree-of-freedom. That means if one of the ends of the beam is fixed, then, it's displacement is zero and the model has $2n+1$ degree-of-freedom.

Let $W_1, W_2, \ldots, W_n$ represent the global generalized coordinates. Each local generalized coordinate is one of the global generalized coordinates, unless that element is subject to a geometric boundary condition. The local mass and stiffness matrices can be expanded to include all global generalized coordinates. The total kinetic energy of the system is the sum of the kinetic energies of the elements.

If $T_i = \frac{1}{2}\dot{w}_i^T m_i \dot{w}_i$ is the kinetic energy of the i^{th} element, the local mass matrix can be enlarged and the kinetic energy written in terms of the global generalized coordinates as $T_i = \frac{1}{2}\dot{W}^T \tilde{M}_i \dot{W}$. Hence the total kinetic energy of the system is:

$$T = \sum_{i=1}^{n} T_i = \frac{1}{2}\sum_{i-1}^{n} \dot{W}^T \tilde{M}_i \dot{W} = \frac{1}{2}\dot{W}^T \left(\sum_{i-1}^{n} \tilde{M}_i \right) \dot{W} \qquad (2.2.24)$$

Thus the global mass matrix M can be assembled by the element masses m_1, m_2,..., m_n. Similarly, the global stiffness matrix K can be assembled by the element stiffness k_1, k_2,..., k_n.

The finite element interpolation of w must be such that w, $\frac{\partial w}{\partial n}$ and $\frac{\partial w}{\partial s}$ are continuous across the inter-element boundaries. Note that $\frac{\partial}{\partial n}$, and $\frac{\partial}{\partial s}$ are related to the global derivatives $\frac{\partial}{\partial x}$ and $\frac{\partial}{\partial y}$ by relations $\frac{\partial}{\partial n} = n_x \frac{\partial}{\partial x} + n_y \frac{\partial}{\partial y}$ and $\frac{\partial}{\partial s} = n_x \frac{\partial}{\partial y} + n_y \frac{\partial}{\partial x}$.

Thus, the primary variables at the nodes should be w, $\frac{\partial w}{\partial x}$ and $\frac{\partial w}{\partial y}$.

Finite elements that require continuity of w and its first derivatives are called C^1 elements.

Suppose that w is interpolated by expression of the form $w = \sum_{j=1}^{n} \Delta_j \phi(x,y)$, where the Δ_j denote the nodal values of w and its derivatives, and $\phi_j(x,y)$ are Hermite interpolation functions.

For the n-element beam with a DVA, we could use an $n+1$ or an $n+2$ degrees-of-freedom model for analysis, where the component of the vibration absorber in the global stiffness matrix and the global force vector can be easily obtained by the methodology discussed in Section 2.1.3.

2.2.3. Plate with dynamic vibration absorber under harmonic excitation

The analysis method for beam vibration suppression using a dynamic vibration absorber can be extended for plate vibration suppression with a dynamic vibration absorber in the following manner. The transverse vibration of plate is described by a two-dimensional boundary-value problem, which is materially more complex than a one-dimensional one. Indeed, as explained in 2.2.2, an important consideration in two-dimensional problems is the shape of the boundary.

The general ideas behind the assembly process for two-dimensional domains are essentially the same as for the one-dimensional domains, but the details are more involved, which can be attributed to the fact that there is no longer a simple correspondence between the node number and element number.

To introduce the idea we consider part of a uniform plate consisting of four triangular elements as shown in figure 2.2.6, in which the encircled number represent the element number, the outside numbers represent the global node number and the smaller size inside numbers represent the local node number for the individual element.

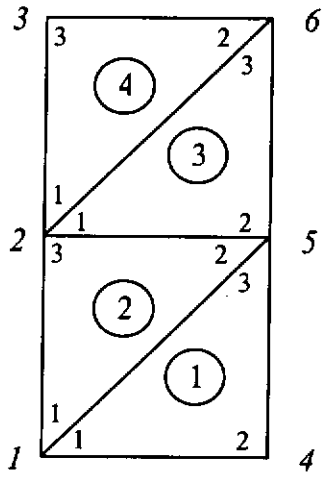

Fig 2.2.6. Four triangular elements with numbering scheme

The plate is free on its sides. The two types of element stiffness matrices are:

$$K^{(j)} = \frac{T}{2}\begin{bmatrix} 1 & -1 & 0 \\ -1 & 2 & -1 \\ 0 & -1 & 1 \end{bmatrix}, \qquad \text{for } j = 1, 3;$$

$$K^{(j)} = \frac{T}{2}\begin{bmatrix} 1 & 0 & -1 \\ 0 & 1 & -1 \\ -1 & -1 & 2 \end{bmatrix}, \qquad \text{for } j = 2, 4 \qquad (2.2.25)$$

And the element mass matrix is:

$$M^{(j)} = \frac{mh^2}{24}\begin{bmatrix} 2 & 1 & 1 \\ 1 & 2 & 1 \\ 1 & 1 & 2 \end{bmatrix}, \qquad \text{for } j = 1, 2, 3, 4 \qquad (2.2.26)$$

Since the motion of the plate is defined by the global nodal displacements and the entries of the element stiffness and mass matrices correspond to local nodal displacements, it is necessary to develop a scheme for placing the element entries in the proper position in the global matrices. To this end, we define the connectivity array $C = [c_{jk}]$, where j identifies the element number and k represents the global node numbers listed in the order specified by the local nodes. And C is simply:

$$C = \begin{bmatrix} 1 & 4 & 5 \\ 1 & 5 & 2 \\ 2 & 5 & 6 \\ 2 & 6 & 3 \end{bmatrix} \tag{2.2.27}$$

As an illustration of the use of the connectivity, an example of a 6 X 6 global stiffness matrix for the system of Figure 2.2.6. The first row in C represents the first element and it instructs us to place the entries $k_{11}^{(1)}$, $k_{12}^{(1)}$, $k_{13}^{(1)}$, $k_{22}^{(1)}$, $k_{23}^{(1)}$ and $k_{33}^{(1)}$ of the element stiffness matrix $K^{(1)}$ in the positions (1, 1), (1, 4), (1, 5), (4, 4), (4, 5) and (5, 5) of the global stiffness matrix K. Repeating the process for the remaining three rows of C, global stiffness matrix is obtained:

$$k = \begin{bmatrix} k_{11}^{(1)} + k_{11}^{(2)} & k_{13}^{(2)} & 0 & k_{12}^{(1)} & k_{13}^{(1)} + k_{12}^{(2)} & 0 \\ & k_{33}^{(2)} + k_{11}^{(3)} + k_{11}^{(4)} & k_{13}^{(4)} & 0 & k_{23}^{(2)} + k_{12}^{(3)} & k_{13}^{(3)} + k_{12}^{(4)} \\ & & k_{33}^{(4)} & 0 & 0 & k_{23}^{(4)} \\ & & & k_{22}^{(1)} & k_{23}^{(1)} & 0 \\ & \textit{Symmetric} & & & k_{33}^{(1)} + k_{22}^{(2)} + k_{22}^{(3)} & k_{23}^{(3)} \\ & & & & & k_{33}^{(3)} + k_{22}^{(4)} \end{bmatrix}$$

$$= \begin{bmatrix} 2 & -1 & 0 & -1 & 0 & 0 \\ & 4 & -1 & 0 & -2 & 0 \\ & & 2 & 0 & 0 & -1 \\ & & & 2 & -1 & 0 \\ & \textit{symmetric} & & & 4 & -1 \\ & & & & & 2 \end{bmatrix} \tag{2.1.28}$$

and the same process applies to the construction of the global mass matrix.

The generation of the finite element mesh amounts to dividing the domain D into triangular domains D_j in such a way that no vertex of one triangle lies on the edge of another triangle. It is common practice to begin with a coarse mesh and refine the mesh so as to improve the accuracy of the eigen-solutions.

2.2.4. Position determined for attaching the vibration absorbers

In order to suppress the resonant vibration of a structure by attaching a translational type dynamic vibration absorbers, the absorber may be attached to somewhere with high translational amplitude such that there is high energy transmission from the structure to the absorber. Hence, an area with high vibration amplitude would be good for attaching the translational type vibration absorbers.

To use a rotational vibration absorber for suppression of a resonant vibration, the absorber may be added to somewhere with a high rotation amplitude. In most of the cases, the nodal points or lines of a structure have vibrations with no translational movement but large amounts of rotational motion. A rotational type vibration absorber may be attached to a nodal point to provide significant vibration suppression when the system is under resonance.

In a forced harmonic vibration not at a resonance, the participation of each mode to the forced vibration can be determined by the normal mode theory as discussed in Chapter 2.2.1.

Figure 2.2.9 shows the frequency spectrum of a continuous system, according to equation 2.2.14, vector of generalized force associated with the generalized coordinates $q(t)$ can be

expressed as a linear combination of normal mode by means of the expression theorem:

$$q_i(t) = q_i(0)\cos\omega_i t + \left(\frac{\dot{q}(0)}{\omega_i}\right)\sin\omega_i t + \frac{1}{\omega}\int Q(\tau)\sin\omega_i(t-\tau)d\tau$$

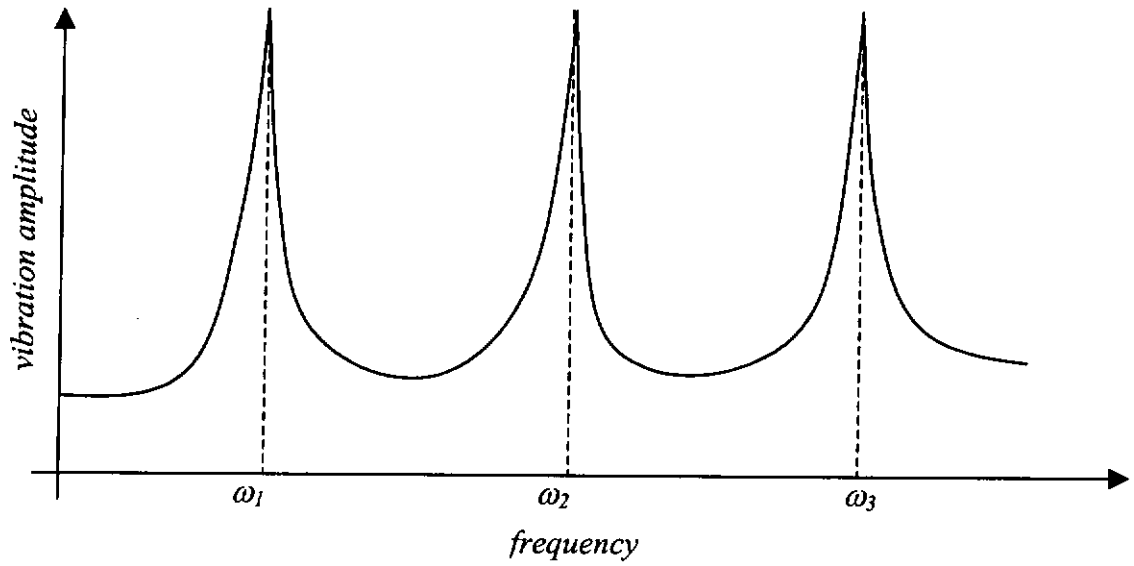

Figure 2.2.7 A typical frequency spectrum of a lightly damped continuous system.

Hence, the frequency spectrum of a continuous system shown in figure 2.2.7 can be expressed as the separated modal contribution of modes of a continuous system as shown in Figure 2.2.8.

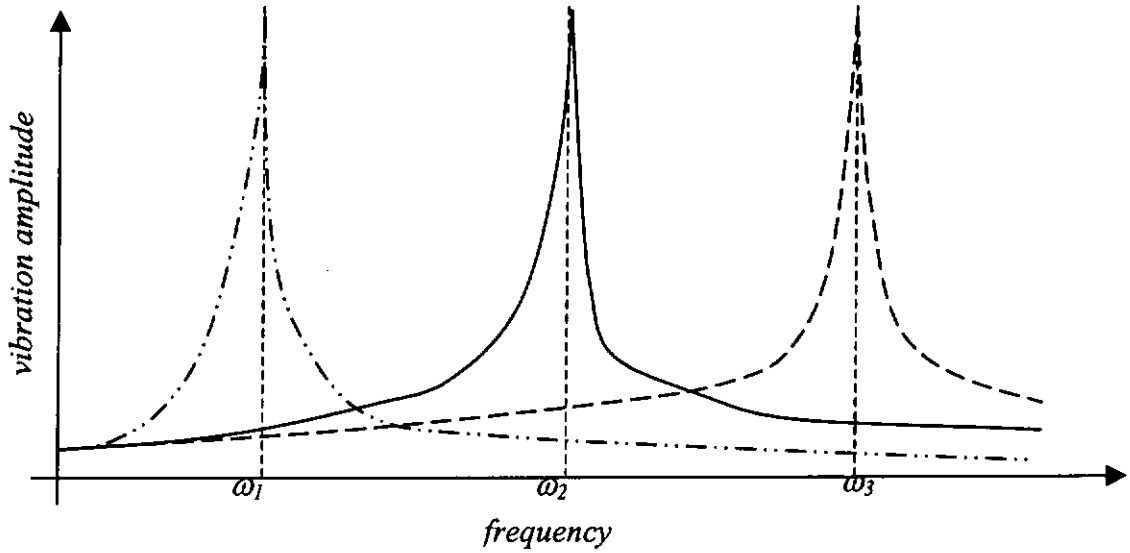

Figure 2.2.8 Illustration of the individual modal contribution of a continuous system.

In harmonic excitation, a rotational absorber may be added to an intersection of the nodal lines of the modes that have high contribution to the vibration. For example, if a force with a driving frequency which is higher than the second mode of a system but lower than the third mode of that system. Modal frequencies and shapes may be determined in order to know which modal response is the most significant. The absorber can then be attached onto the corresponding nodal position for maximum absorption of the energy and the rotational vibration absorber there may be attached at a nodal point of the corresponding mode. It is useful to find the location of these intersections because the position may be good for attaching the absorber for suppressing any vibration of frequency that lies between the second and the third modes of the system. This is important if the excitation frequency is not of one single frequency, but may fluctuate within a narrow frequency band.

3. Computer simulations and experimental results

3.1. Computer simulations

3.1.1. Comparison of different types of DVA in absorbing rigid body motions

A numerical solution for a rigid beam mounted on springs was simulated by means of a self-written Matlab program.

The effects of using a translational type and a rotational type DVAs were studied. The natural frequencies of the system were found by calculating the roots of the determinants of the matrices in equation (2.1.6), (2.1.10), and (2.1.15) as shown in Chapter 2.1. They are:

The equation of motion of a rigid body:

$$\begin{bmatrix} k_1+k_2-m\omega^2 & k_2l_2-k_1l_1 \\ k_2l_2-k_1l_1 & k_1l_1^{\,2}+k_2l_2^{\,2}-I\omega^2 \end{bmatrix}\begin{bmatrix} x \\ \theta \end{bmatrix}=0 \qquad (2.1.6)$$

The equation of motion of a rigid body with a translational type DVA:

$$\begin{bmatrix} k_1+k_2+k_t-m\omega^2 & k_2l_2-k_1l_1 & -k_t \\ k_2l_2-k_1l_1 & k_1l_1^{\,2}+k_2l_2^{\,2}-I\omega^2 & 0 \\ -k_t & 0 & k_t-m_t\omega^2 \end{bmatrix}\begin{bmatrix} x_1 \\ \theta \\ x_2 \end{bmatrix}=\begin{bmatrix} F \\ y_aF \\ 0 \end{bmatrix}\sin\omega t \qquad (2.1.10)$$

and the equation of motion of a rigid body with a rotational type DVA:

$$\begin{bmatrix} k_1+k_2-m\omega^2 & k_2l_2-k_1l_1 & 0 \\ k_2l_2-k_1l_1 & k_1l_1^{\,2}+k_2l_2^{\,2}+k_r-I\omega^2 & -k_r \\ 0 & -k_r & k_r-I_r\omega^2 \end{bmatrix}\begin{bmatrix} x_1 \\ \theta \\ \phi \end{bmatrix}=\begin{bmatrix} F \\ y_aF \\ 0 \end{bmatrix}\sin\omega t \qquad (2.1.15)$$

From the determinants of the coefficient matrices of the equations above, the vibration amplitude of displacement and rotation of the rigid beam, with and without a translational

or rotational absorber were found and they are plotted in Figure 3.1.1a and 3.1.1b respectively.

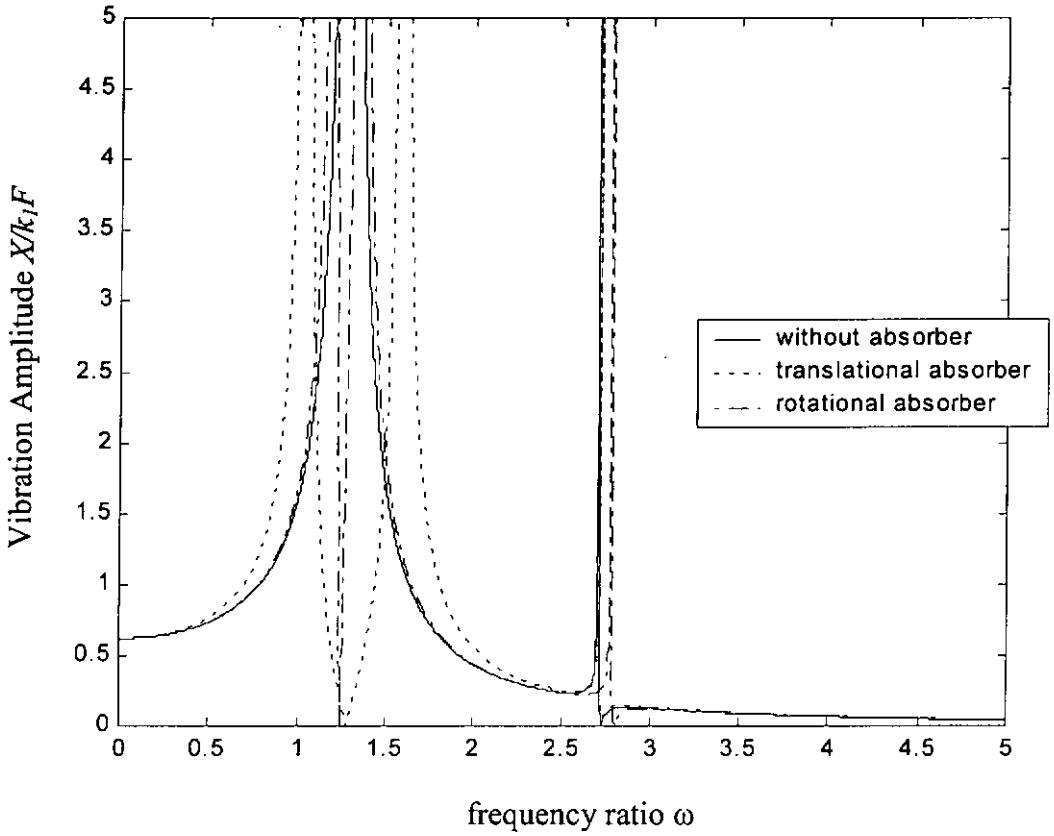

Figure 3.1.1a. Frequency response of a beam model with translational and rotational absorbers tuned at the lower natural frequency of the rigid beam model. (`z=1/12; l=0.7; k=1; ya=0.1; mr=0.2`)

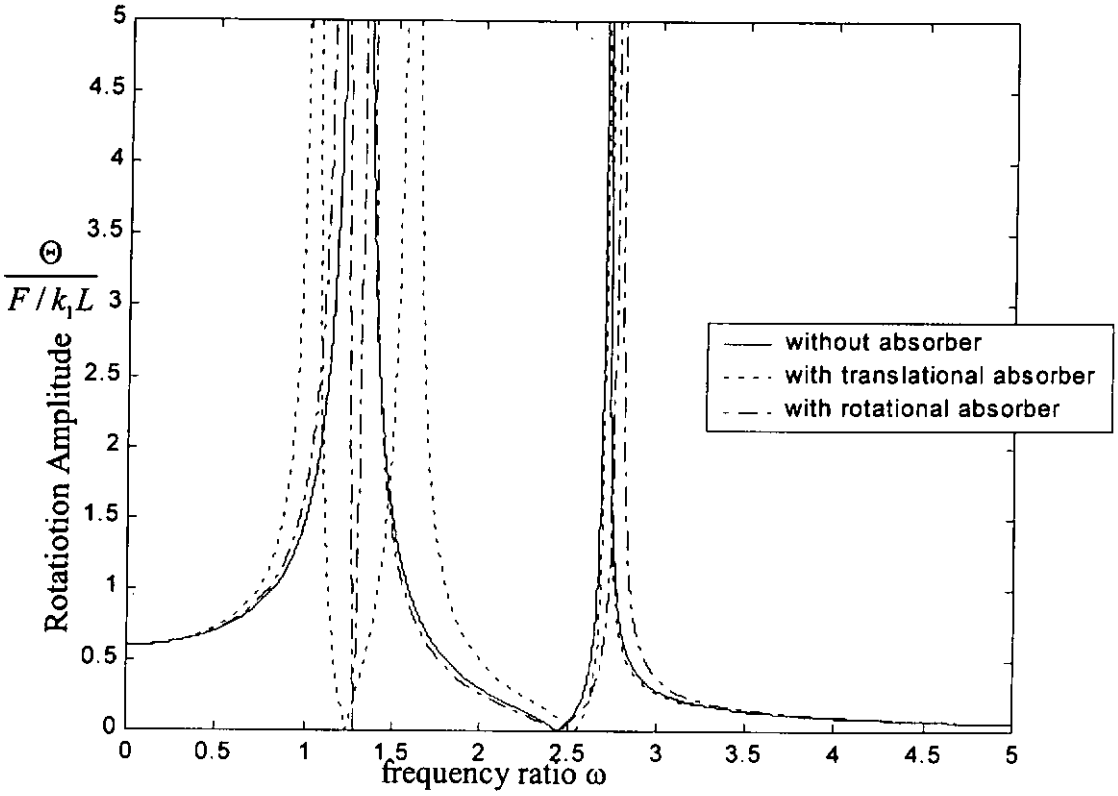

Figure 3.1.1b. Frequency response of a beam modal with translational and rotational absorbers tuned at the lower natural frequency of the rigid beam model (`z=1/12; l=0.7; k=1; ya=0.1; mr=0.2`)

From the results, it was found that when the system was forced to vibrate at a lower frequency around the first natural frequency as shown in Figure 2.1.5, the translational vibration absorber is more effective in shifting away the original natural frequency from the excitation frequency than using the rotational one.

The plots are the results of a simulation where an absorber is attached to a rigid beam. When the absorbing frequency of the absorber is tuned at the natural frequency of the first mode of the rigid beam, the natural frequencies of the beam changes. Figure 3.1.1a shows

that both the translational and rotational absorbers have effects in suppressing the vibration. However, the translational absorber tends to shift the new natural frequency further away from the original natural frequency in comparsion to the rotational one. This implies that after the translational absorber is added, the vibration level of a larger frequency band around the tuned frequency were suppressed. So, the "useable" frequency range of the system is wider if a translational absorber is attached to the system.

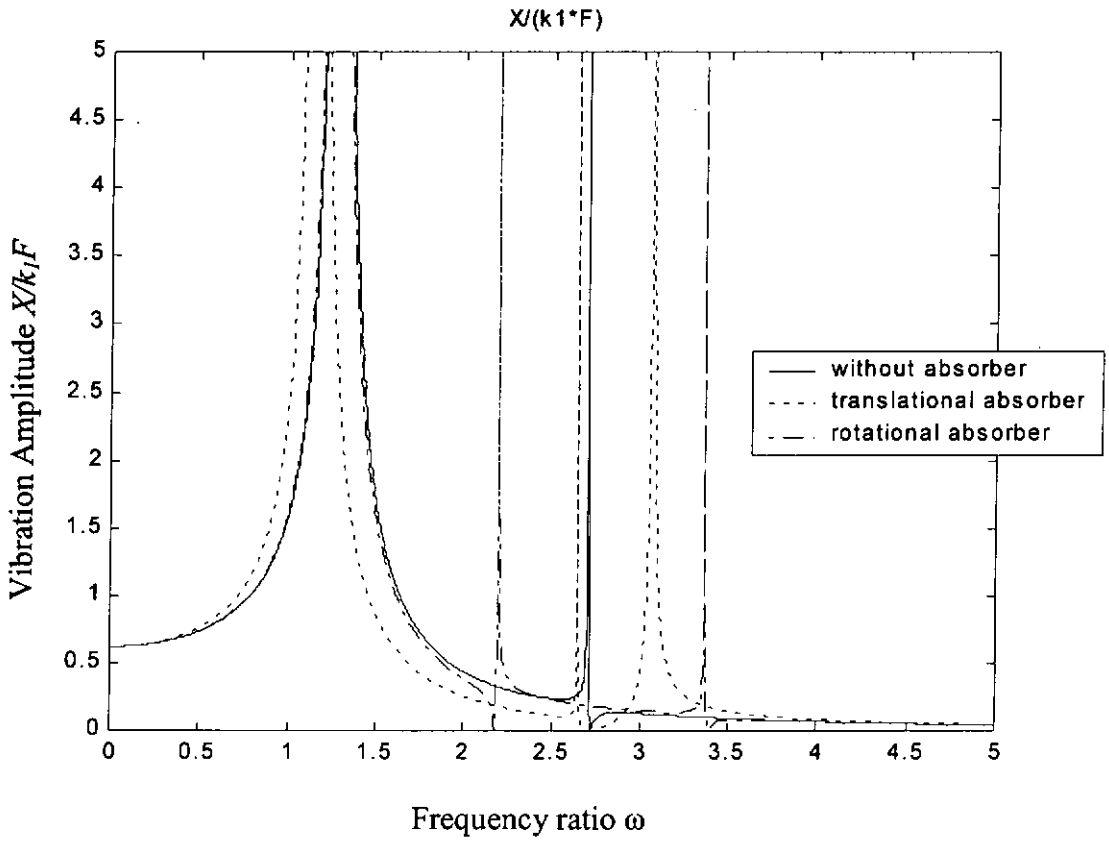

Figure 3.1.2a. Frequency response of a beam model with translational and rotational absorbers tuned at the higher natural frequency of the rigid beam model. (`z=1/12; l=0.7; k=1; ya=0.1; mr=0.2`)

On the other hand, Figure 3.1.2 shows the system with the same configuration as the previous model but tuned to the higher natural frequency of the rigid beam model (rotation dominant as shown in Figure 2.1.4).

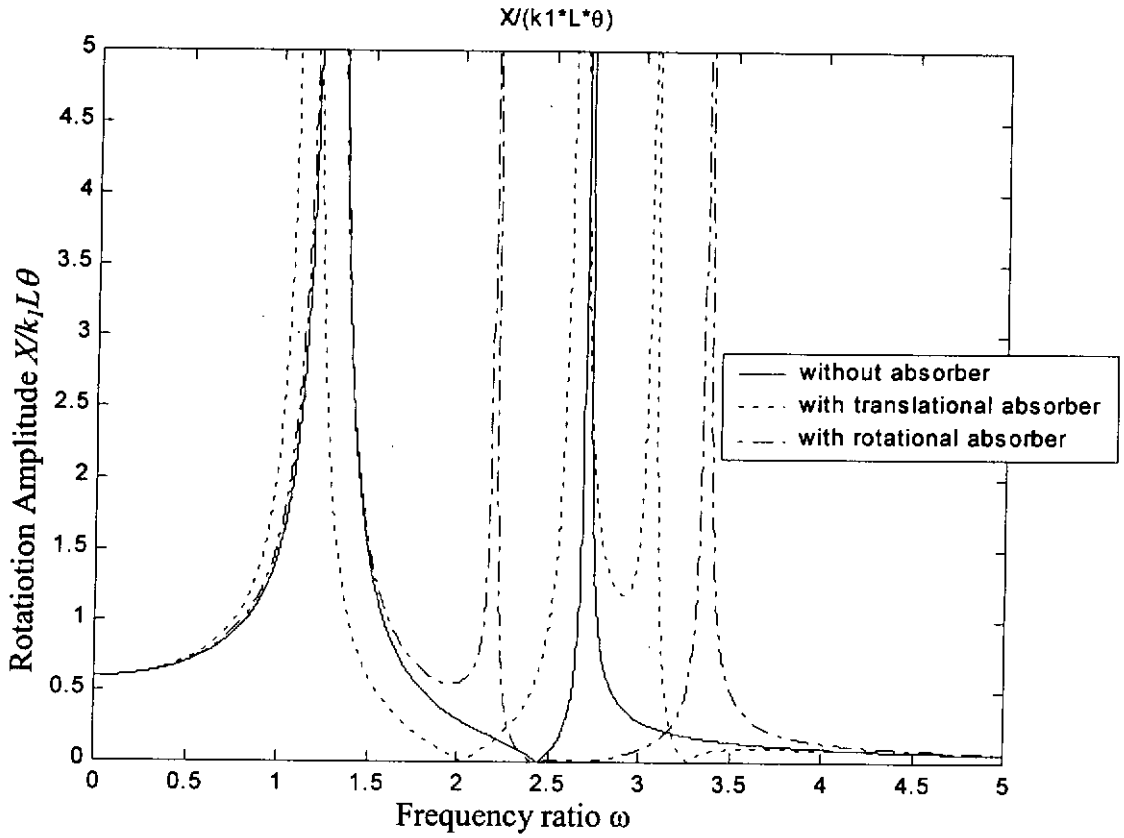

Figure 3.1.2b. Frequency response of a beam model with translational and rotational absorbers tuned at the higher natural frequency of the rigid beam model. (`z=1/12; l=0.7; k=1; ya=0.1; mr=0.2`)

Figures 3.1.2a and 3.1.2b show a very different result in comparison with the results as shown in Figure 3.1.1a and 3.1.2 b, which show that the system vibrates at the lower natural frequency. This time, the rotational absorber rather than the translational absorber, shifts the new natural frequency further away from the original natural frequency. This means that when using the rotational absorber in suppressing the vibration amplitude of the second natural frequency of the system, the "useable" frequency band of the system is wider than the case of applying the translational absorber.

In addition, it is found that the range of suppressed frequencies was wider when using the rotational absorber to suppress the rotational dominant mode (second mode) than using the translational absorber to suppress the translational dominant mode (first mode).

Figures 3.1.3 to 3.1.6 show the effective range of vibration suppression by using the translational and rotational absorbers with different mass ratios and stiffness ratios combinations. ω_{t1}, ω_{t2} and ω_{t3} are the natural frequencies of the system after adding the translational absorber (where $\omega_{t1} > \omega_{t2} > \omega_{t3}$). Similarly, ω_{r1}, ω_{r2} and ω_{r3} are the natural frequencies of the system attached to the rotational absorber (where $\omega_{r1} > \omega_{tr2} > \omega_{r3}$).

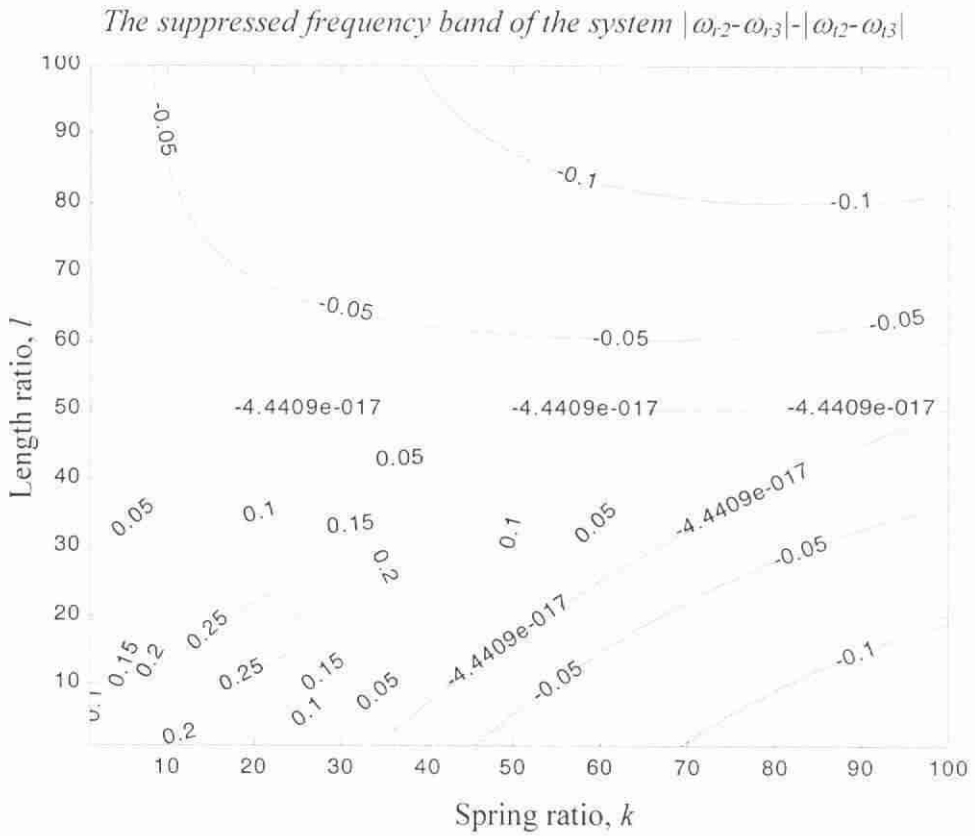

Figure 3.1.3a. The suppressed frequency range comparison for absorbers tuned at lower natural frequency of the system. (`z=1/4; mr=0.2`)

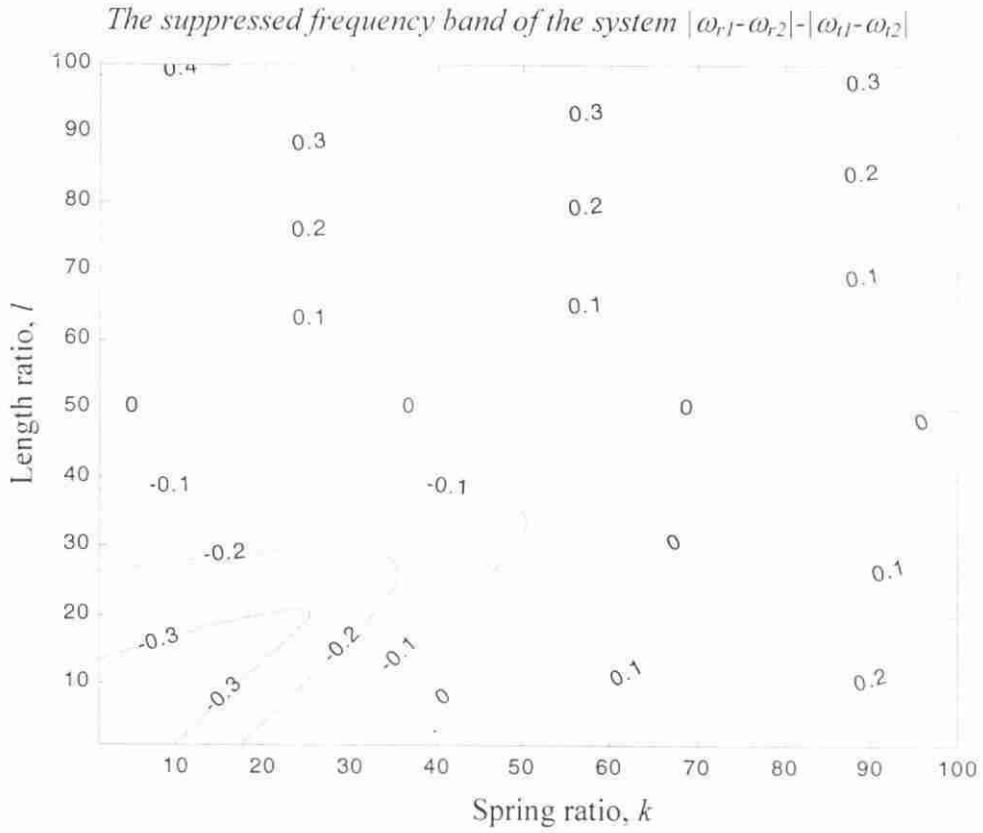

Figure 3.1.3b. The suppressed frequency range comparison for absorbers tuned at higher natural frequency of the system. (`z=1/4; mr=0.2`)

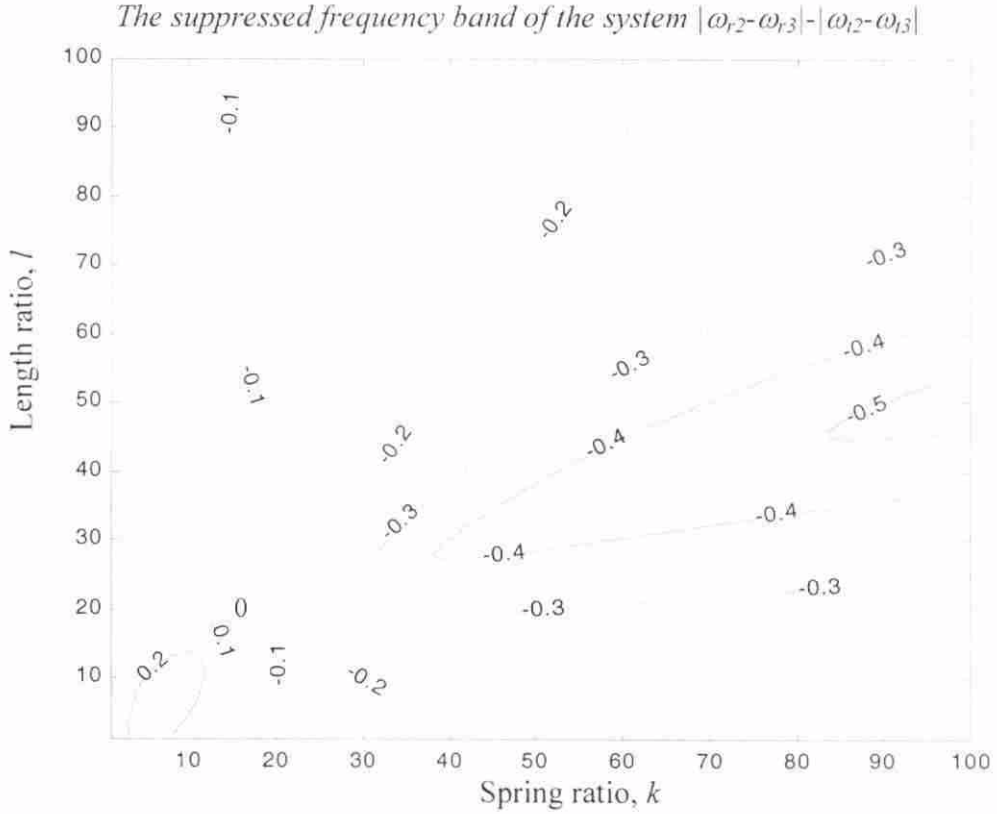

Figure 3.1.4a. The suppressed frequency range comparison for absorbers tuned at lower natural frequency of the system. (z=1/8; mr=0.2)

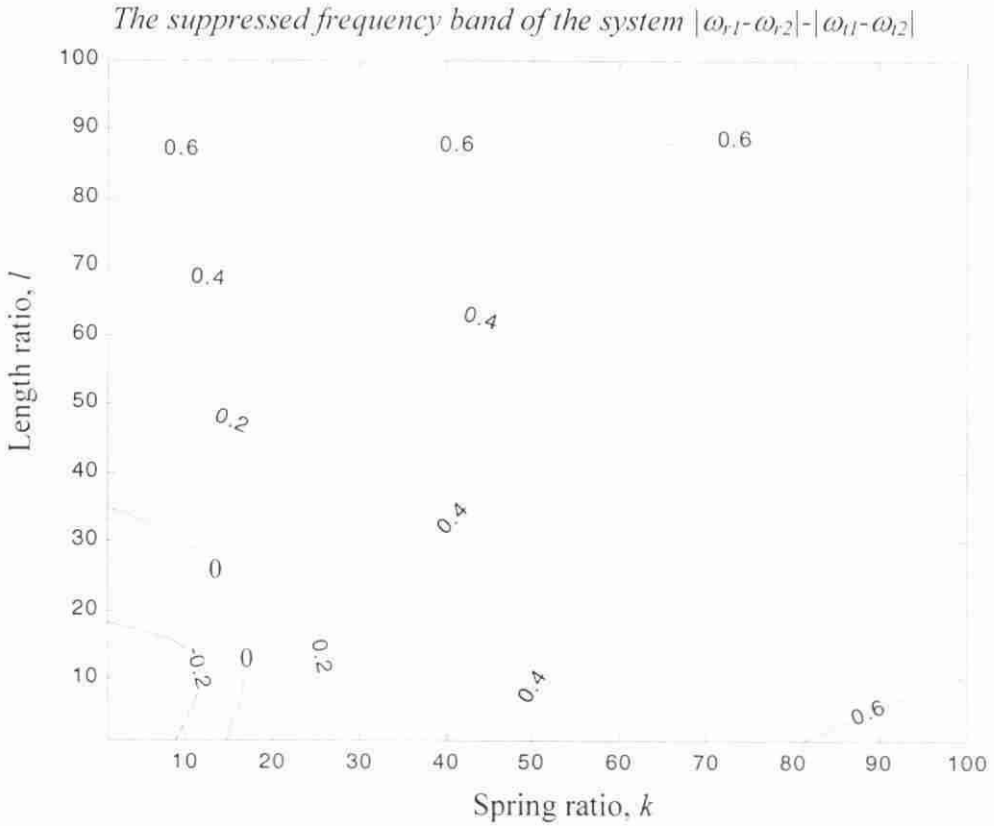

Figure 3.1.4b. The suppressed frequency range comparison for absorbers tuned at higher natural frequency of the system. (z=1/8; mr=0.2)

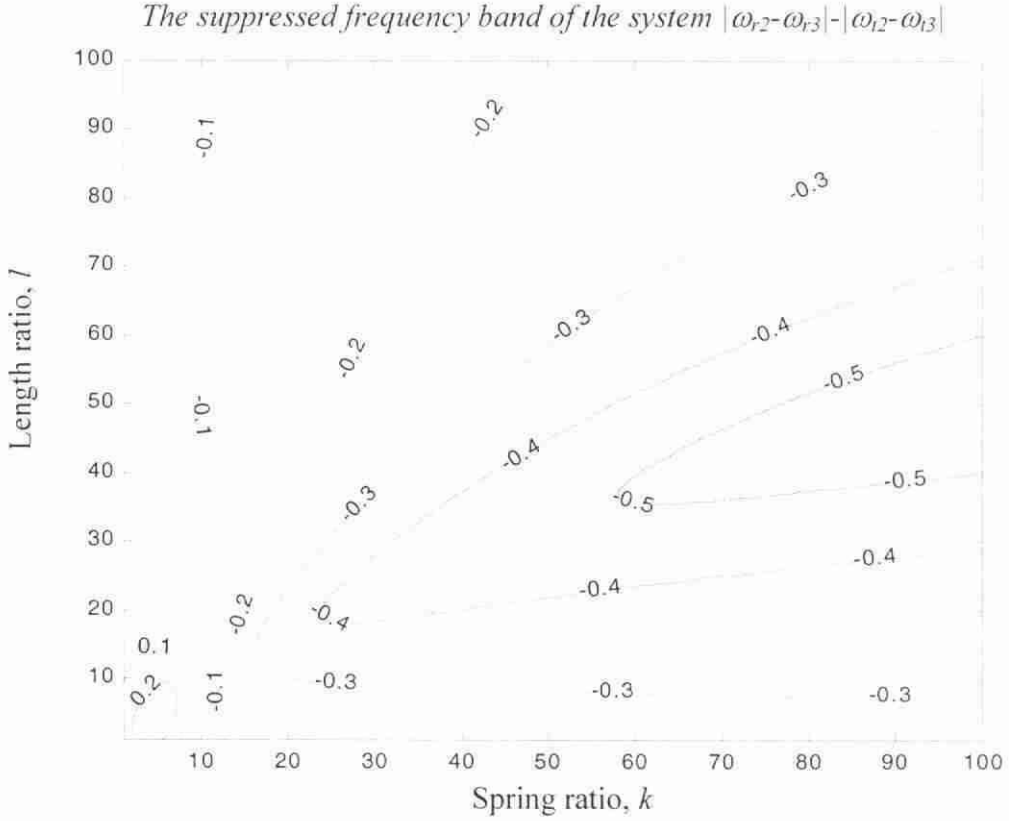

Figure 3.1.5a. The suppressed frequency range comparison for absorbers tuned at lower natural frequency of the system. (`z=1/12; mr=0.2`)

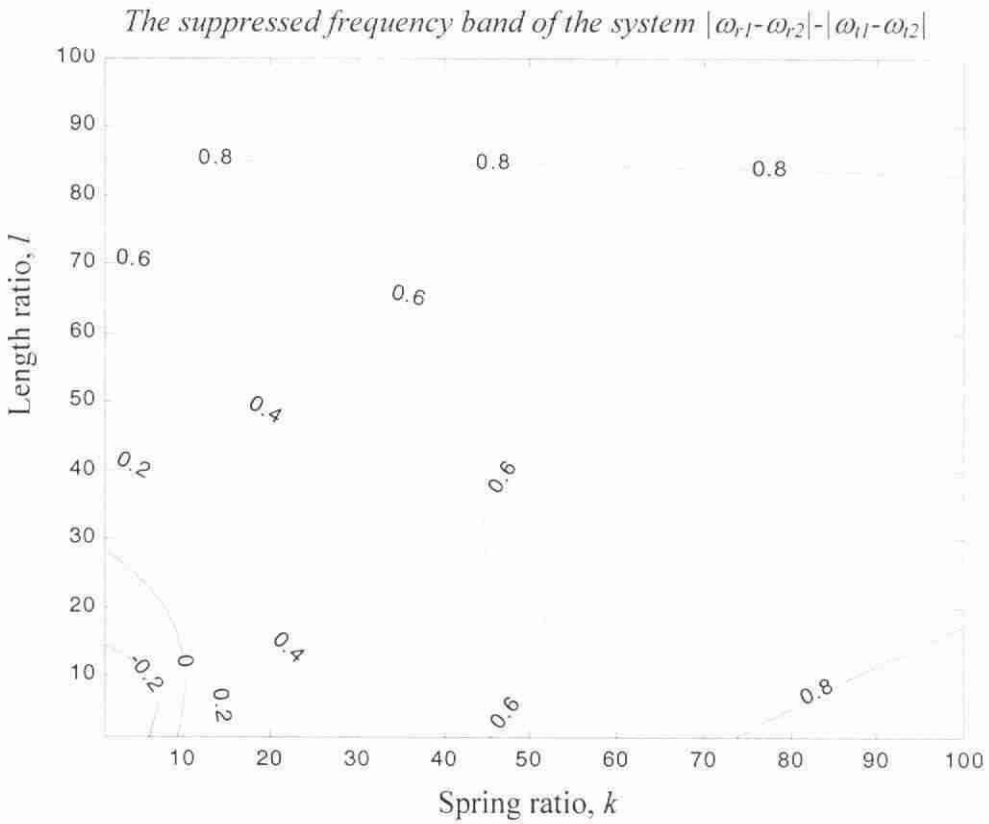

Figure 3.1.5b. The suppressed frequency range comparison for absorbers tuned at higher natural frequency of the system. (`z=1/12; mr=0.2`)

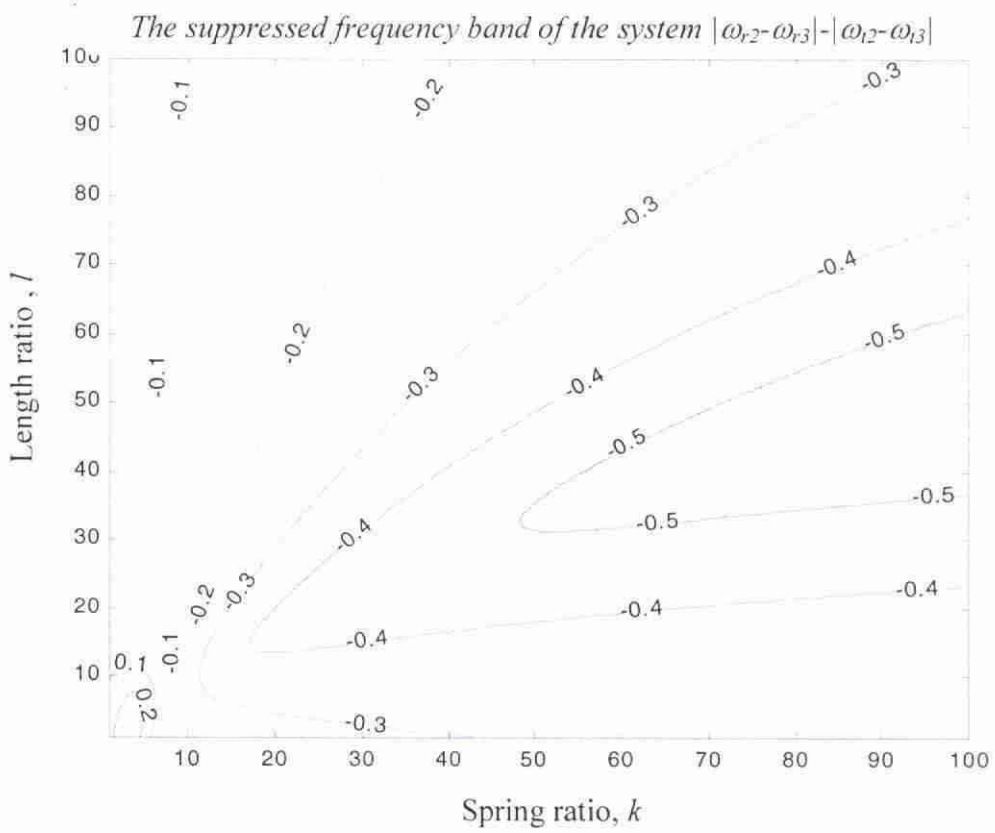

Figure 3.1.6a. The suppressed frequency range comparison for absorbers tuned at lower natural frequency of the system. (z=1/16; mr=0.2)

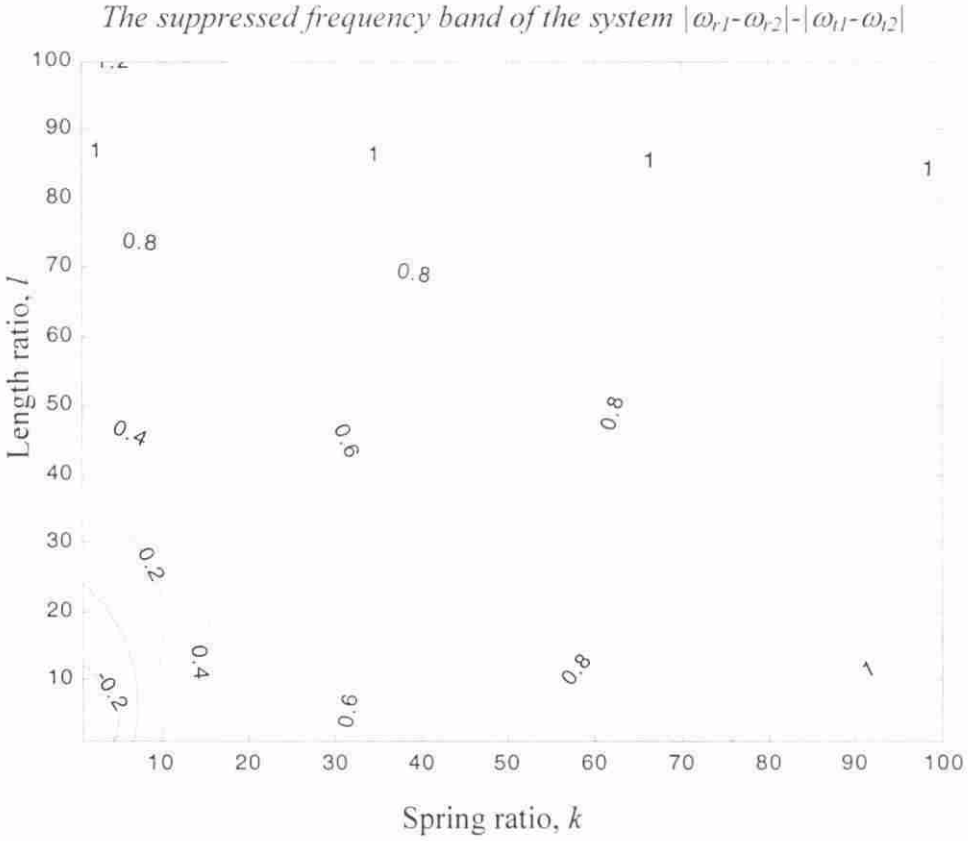

Figure 3.1.6b. The suppressed frequency range comparison for absorbers tuned at higher natural frequency of the system. (`z=1/16; mr=0.2`)

According to the results, it was observed that the translational absorber is more effective in suppressing the low frequency vibrations (on the other hand, a rotational absorber is better in shifting away the second natural frequency and hence suppressing higher frequency vibrations), it is found that the effect of the absorber was affected by the $\tilde{z}$ value, which is the inertia ratio $\frac{I}{mL^2}$.

When trying to suppress low frequency vibration (i.e. absorber tuned at the lower mode natural frequency), the negative region increased if the value of $\tilde{z}$ is smaller. This means that the effect of vibration suppression is better if the value of $\tilde{z}$ is smaller.

In the case of suppressing higher frequency vibration, the rotational absorber would have a better performance if the value of $\tilde{z}$ is smaller.

With the aid of the derived equations, the effect of attaching both rotational and translational absorbers to the rigid beam at the same point was investigated. It was found that it would be possible to make the beam transmit all the kinetic energy to the absorbers, i.e. the beam would not move. This impressive result motivated the study of the response of a continuous system such as a flexural beam or plate when both the rotational and translational vibration absorbers were utilized.

3.1.2. Simulation of vibration suppression of beams using dynamic absorbers

Some initial tests on the sensitivity to location when adding a translational absorber were carried out by using a self-written Matlab Program. The simulation model was a fixed-fixed beam (as shown in Figure 3.1.9). It showed how the mode shape of the system and the location where the dynamic absorbers was attached affected the effectiveness in suppression of vibration. Also, the simulation showed that the force transmissibility was high when the absorber was attached at the anti-node of the object (the transmissibility when the absorber attached at an anti-node was at least three times higher than at other positions on the beam).

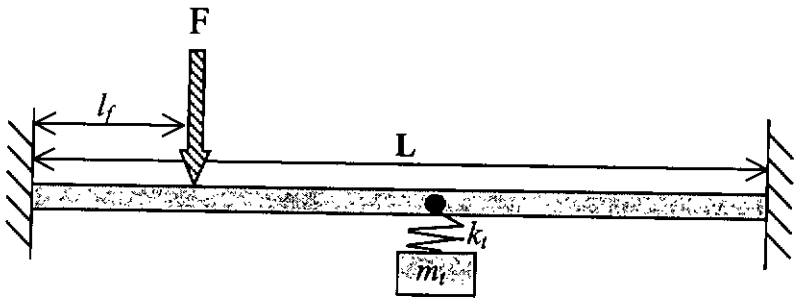

Figure 3.1.9a Model of fixed-fixed beam with a translational absorber.

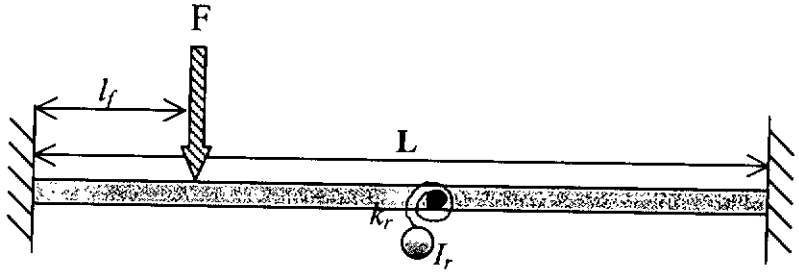

Figure 3.1.9b Model of fixed-fixed beam with rotational absorber

In the simulation, the vibration absorbers were attached at the center of the beam with a harmonic force applying to the beam at l_f as shown in Figure 3.1.9a and Figure 3.1.9b. The parameters of the simulation were shown in the Table 5.1.1 in the Appendix I.

Excitations at resonant or non-resonant frequency were tried in the simulations and the results are shown in figures 3.1.10 to 3.1.17.

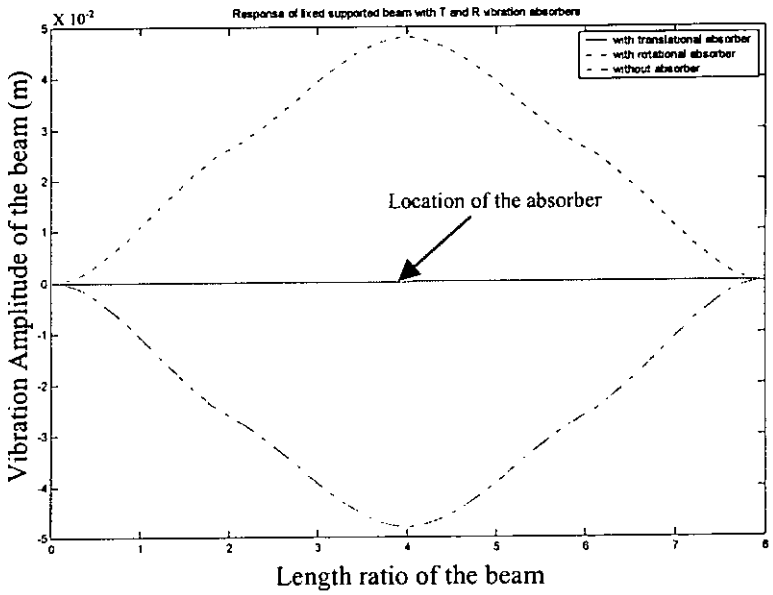

Figure 3.1.10 Frequency response of the beam at forcing frequency at 37.9rad/s. (natural frequencies of the beam are 37.9rad/s, 105.2rad/s, 208.7rad/s, 394.8rad/s, 652.9rad/s and 1052rad/s)

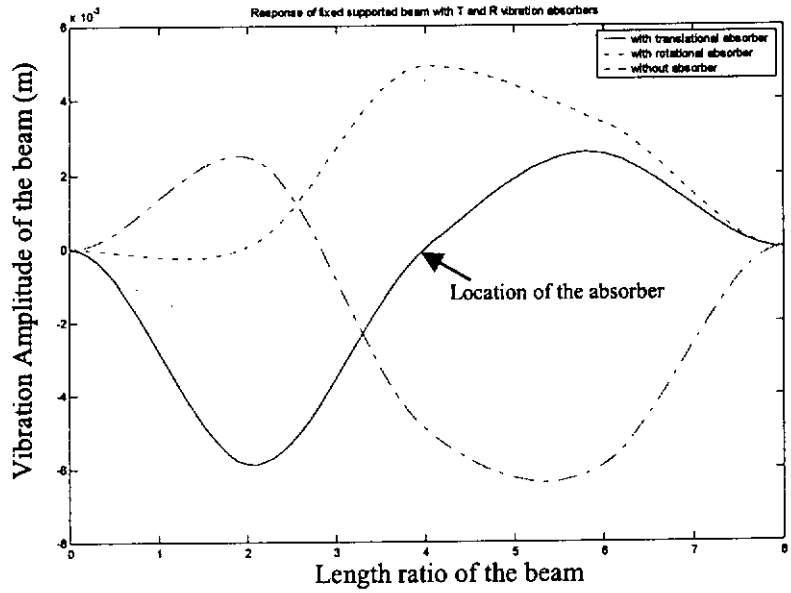

Figure 3.1.11 Frequency response of the beam at forcing frequency at 71.5rad/s. (natural frequencies of the beam are 37.9rad/s, 105.2rad/s, 208.7rad/s, 394.8rad/s, 652.9rad/s and 1052rad/s)

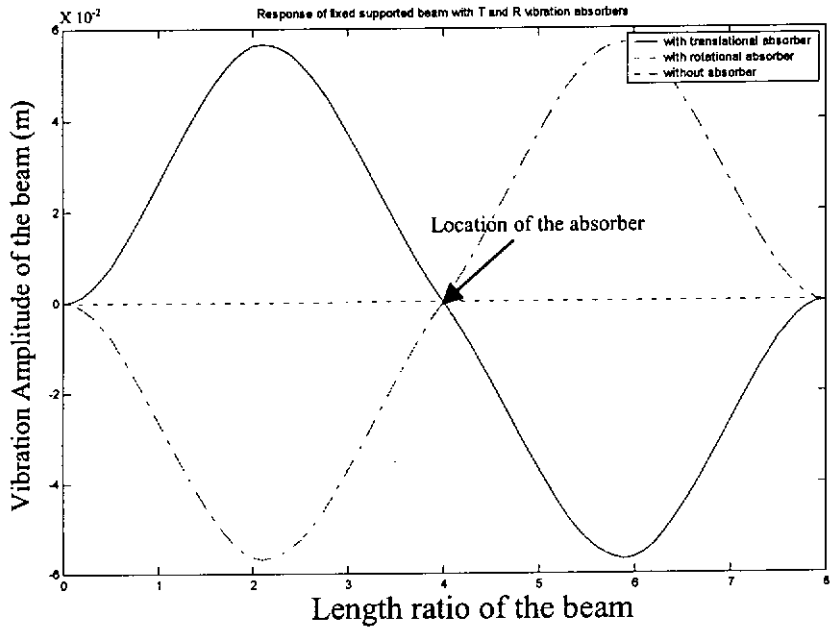

Figure 3.1.12 Frequency response of the beam at forcing frequency at 105.2rad/s. (natural frequencies of the beam are 37.9rad/s, 105.2rad/s, 208.7rad/s, 394.8rad/s, 652.9rad/s and 1052rad/s)

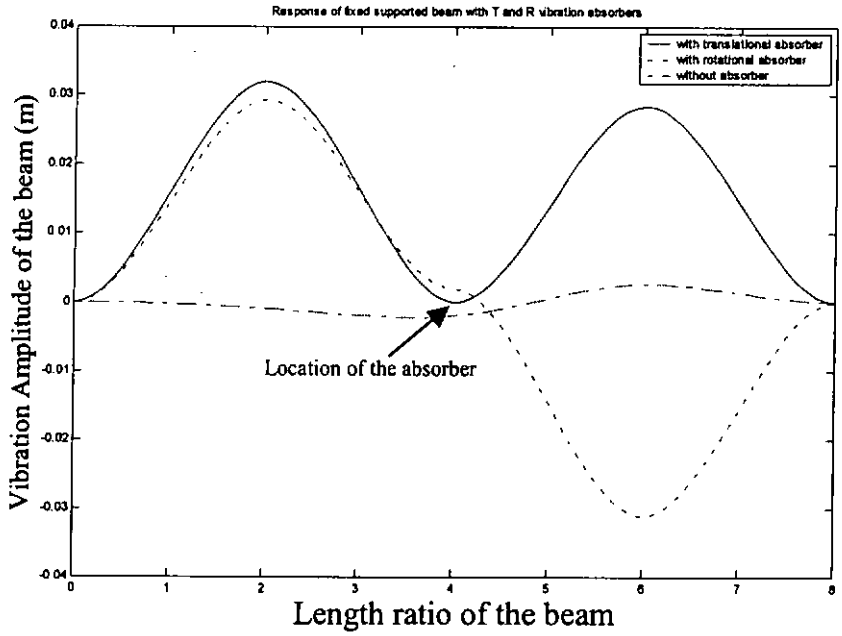

Figure 3.1.13 Frequency response of the beam at forcing frequency at 156.95rad/s. (natural frequencies of the beam are 37.9rad/s, 105.2rad/s, 208.7rad/s, 394.8rad/s, 652.9rad/s and 1052rad/s)

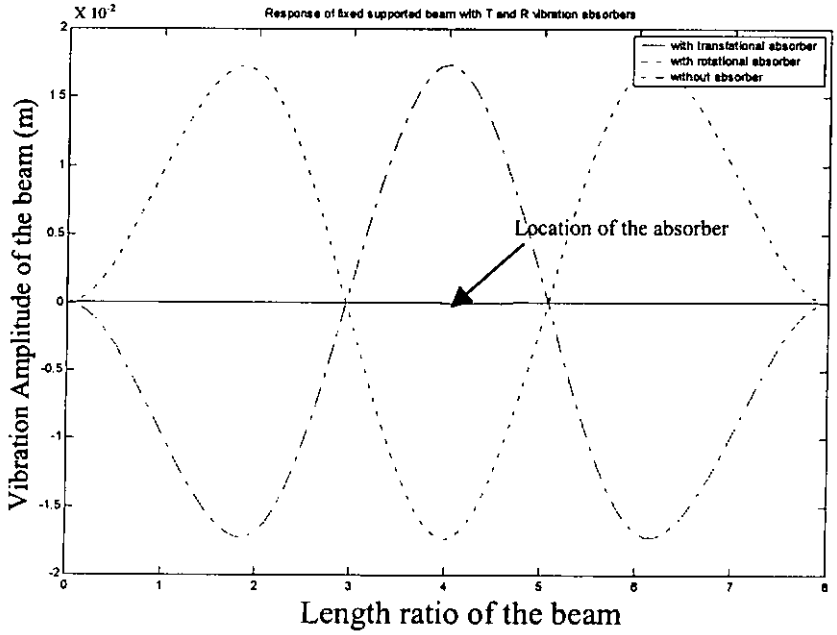

Figure 3.1.14 Frequency response of the beam at forcing frequency at 208.7rad/s. (natural frequencies of the beam are 37.9rad/s, 105.2rad/s, 208.7rad/s, 394.8rad/s, 652.9rad/s and 1052rad/s)

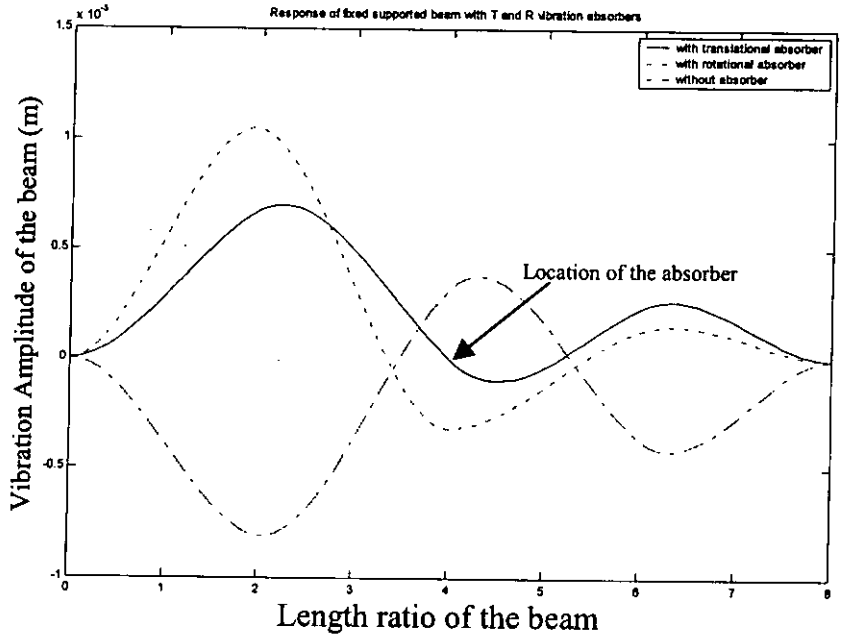

Figure 3.1.15 Frequency response of the beam at forcing frequency at 301.75rad/s. (natural frequencies of the beam are 37.9rad/s, 105.2rad/s, 208.7rad/s, 394.8rad/s, 652.9rad/s and 1052rad/s)

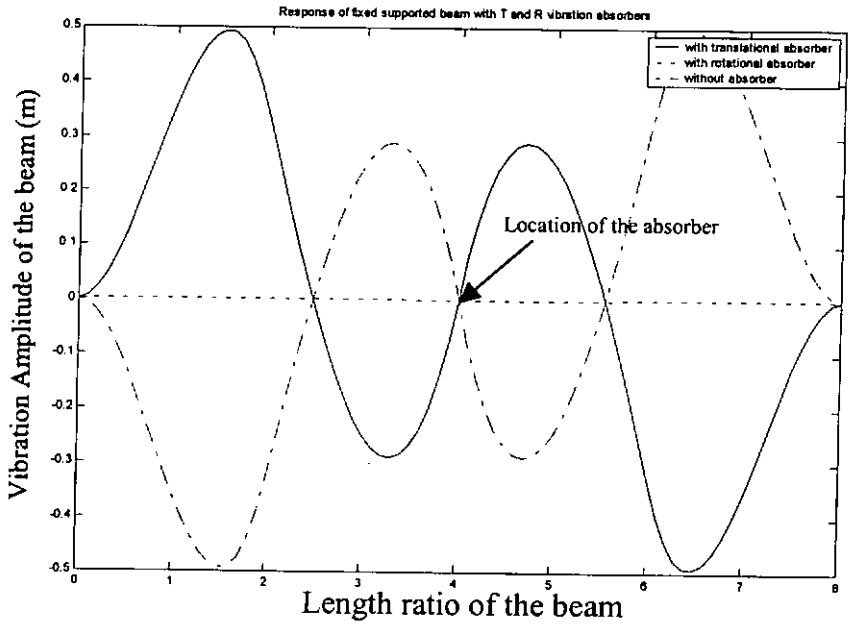

Figure 3.1.16 Frequency response of the beam at forcing frequency at 394.8rad/s. (natural frequencies of the beam are 37.9rad/s, 105.2rad/s, 208.7rad/s, 394.8rad/s, 652.9rad/s and 1052rad/s)

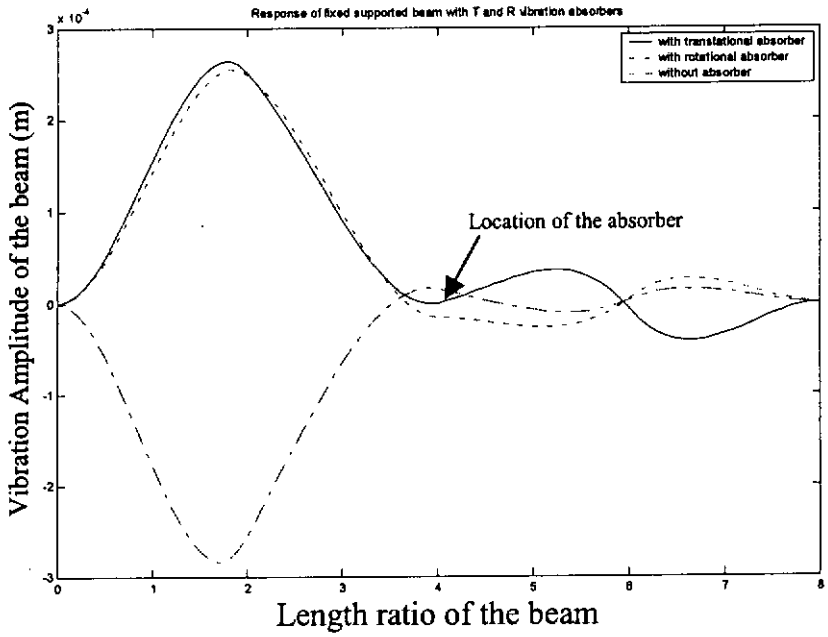

Figure 3.1.17 Frequency response of the beam at forcing frequency at 523.85rad/s. (natural frequencies of the beam are 37.9rad/s, 105.2rad/s, 208.7rad/s, 394.8rad/s, 652.9rad/s and 1052rad/s)

From the results, as expected, the translational absorber has a very good effects on vibration suppression if the absorber was added to somewhere of large vibration amplitude (near the anti-node if resonant) of the beam. Rotational absorber had very good performance in vibration absorption at positions of large rotation of the beam (somewhere near the node if resonant).

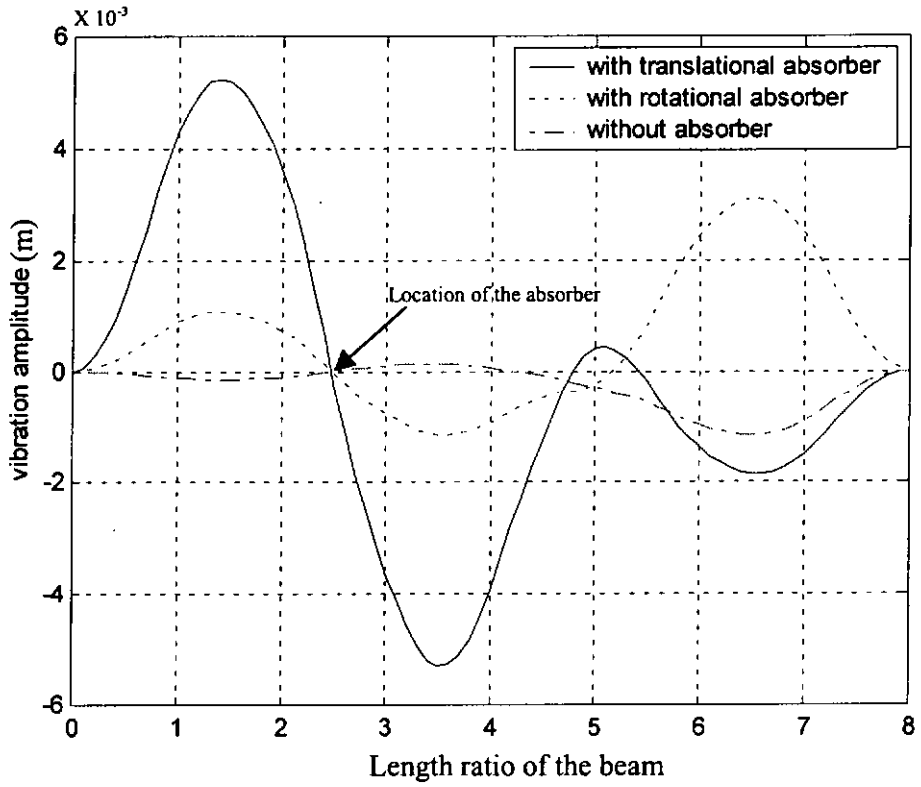

Figure 3.1.18 Frequency response of a fixed-fixed beam attached with the translational and the rotational absorber.

Simulation for the clamped-clamped beam without any vibration absorber, with a translational absorber attached at a point of length ratio 2.5 and with a rotational absorber attached at length ratio 2.5 were made and the results are shown in Figure 3.1.18. The simulation shows that the attachment of translational absorber at an improper location may induce amplification in vibration amplitude. This shows the importance of finding a suitable location for attaching a suitable absorber in vibration suppression.

In concluding the simulations in this section, nodes of a beam would be good locations for attaching the rotational absorber and anti-nodes of the beam would be good locations for attaching the translational absorber. In addition, the result shows that implementing the rotational absorber could obtain a wider frequency range for vibration suppression if the excitation frequency is relatively high.

3.1.3. Simulation of vibration suppression of beam using a combined type of dynamic vibration absorber

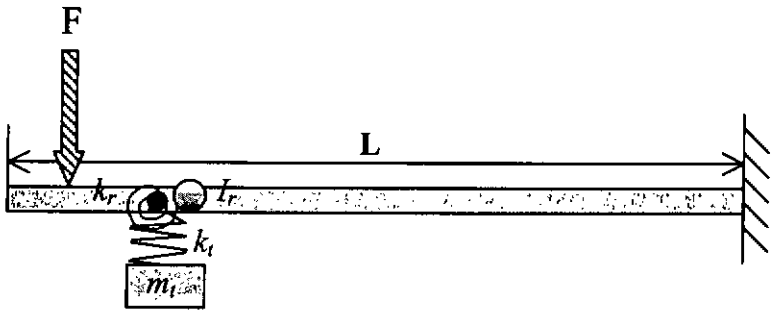

Figure 3.1.19 Model of a beam with both a translational and a rotational DVAs.

In Section 3.1.1, it was found that it is effective to suppress the vibration of a rigid beam if both translational and rotational type vibration absorbers were used. A simulation of the absorbers on a continuous system was done by means of a self-written MATLAB program.

The model of the simulation is shown in Figure 3.1.19, a cantilever beam under a harmonic excitation used. The parameters of the simulation were shown in the Table 5.1.2 in Appendix I.

Comparison between the amplitude of vibration after adding translational absorbers, the combined type absorber and no absorber are shown in the plot below.

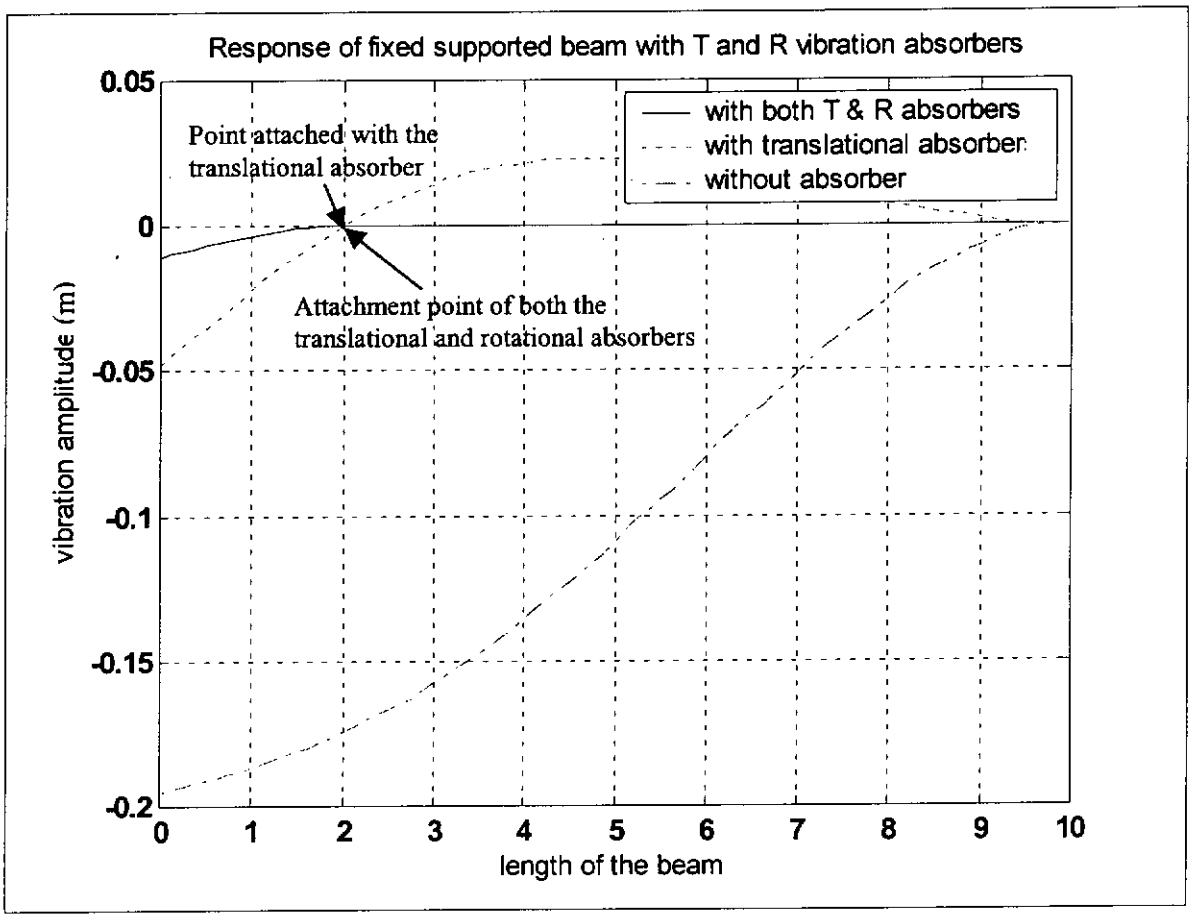

Figure 3.1.20. Comparison of the response of beam with "Rotational and Translational Absorbers" and "Translational Absorbers"

In the simulation, a non-resonant single harmonic excitation was applied. Translational absorbers and a combined type of absorber were tuned at the excitation frequency and added to beam. The response of the beam was simulated and is shown in Figure 3.1.20. The results show that the translational absorber was effective in vibration suppression; the maximum vibration amplitude is only about twenty-five percent of the maximum amplitude of beam without any absorber. Although the translational absorbers have good performance in vibration suppression, the combined type of vibration absorber have a better performance. The result not only shows that there is higher suppression in the maximum vibration level when using the combined type of absorber in comparison to the case of translational absorbers, the result also show that when the combined type of absorber is attached to the system, vibration can be isolated such that the beam section beyond the absorbers has no movement at all.

3.1.4. Simulation of vibration suppression of plate vibration using dynamic vibration absorbers

To investigate the vibration suppression of plates with a dynamic vibration absorber, a simulation was done by means of a finite element program. This shows the effectiveness of the different type of absorbers including the combined type of dynamic absorber on a plate under a non-resonant single harmonic excitation.

In this simulation, an aluminum plate with dimension 50mmX20mmX2mm was modeled. The plate as shown in Figure 3.1.21 was modeled by 4000 square elements which were meshed by the MSC Patran finite element program.

The natural frequencies of the plate was found after the normal mode analysis, the first natural mode of the plate was shown in Figure 3.1.22 which is the first cantilever plate mode with natural frequency equal to 3384Hz. In Figure 3.1.23, it shows the second natural mode of the plate which is a butterfly mode with a nodal line at the center of the plate and it's natural frequency was found as 17091Hz. In Figure 3.1.24, it shows the third natural mode of the plate with a nodal line and the natural frequency of this mode was found as 21063Hz.

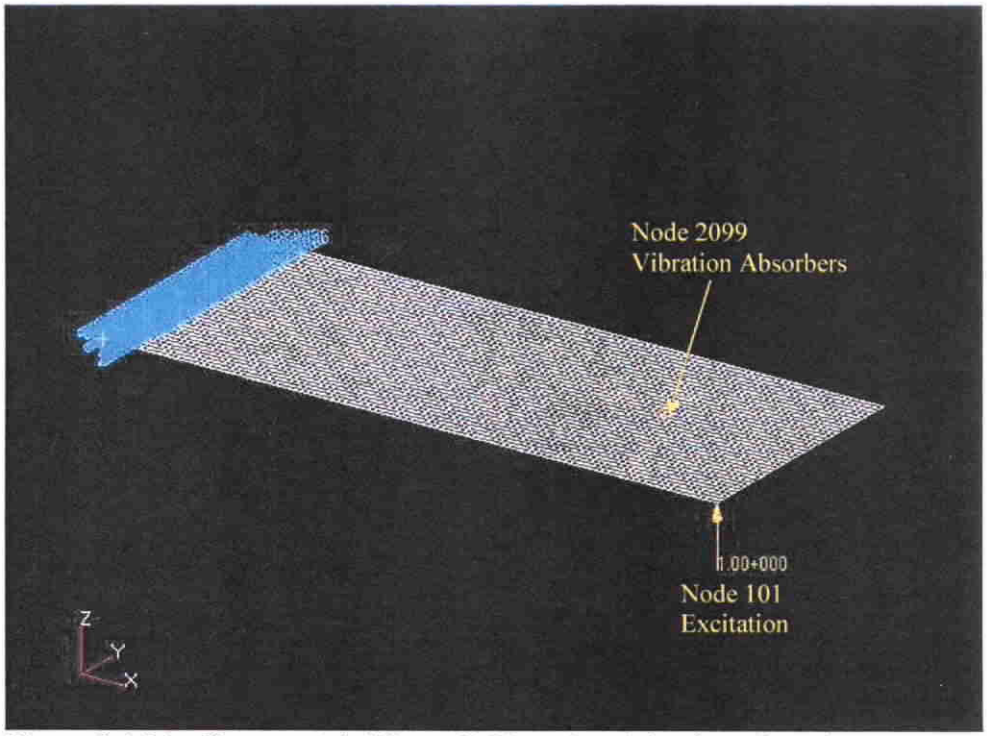

Figure 3.1.21. Plate model (50mm X 20mm) and the force location.

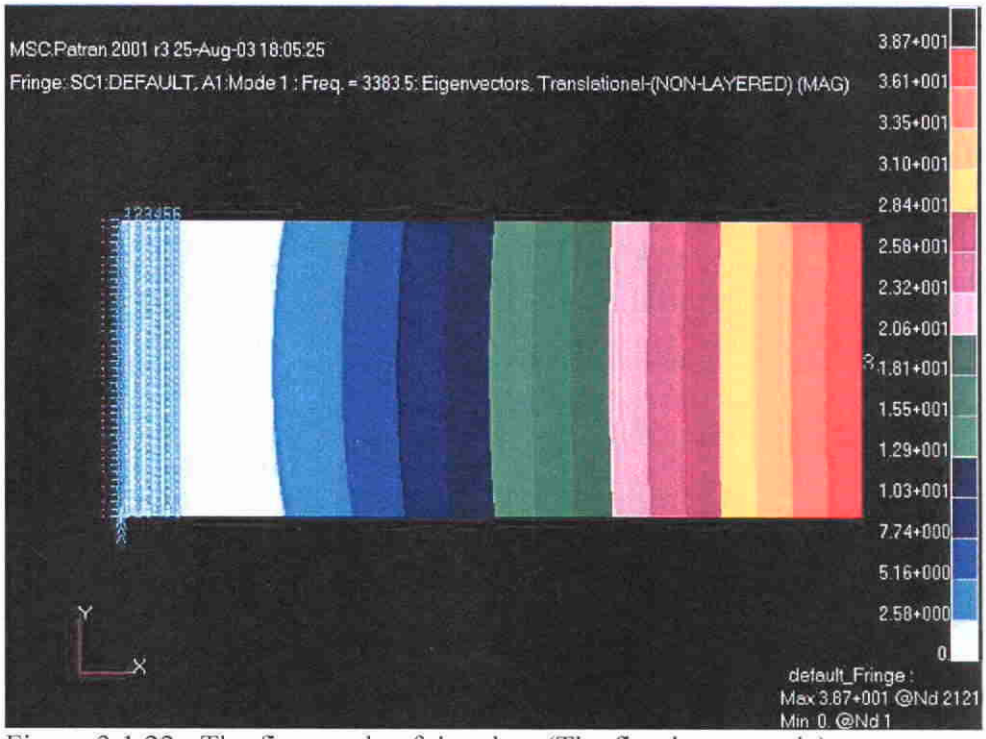

Displacement level of the plate

Figure 3.1.22. The first mode of the plate (The first beam mode)

The effect of vibration absorbers on a plate vibrating at a non-resonant frequency was investigated by exciting the plate with a single harmonic excitation of frequency far away from any of its natural frequencies in this simulation. In the simulation, a frequency between the natural frequencies of the second and the third plate mode was used as the excitation frequency. The dynamic vibration absorbers were attached at the intersection of the nodal lines of the second mode (Figure 3.1.23) and the third mode (Figure 3.1.24) of the plate. Figures 3.1.25, .3.1.26, 3.1.27 and 3.1.28 show the simulated results of the forced vibration of the plate without an absorber, with a translational absorber, with a rotational absorber and with the combined type of absorber respectively where the excitation location and frequencies in every single case are the same (please refer to Figure 3.1.21.)

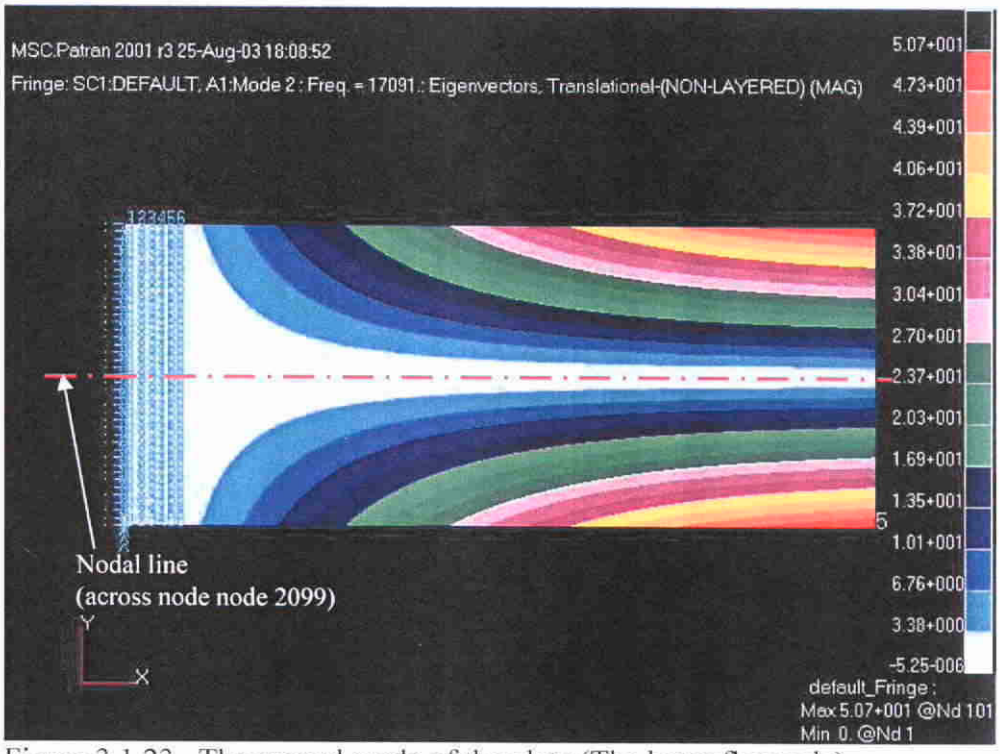

Figure 3.1.23. The second mode of the plate (The butterfly mode)

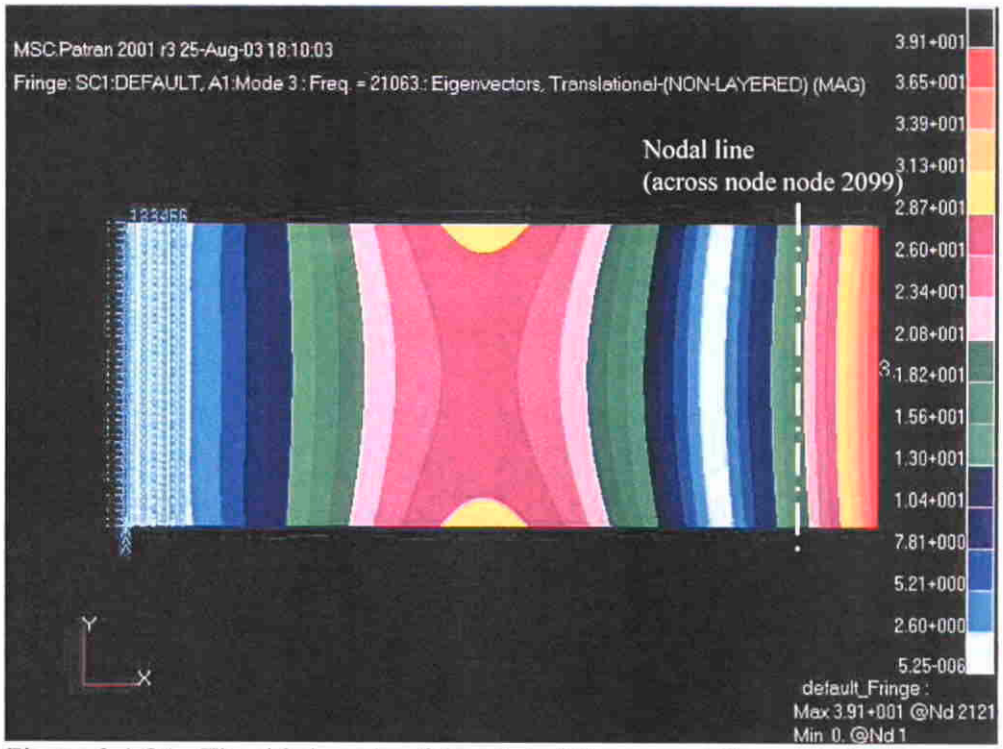

Figure 3.1.24. The third mode of the plate (The second Beam mode)

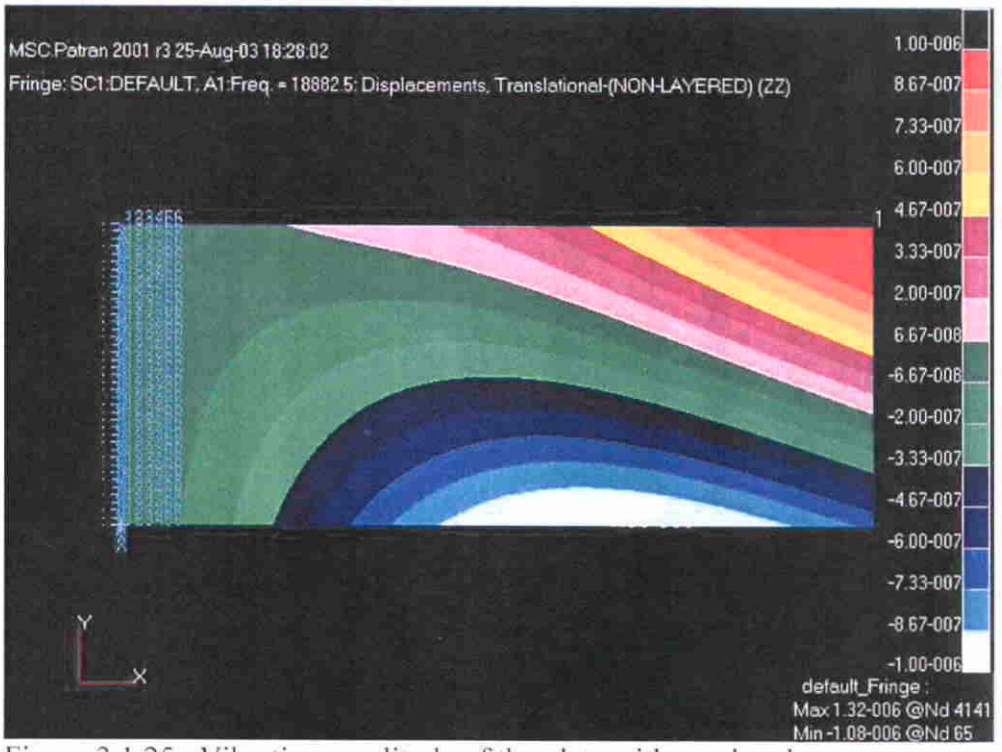

Figure 3.1.25. Vibration amplitude of the plate without absorber

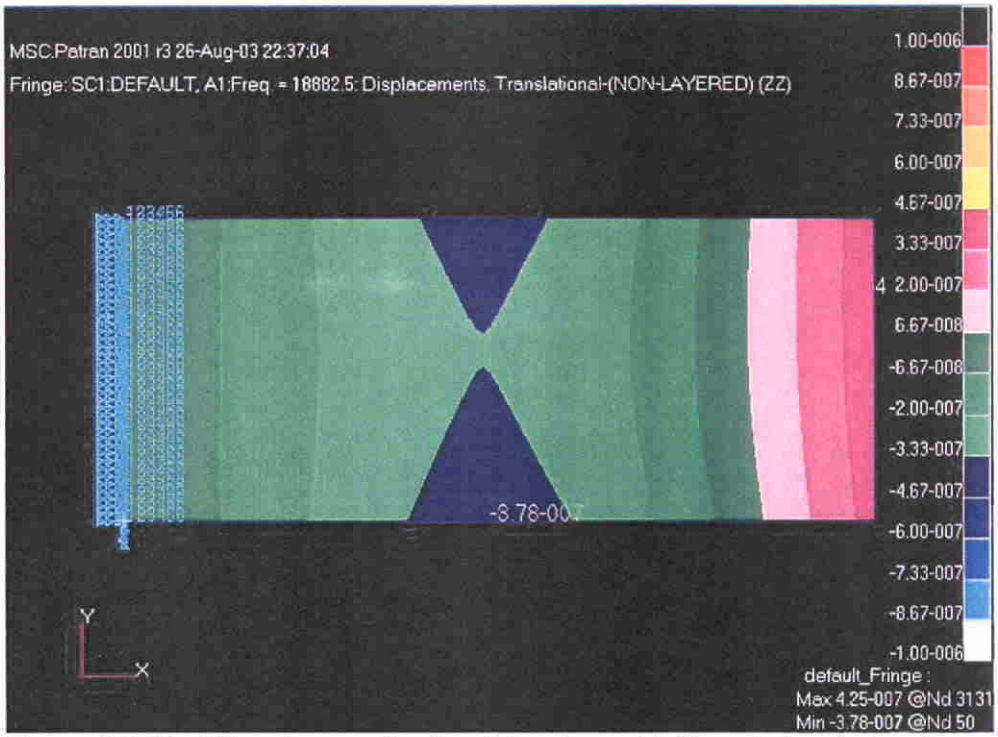

Figure 3.1.26. Vibration amplitude of the plate with Translational absorber

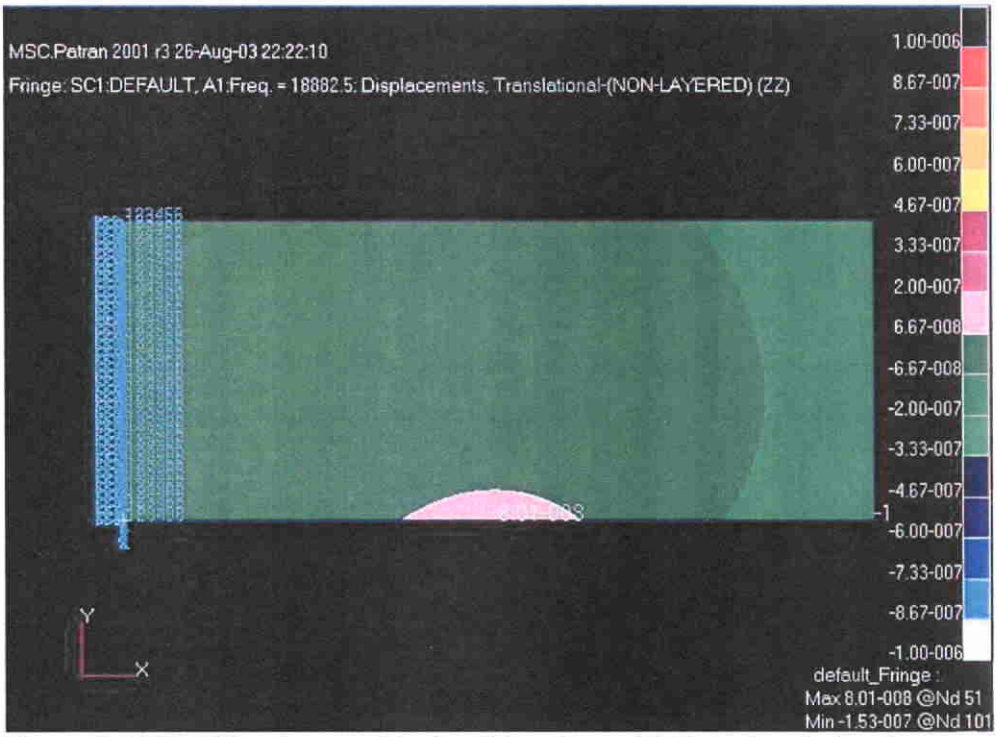

Figure 3.1.27. Vibration amplitude of the plate with Rotational absorber

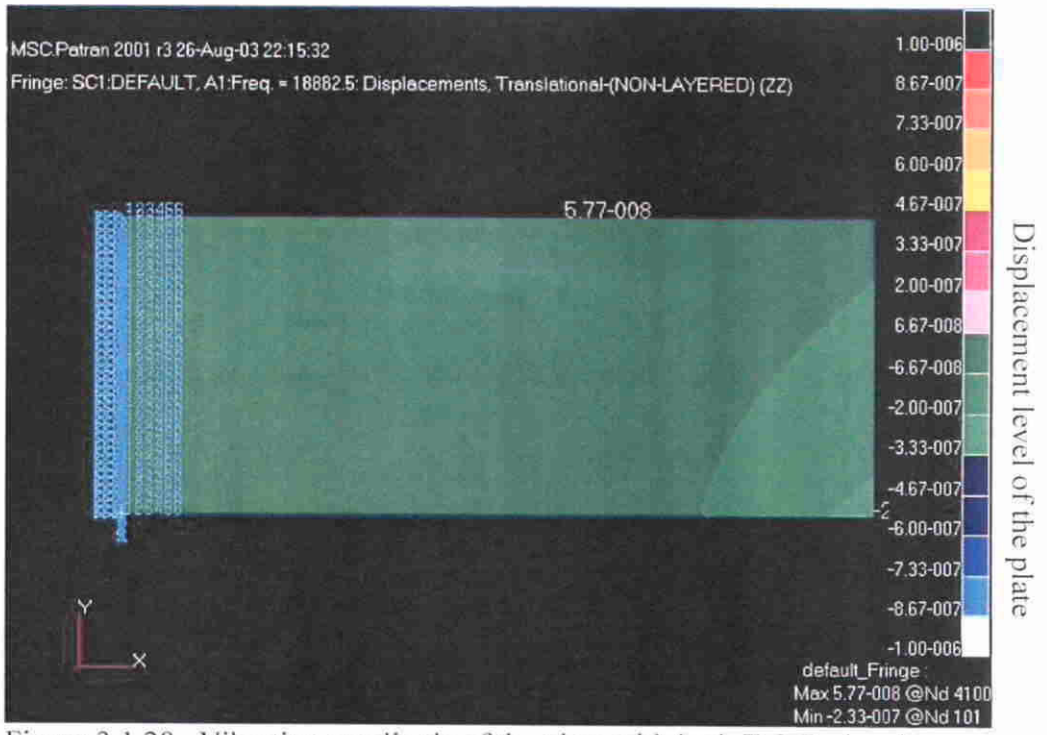

Figure 3.1.28. Vibration amplitude of the plate with both T & R absorber

Vibration absorber used	*Vibration amplitude range (m)*	*Peak-to-peak vibration amplitude (m)*
Without dynamic absorber	-1.32×10^{-6} to 1.08×10^{-6}	2.4×10^{-6}
Translational absorber	-4.25×10^{-7} to 3.78×10^{-7}	8.03×10^{-7}
Rotational absorber	-5.77×10^{-8} to 2.33×10^{-7}	2.907×10^{-7}
Combined type of absorber	-8.01×10^{-8} to 1.53×10^{-7}	2.331×10^{-7}

Table 3.1.1 Simulated vibration amplitude of the plate with different kinds of dynamic vibration absorber.

By comparison with the peak-to-peak vibration amplitude of the plate without any absorber as shown in Table 3.1.1, there is about 3 times vibration suppression if the translational vibration absorber was used, while there are about 8 times and 10 times of vibration suppression if the rotational and combined type of vibration absorber were used respectively.

The simulated results showed that the combined type of absorber was the most effective dynamic vibration absorber in vibration suppression within the frequency range. The combined type of vibration absorber gives a good performance in vibration suppression in the simulations, and match with the theoretical predictions in Chapter 2.3.3. The chosen location was a suitable place for attaching the DVA in suppressing the vibration excited by the force. This varies within that frequency range (in between the natural frequency of the second mode and the third mode).

To consider the sound radiation by vibrating surfaces, the radiated power can be obtained by integrating the far-field intensity over a hemispherical surface centered on the panel. The time-averaged power may be written as [20]:

$$\overline{P} = \int_S I(\theta,\phi)dS = \int_0^{\pi}\int_0^{2\pi} I(\theta,\phi)r^2 d\theta d\phi \qquad (3.1.1)$$

A measure of the velocity of vibration is the space-averaged value of the time-averaged normal vibration $\langle \overline{v}_n^{\,2} \rangle$ defined by:

$$\langle \overline{v}_n^{\,2} \rangle = \frac{1}{S}\int_x\left[\frac{1}{T}\int_0^T v_n^{\,2}(x,y,t)\right]dS \qquad (3.1.2)$$

where T is a suitable period of time over which to estimate the mean square velocity $\overline{v_n^2(x,y)}$ at a point (x, y), and S extends over the total vibrating surface: $\langle \bar{v}_n^2 \rangle$ is sometimes known as the "average mean square velocity".

A radiation efficiency, ratio (index) is defined by reference to the acoustic power radiated by a uniformly vibrating baffled piston at a frequency for which the piston circumference greatly exceeds the acoustic wavelength: $ka>>1$. With integration over a hemisphere, this yields the following expression for radiated power in this case:

$$\overline{P} = \frac{1}{2}\rho_0 c\pi a^2 |\bar{v}_n^2| \tag{3.1.3}$$

As a definition of reference radiation efficiency σ, we have:

$$\overline{P} = \sigma\rho_0 cS\langle \bar{v}_n^2 \rangle \tag{3.1.4}$$

which shows that if the far-field intensity is directly radically, the time-averagedd power is closely related to the mean square velocity $\langle \bar{v}_n^2 \rangle$ of the object's surface.

To investigate the acoustical power radiated by the plate with absorbers at different frequencies, the means square velocity $\langle \bar{v}_n^2 \rangle$ spectrum curve is shown in Figure 3.1.34. In this simulation, the plate without absorber (plate), the plate with a translational DVA (1T) , the plate with two rotational DVAs – one is oriented in the horizontal direction and the other in vertical direction (2R), and the plate with both kinds of the absorber (1T+2R) were compared.

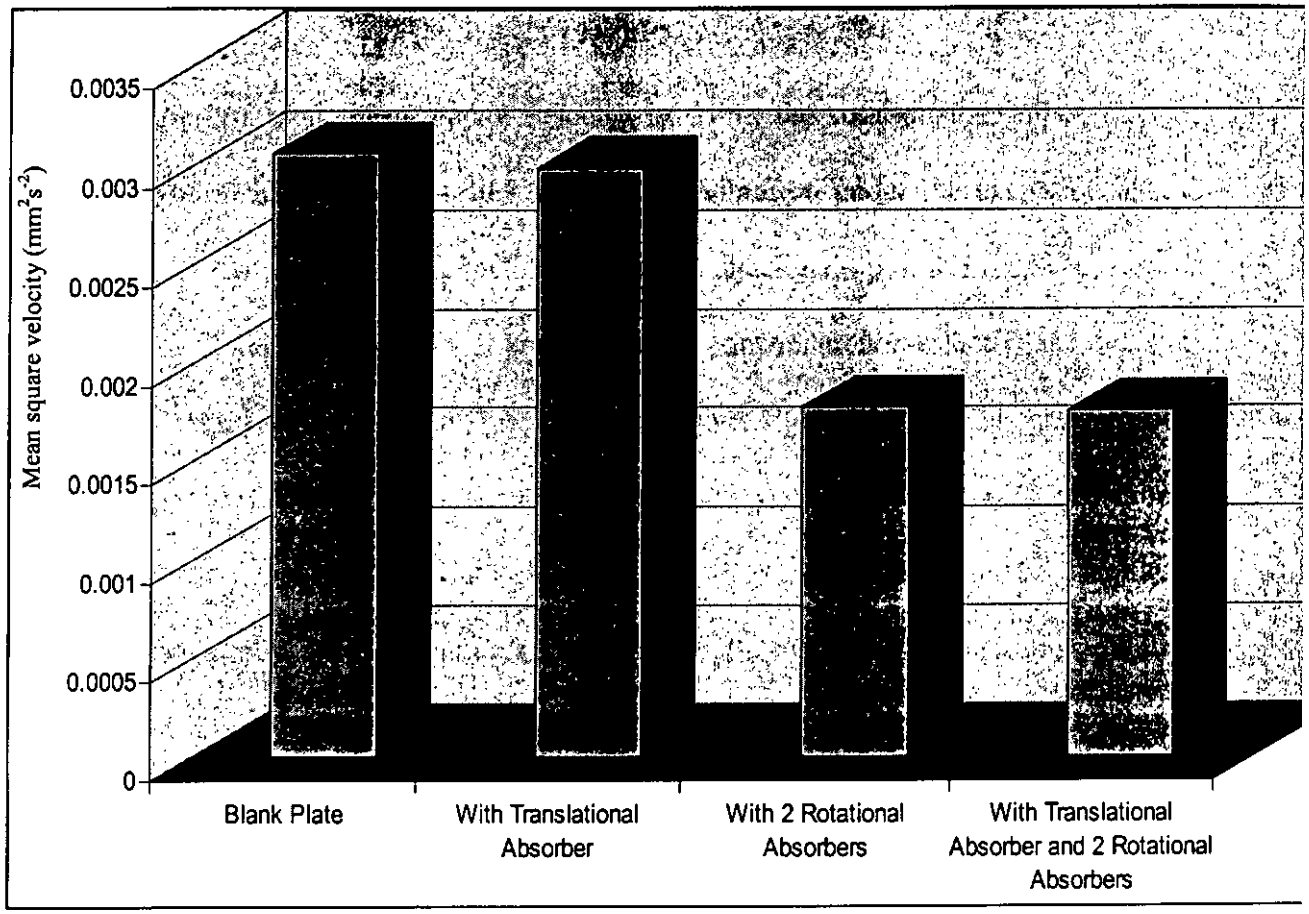

Figure 3.1.34. Mean square velocity of the plate with/without DVA at 19000Hz.

From the simulation, it was found that the translational type DVA does not suppress the vibration level of the plate at the tuned frequency. On the other hand, the result of the simulation shows that the attachment of rotational absorber or the combined type absorber lead to about 40% reduction of mean square velocity reduction at the tuned frequency compare with the plate without absorber.

The reductions of total mean square velocity in using the rotational absorber and the combined type of absorber are similar because the vibration under the excitation has no translational motion but high rotational motion at the attachment point of the absorbers. It shows that the "intersections of nodal lines" could be convenient and effective locations for attaching the absorbers within a frequency range; knowledge of the nodal positions of the contributing modes is useful for the determination of the attachment point of the absorbers. Although they may not be the optimum locations for attaching the absorbers, they would be convenient locations for attaching the absorber with high performance in vibration suppression.

3.2. Experimental tests and results

3.2.1. Suppression of a forced beam vibration using a dynamic vibration absorber

Experimental procedure and design of the absorber.

The test rig setup is illustrated in Figure 3.2.1 below:

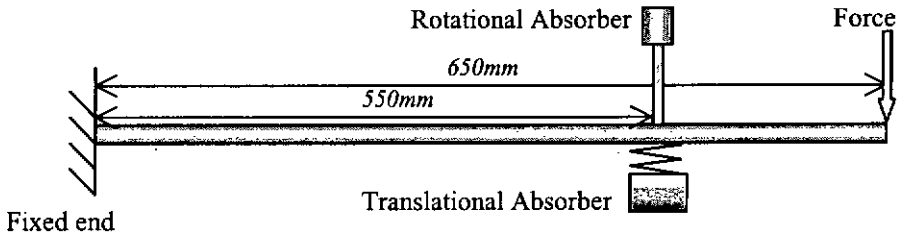

Figure 3.2.1a. Illustration of the experiment for testing the effect of the combined type of absorber.

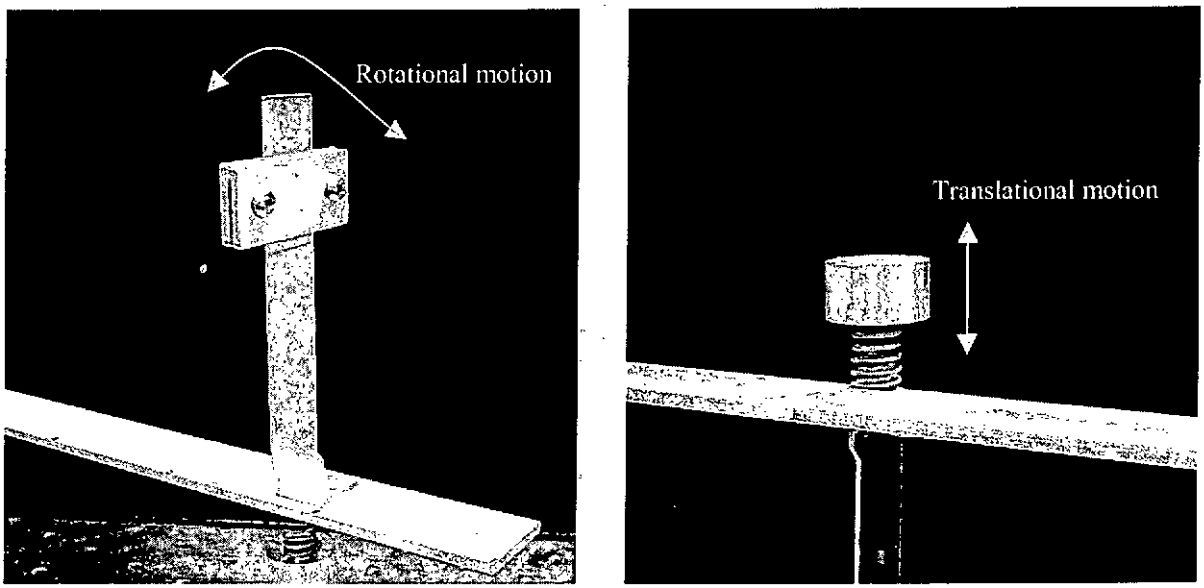

Figure 3.2.1b. The rotational absorber and translational vibration absorber designed for the experiment.

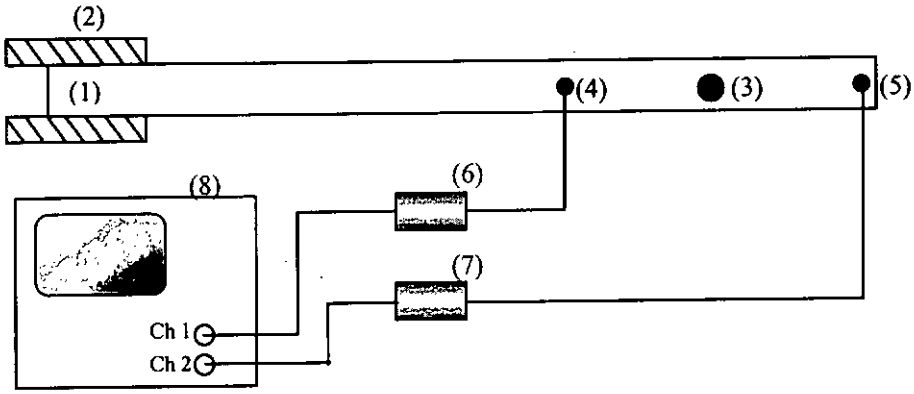

(1) 650mmX20mmX2mm aluminum beam
(2) Clamp
(3) Combined type of dynamic absorber
(4) Brüel & Kjær Charge Accelerometer Type 2032
(5) Brüel & Kjær Impact Hammer Type 8202
(6) Brüel & Kjær Charge Amplifier Type 2637
(7) Brüel & Kjær Charge Amplifier Type 2637
(8) Brüel & Kjær Dual Channel Signal Analyzer Type 2032

Figure 3.2.1c. Illustration of the setup for testing the effect of the combined type DVA.

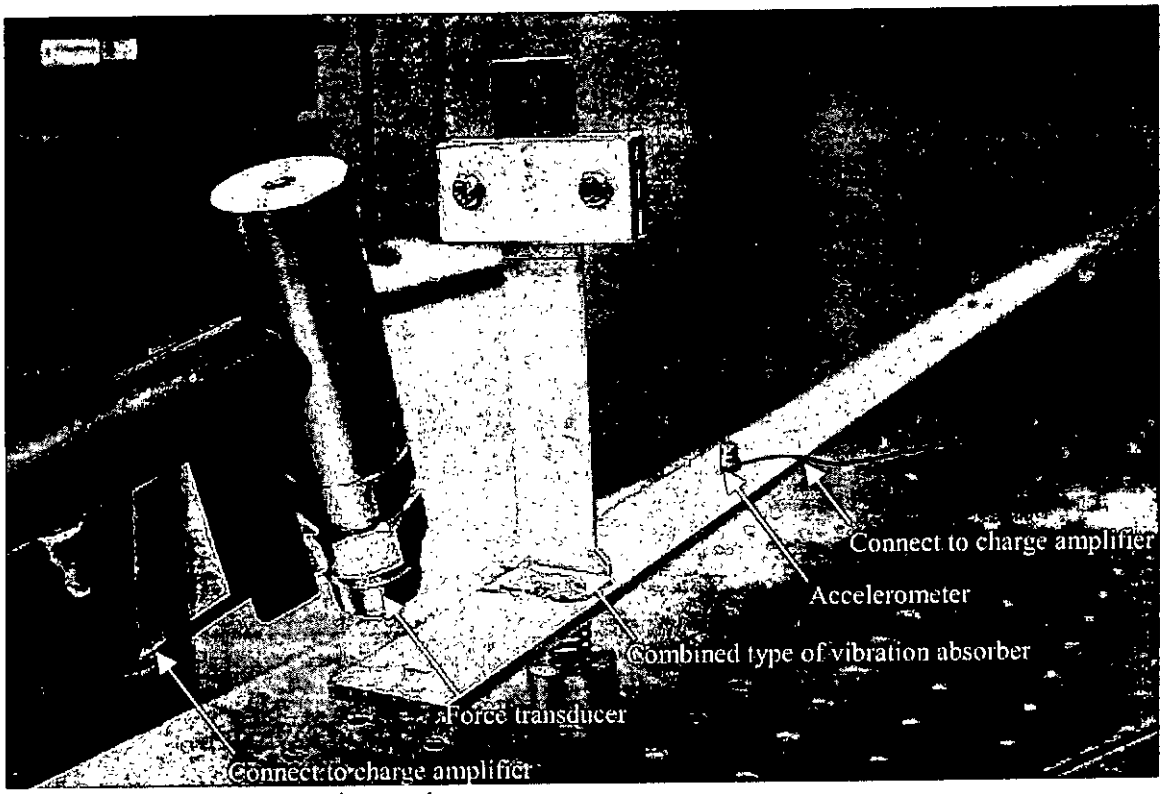

Figure 3.2.1d. The Experimental setup.

In order to evaluate the effect of the combined type of absorbers, a traditional sprung mass was hung on to the beam as an translational absorber. As shown in Figure 3.2.1b, a rotational absorber was also designed and mounted on the beam with the same distance measured from the clamped end as that of the sprung mass absorber. The natural frequencies of both absorbers were tuned at 230Hz. Since the two absorbers are practically mounted at the same location, they are considered as a combined type of absorber in this thesis.

In the experiment, the beam without any absorber was fixed on a table, and an impact excitation was applied at the free end of the beam. The vibration of the beam was measured by an accelerometer and analyzed by a B&K frequency analyzer; the frequency response of the beam at 230Hz was recorded.

Then the translational absorber was attached at 585mm from the fixed end of the beam, a similar vibration test as for the beam without any DVA was conducted. The frequency response of beam at 230Hz was also recorded.

Finally, attaching the rotational absorber at the same position as the translational absorber, the translation vibration response of the beam with both translational and rotational absorber on 230Hz excitation was recorded. The results were plotted in Figure 3.2.2.

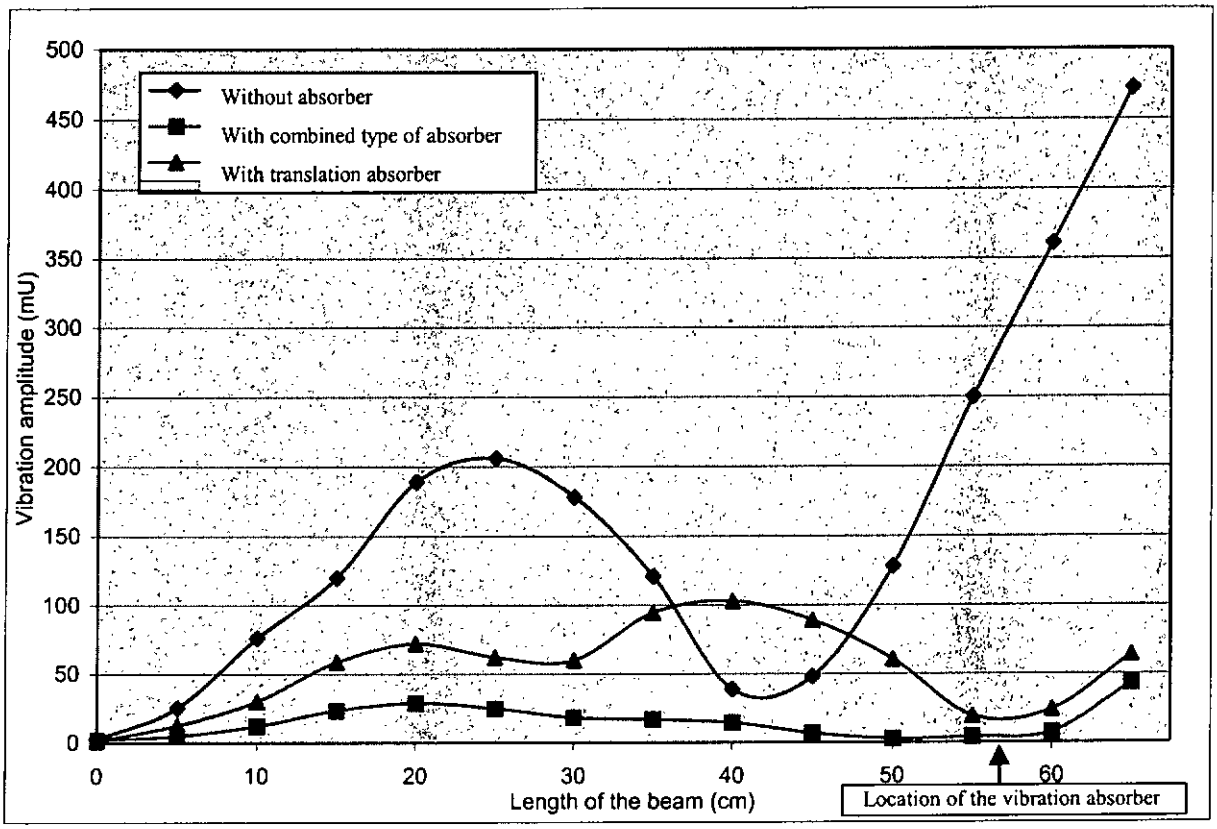

Figure 3.2.2. The response of "the beam without absorber", "the beam with rotational and translational absorber" and "the beam with translational absorber only".

The experimental result as shown in Figure 3.2.2 shows that if the combined type of absorber was implemented, the vibration level of the whole beam was suppressed greatly. The effectiveness of using the combined type of absorber in vibration suppression was better than just using a translational absorber at all points of the beam. At some points, the vibration amplitude of the beam after using the combined type of absorber was 8 times lower than that of the case without any absorber and 5 times lower than that of the case with the translational vibration absorber.

According to the simulation at Chapter 3.1.3, the vibration of the beam should be completely isolated after the combined type of vibration absorber was added at the location where the translational absorber was installed before. The experimental result showed that the beam still vibrated slightly after the combined type of absorber was added, this may be due to the fact that vibration absorber in the experiment cannot occupy the whole width of the beam, leakage of energy to the remaining portion of the beam caused the experimental result to be a little bit different from the simulation result.

As the figure shows, although the combined type of dynamic vibration absorber cannot isolate the vibration from the excitation completely, the vibration level was reduced dramatically.

3.2.2. Suppression of forced vibration of a resonant plate using dynamic absorber

An experiment was designed similar to the numerical experiment in Chapter 3.1.4. The numerical results showed that the performance of the combined type of absorbers was similar to that of the rotational absorbers alone for that particular configuration as described in Chapter 3.1.4. In the physical experiment, only a combined rotational absorber was therefore designed and tested for vibration suppression of the plate. The rotation absorber used in experiment before (Figure 3.2.1b) was a single axis vibration absorber that was able to absorb the rotation along a plane, which is good enough to be implemented on the one-dimensional vibration system such as the beam vibration as shown before. As the rotational absorber used in this experiment (Figure 3.2.3b and Figure 3.2.3c) was able to bend at multi-directions, it is good for use on the two-dimensional system such as plate vibration.

There is a limited amount of information concerning the response on different position of the dynamic vibration absorber attached to a plate under forced vibrations. Simple experiments were carried out; Figure 3.2.3a shows the geometry of the plate being studied, the position of vibration absorber being attached (attached at hole 1-7) and the points of measurements (Positions 1- Positions 21 are measuring the amplitude of displacement of the plate, and Position A1 & Position A2 are measuring the amplitude of displacement of the absorber). The experiment was under a periodic excitation at a position shown in

Figure 3.2.3a and the experimental setup was shown in Figure 3.2.3b. The plate used was a 85mm X 220mm aluminum plate with 2mm thickness. Where the vibration absorber was made of a copper mass and a steel rod with mass ratio to the plate equal to 0.15.

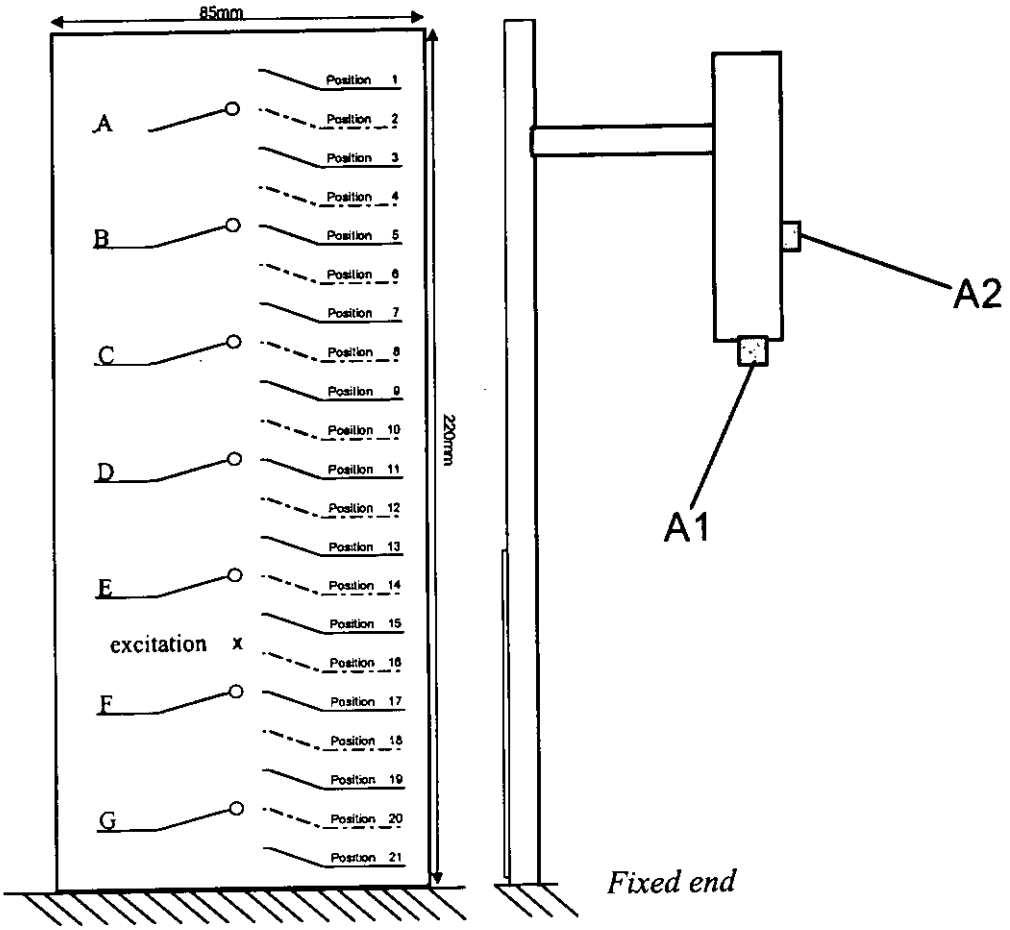

Figure3.2.3a. The geometry of the measured plate and points of measurement

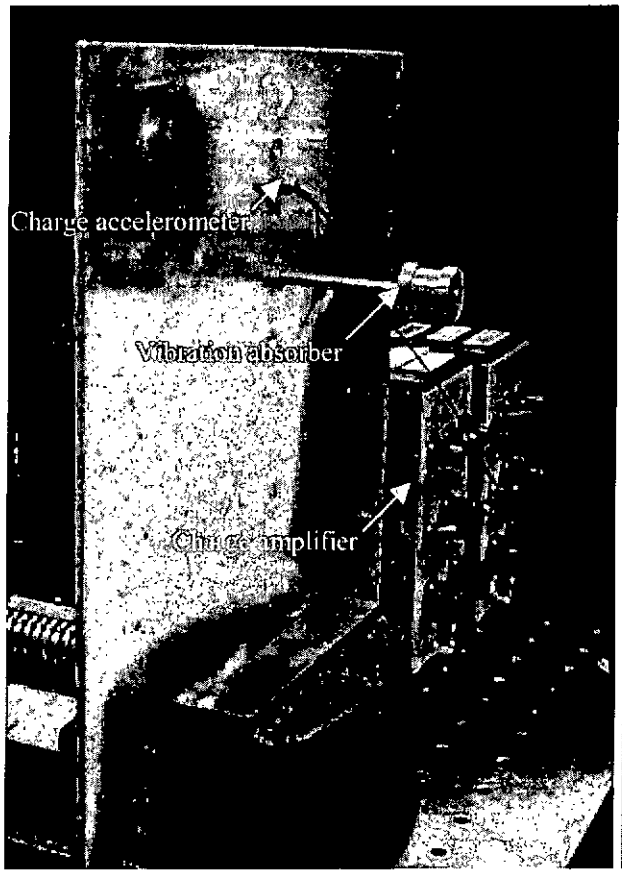

Figure 3.2.3b. The experimental setup

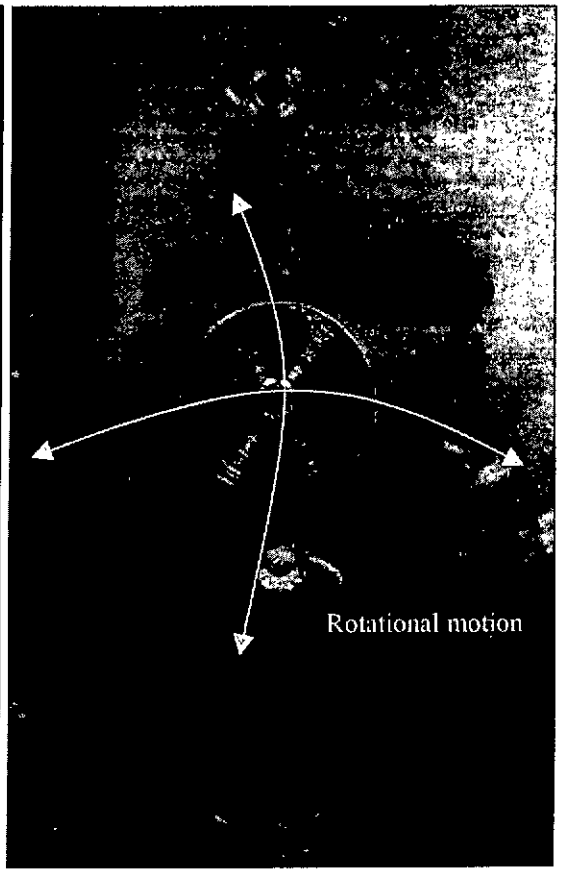

Figure 3.2.3c. The Rotational Absorber

Figure 3.2.3c shows the specially designed rotational absorber used, it is able to absorb multi-directional rotational motion. A signal generator was used to provide a signal for the shaker to give a harmonic vibration at the source of excitation, which was attached to a point between location E and F that shown in Figure 3.2.3a. After the accelerometer and the force transducer obtained the signal from the point of measurement and the excitation source respectively, the signal was conditioned by the charge amplifiers and send to the dual channel signal analyzer. The frequency response results were obtained from the spectrum analyzer.

The resonant frequencies of the first mode and second mode of the cantilever plate were measured to be 50Hz and 300Hz respectively by random excitation test [37]. In order to see the effect of the dynamic vibration absorber at different positions, the plate was excited at its resonant frequency to see the response of the absorber to the excitation. Two different amplitudes of input Signal Amplitude were used to drive the vibrator, they are 0.5Vpp and 2Vpp, where the 0.5Vpp excitation gives a weaker force than the 2Vpp. The results obtained from the experiment is summarized in the figures below:

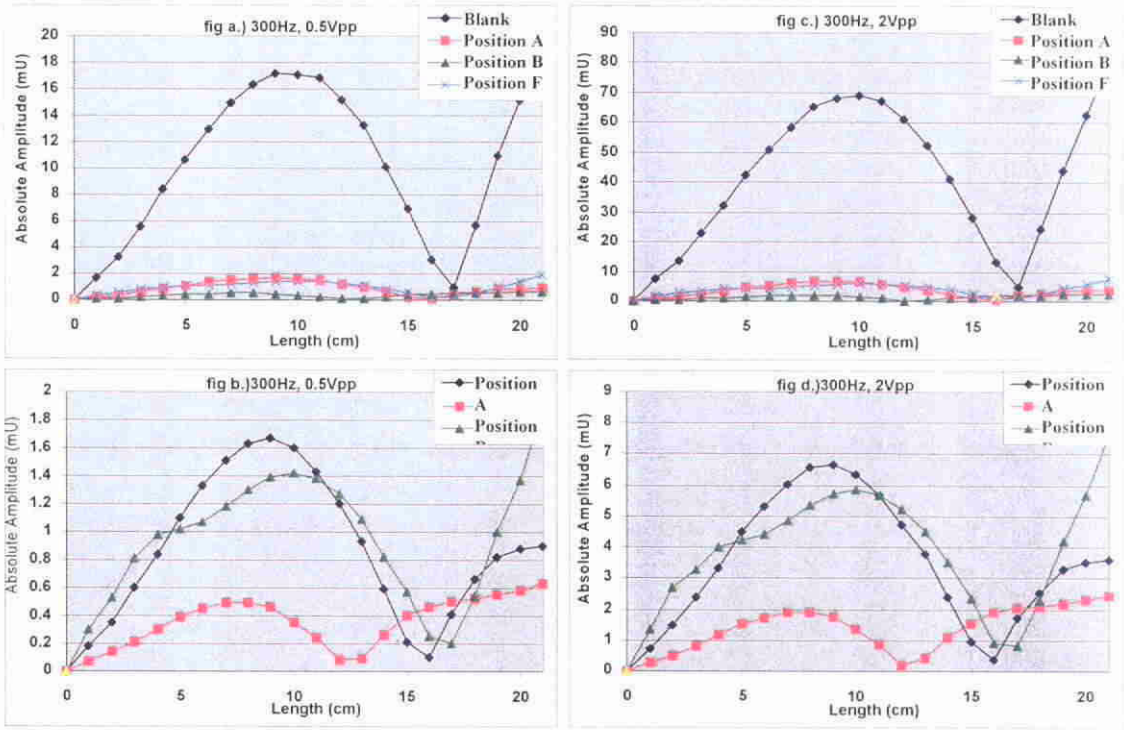

Figure 3.2.4. Vibration suppression by dynamic absorber comparison - a. Excitation voltage=0.5Vpp, b.)Excitation voltag =0.5Vpp (zoom), c. Excitation voltage=2.0Vpp. d.)Excitation voltage=2.0Vpp (zoom)

From Figure 3.2.4a. and Figure 3.2.4c.), the dynamic vibration absorber reduced the vibration amplitude by a factor of 1/9 (the average reduction was 41 times!). To compare

From Figure 3.2.4a. and Figure 3.2.4c.), the dynamic vibration absorber reduced the vibration amplitude by a factor of 1/9 (the average reduction was 41 times!). To compare the effect of the vibration absorber on different location clearly, Figure 3.2.4a and Figure 3.2.4c were enlarged to be Figure 3.2.4b and Figure 3.2.4d. In comparing the amplitudes of vibration with the absorber attached at position A and B, we could find the effectiveness of the absorber at B was averagely 3.5 times better than at position A. These tell us that the absorber is more effective when it is attached at position B, which is the nodal point of the vibrating mode. As the vibration absorber was of the rotational type, mostly likely, the absorber is most effective on the nodal points of vibrating mode and the experiment validated this prediction.

On the other hand, by comparing results of different strength of the excitation force – comparing the figures 3.2.4a & 3.2.4c and figures 3.2.4b & 3.2.4d. It was found that the level of vibration displacement suppression was independent to the excitation forces; where both of the tests give nearly 9 times of vibration reduction.

3.2.3. Suppression of forced vibration of a non-resonant plate using a dynamic absorber

The same plate tested in Chapter 3.2.2 was used to perform the following experiment. This time, the driving frequency of the plate was set at 250Hz. The results obtained from the experiment is attached in Appendix III and summarized in the following figures:

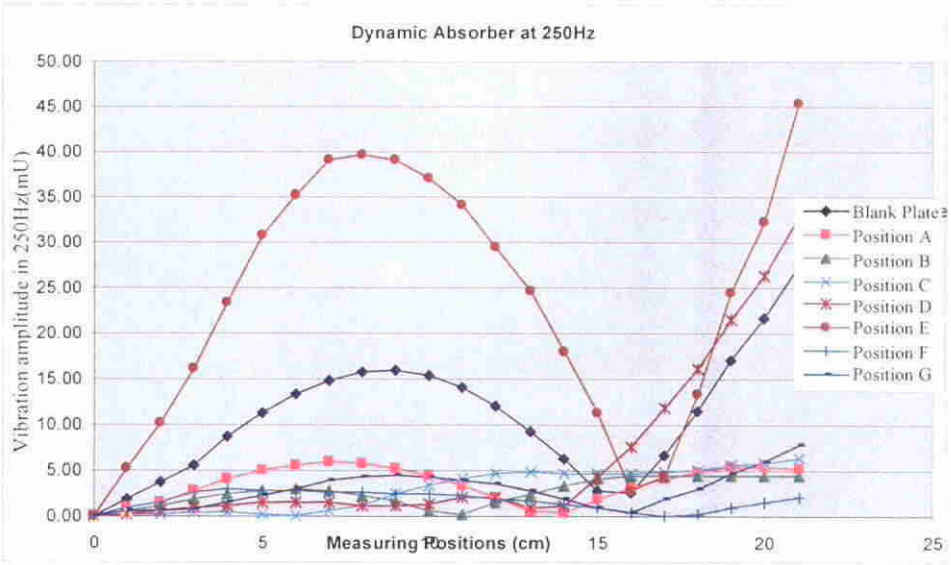

Figure3.2.5. Vibration amplitude of a non-resonant plate with a dynamic vibration absorber

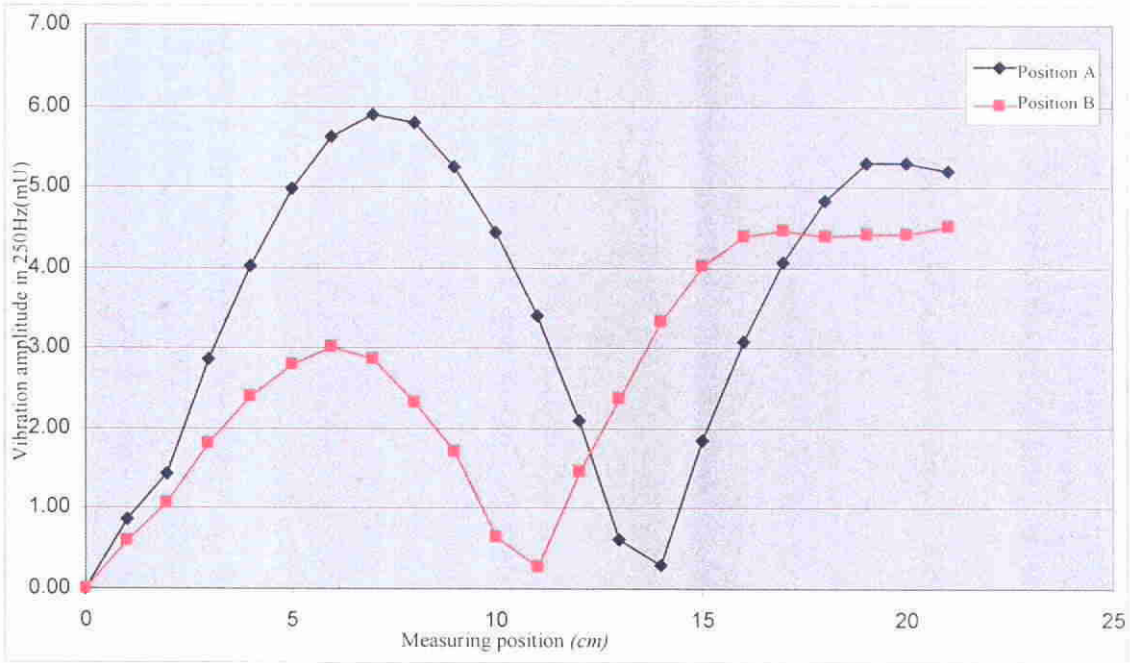

Figure3.2.6. Vibration amplitude of the plate with the Dynamic vibration absorber at different locations.

From Figure 3.2.5, it was found that although the plate was not driven at a resonant frequency, the vibration suppression was still significant at many points. As the excitation frequency was somewhere between the natural frequency of the first and second modes of vibration, the vibration may be dominated by these two modes. By comparing the results from the position of absorber at position A and position B, it was found that the vibration reduction was about one-half on average. As the node of the second mode was at position B, the vibration reduction when the absorber attached at position B was at least 2 times higher than the absorber attached to other points.

3.2.4. Determination of suitable mounting position of dynamic absorber using ESPI

To find a suitable nodal position for attaching the proposed vibration absorber, a full field technique called ESPI described in Chapter 1.3 was tried.

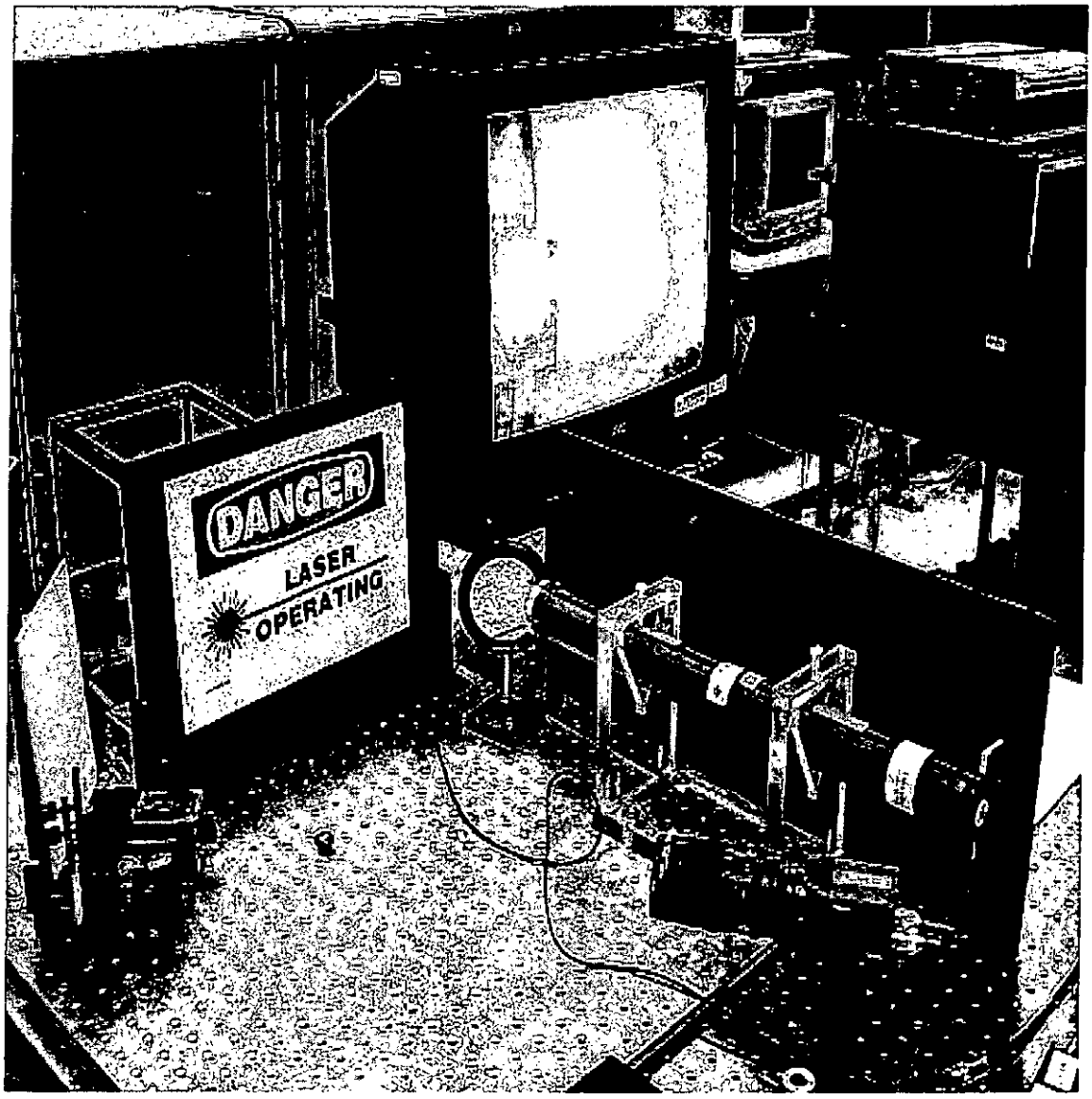

Figure 3.2.7a. Experimental setup of the ESPI system

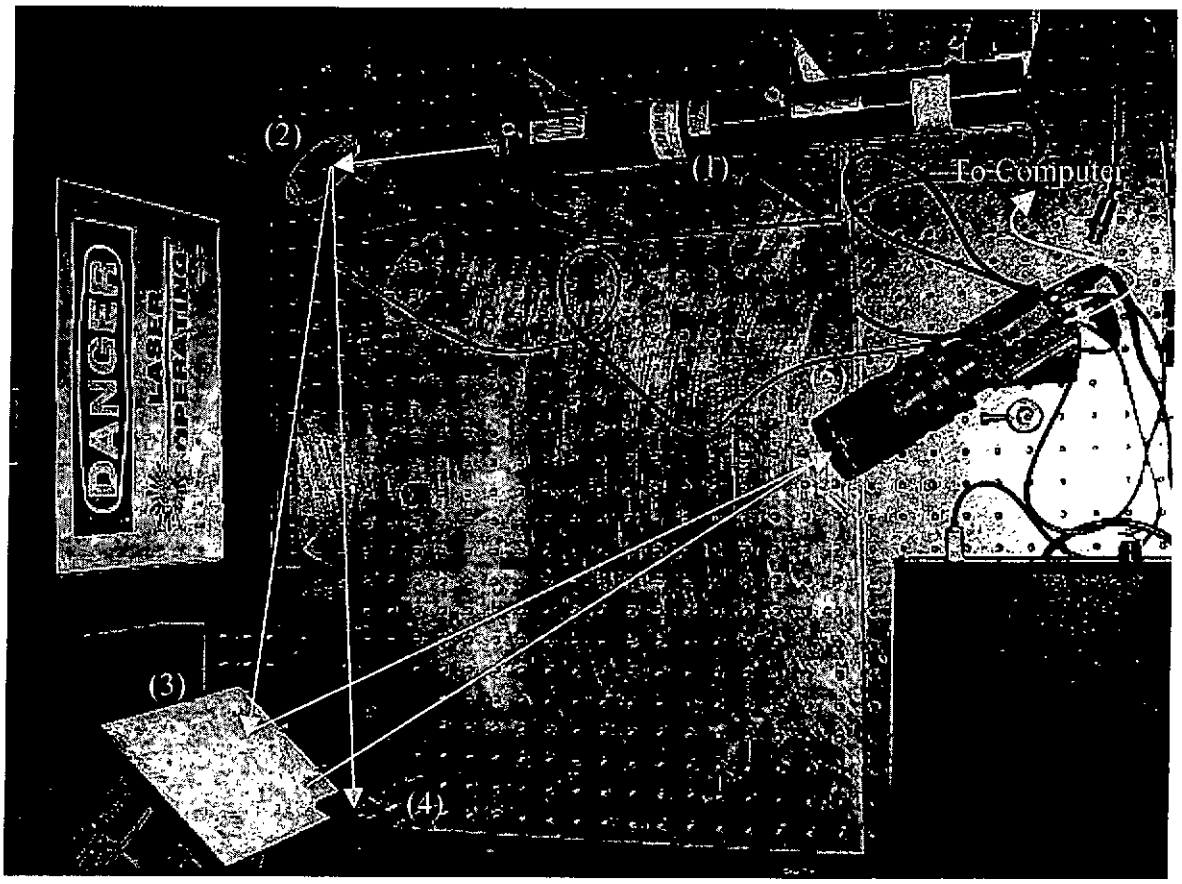

Figure 3.2.7b. The optical path and equipment setup.

(1) Uniphase Helium-Neon 200mW Class IIIb Laser Gun

(2) Reflection Mirror

(3) The aluminum plate

(4) Reflection Mirror

(5) CCD camera

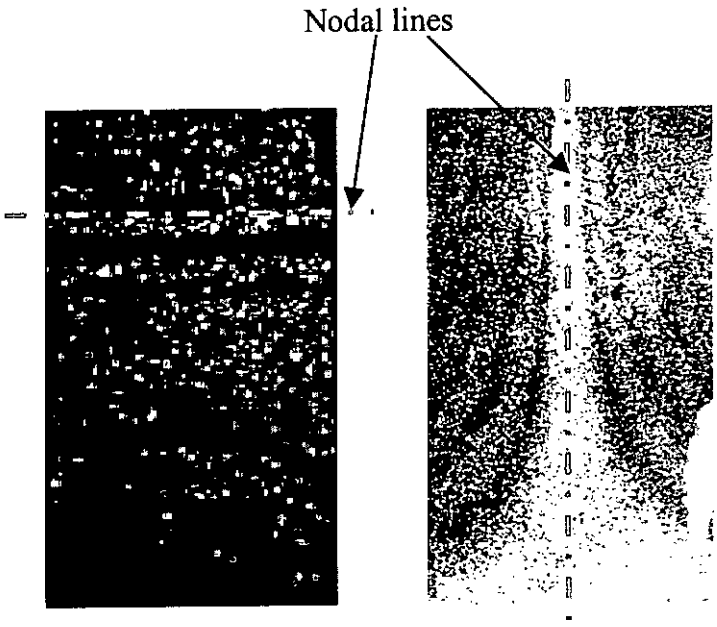

Figure 3.2.8. Pictures taken by ESPI showing the nodal lines of the 2nd and the 3rd mode of a plate.

In the experiment, nodal lines of a vibrating plate at specified modes were found as shown in Figure 3.2.8. Those positions are where the plate vibrates with very high twisting amplitude. According to the theory stated in Section 2.2.3 and simulation shown in Chapter 3.1.4. The intersections of the nodal lines should be good locations for attaching the proposed absorber. It is possible to find such an area conveniently with the aid of a whole field optical technique.

This experiment showed a tool for finding the intersections of the nodal lines. In this experiment the position B of Figure 3.2.3a was found to be the intersections that gave best performance in experiment shown in Section 3.2.2 and 3.2.3. It validated the simulation in Section 2.2.3 as the experimental result matches with the result in simulation.

4. Discussion and Conclusions

In the present study, the proposed combined type of dynamic vibration absorber have been shown to be able to suppress forced vibration significantly in a narrow frequency range, which overcomes the problem of the traditional sprung mass vibration absorber. For suppression of rigid body vibration, the performance of the commonly used translational absorber was compared to those of the rotational absorber and the proposed absorber. From the numerical analysis in Section 3, it was found that the translational one has the poorest performance in terms of the absorption frequency range, the rotational absorber is better while the proposed absorber can completely absorb all the rigid body vibration. This finding is useful for vibration suppression of the rigid body vibration of machine platforms.

For flexural vibration of continuous structures such as beams and plates, the performance of the commonly used translational absorber was compared to those of the rotational absorber and the combined type vibration absorber by finite element analysis and experimental tests. It was found that the combination of translational and rotational type of absorber provides excellent performance than those of the standard sprung mass absorbers, which, in the simulation, the combined translational plus rotational type vibration absorber was able to isolate the vibration efficiently. And it was purposed to install such kinds of combined type absorber close to the excitation of obtaining larger suppressed region.

In the suppression of plate vibration, combining two rotational absorbers of rotation axis perpendicular to each other was used for vibration suppression. The combined absorber was tested and compared with the effect of the traditional translational vibration absorber.

It was found that when putting the proposed multi-axial rotational combined type vibration absorber was effective when installing such kind of absorber at the location at which the structure had a large rotation. Modal analysis was used for predicting the suitable location for installing such kind of vibration absorber.

In conclusion, the proposed absorbers are simple combination of different kinds of vibration absorbers and attached on to the vibrating beam at a single point. With the knowledge of the modal parameters of the structures, it is straightforward to determine an effective attachment point for vibration and the resulting sound radiation as demonstrated by the test cases reported in the previous chapter. In this project, a new type of vibration absorber for structural vibration suppression was developed, a systematic way for choosing a suitable vibration absorber and guidelines for determining a good location for vibration absorber installation were described in this project.

Appendices

Appendix I - Computer simulations of vibration suppression of beams with vibration absorbers with Matlab

The beam parameters	Young's modulus	200e9Pa
	Cross-section area	3.6e-3m^2
	Density	7600kg/m^3
	Length	6m
	Boundary condition	Simply supported
The absorbers parameters	Mass Ratio	0.1
	Inertia Ratio	0.1
Excitation	Translational force	2500N

Table5.1.1. Parameters of fixed-free beam used in the simulation in Section 3.1.2

The beam parameters	Young's modulus	200e9Pa
	Cross-section area	3.6e-3m^2
	Density	7600kg/m^3
	Length	6m
	Boundary condition	Fixed-free supported
The absorbers parameters	Mass Ratio	0.1
	Inertia Ratio	0.1
Excitation	Translational force	2500N

Table5.1.2. Parameters of fixed-free beam used in the simulation in Section 3.1.3

Appendix II – Computer simulations of vibration suppression of beams with vibration absorbers using MSc Nastran

Cantilever beams are common elements of many aeronautical, civil and mechanical engineering structures. Vibration analysis should be required when designing systems using these elements. So, cantilever beam is chosen as a typical model for analyzing the effectiveness of a dynamic absorber for vibration control.

As an initial sensitivity test of the absorber parameters and location of the attachment to the effectiveness of vibration suppression, a commercial FEM software called MSC NASTRAN is used for some quick tests. In this method, the structure is subdivided into a finite number of small regions called elements. Mechanical model can be formed by these elements. Within an element displacements and stresses are approximated using polynomial shape functions. An element connected to adjacent elements at a finite number of points is called grid points. Elemental material properties and geometry are used to generate the stiffness of the entire structure, discretized at the grid points. The center load acting on the structure is represented as the force, also at the grid points. In the simulation presented in this report, a periodic force is used as the excitation. These are then used to generate element results such as force per unit length, stress, strain, etc. Finally, amplitude of vibration for the cantilever beam in concerned area can be known.

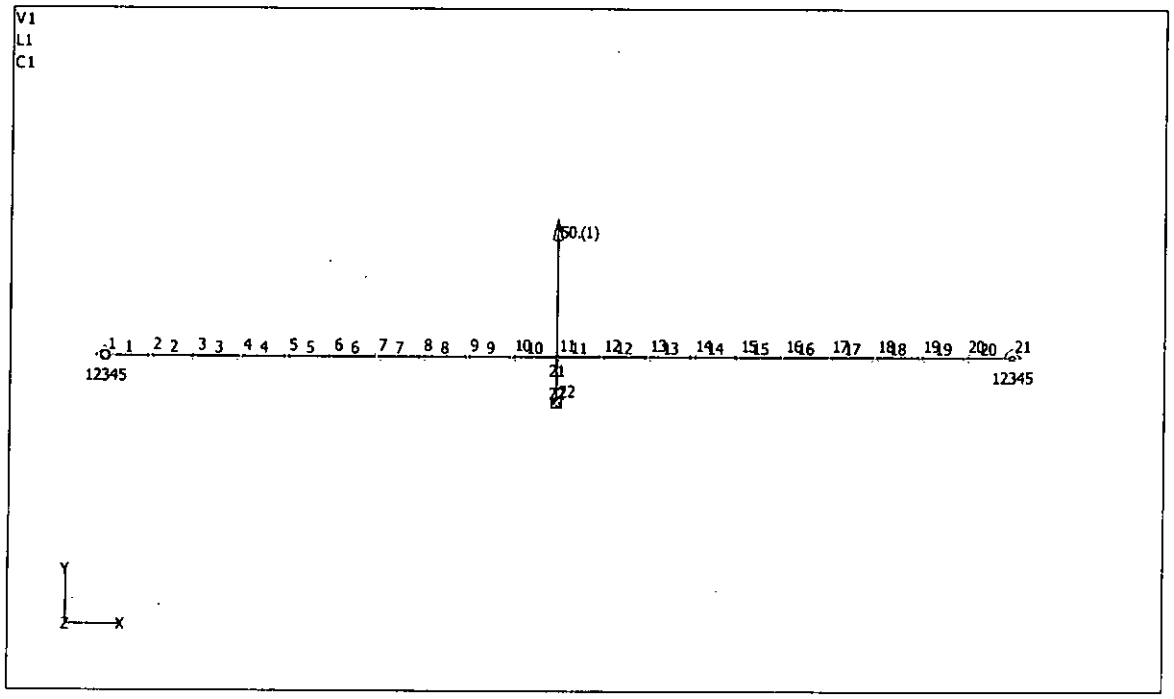

Figure5.1.1. Simply supported cantilever beam model

A simply supported aluminum rectangular beam was modeled and meshed as Figure 5.1.1 above with cross sectional area A = 0.003m^2, moment of inertia I_1 = 5×10^{-8} kgm^2, I_2 = 2.5×10^{-8} kgm^2, mass per unit length = 0.825kg/m. With the assumed information, the first and second mode of vibration of this beam were calculated which are 56.85Hz and 227.40Hz respectively.

The point of attachment of the dynamic vibration absorber was changed in this simulation with other parameters remained constant. There are in total 11 models were done (attach the absorber in node 1 to node 11). To model the absorber, a lumped mass of 16kg (Basic rectangular mass) and a linear spring with stiffness 1579 kN/m was used.

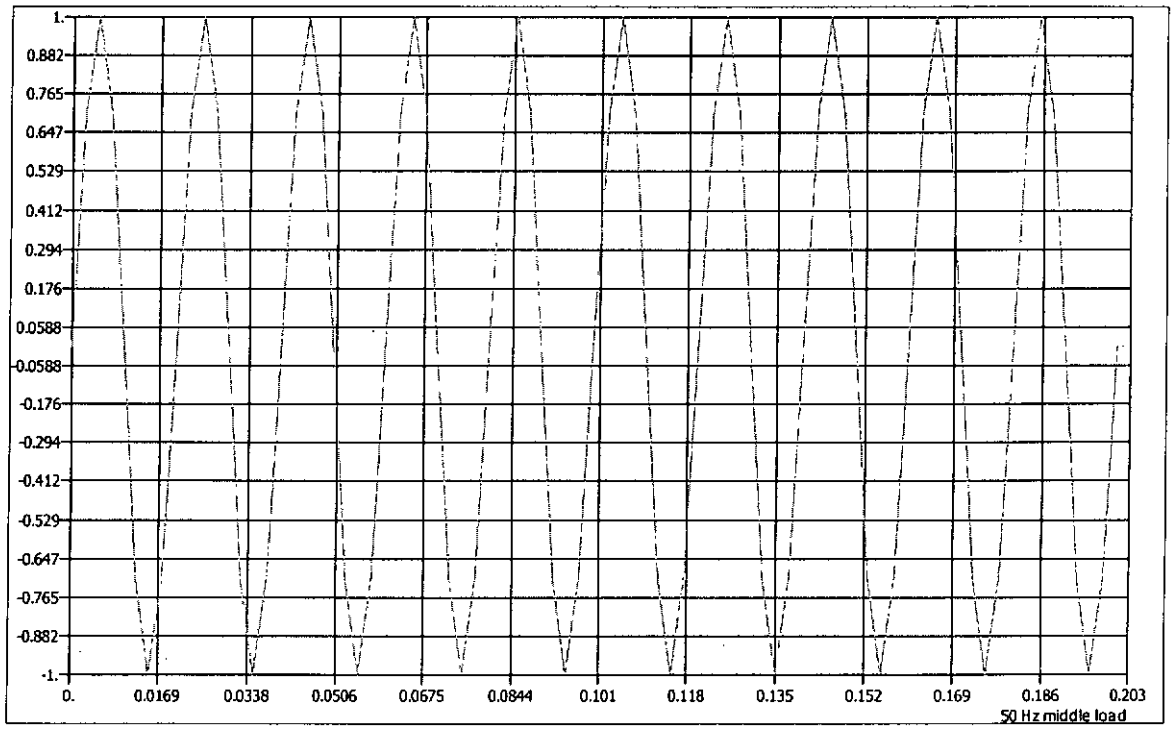

Figure5.1.2. Excitation function used in the simulation of cantilever beam

The excitation was a 50Hz sinusoidal force acted on the mid-point of the beam. Two of the analyzed results were chosen.

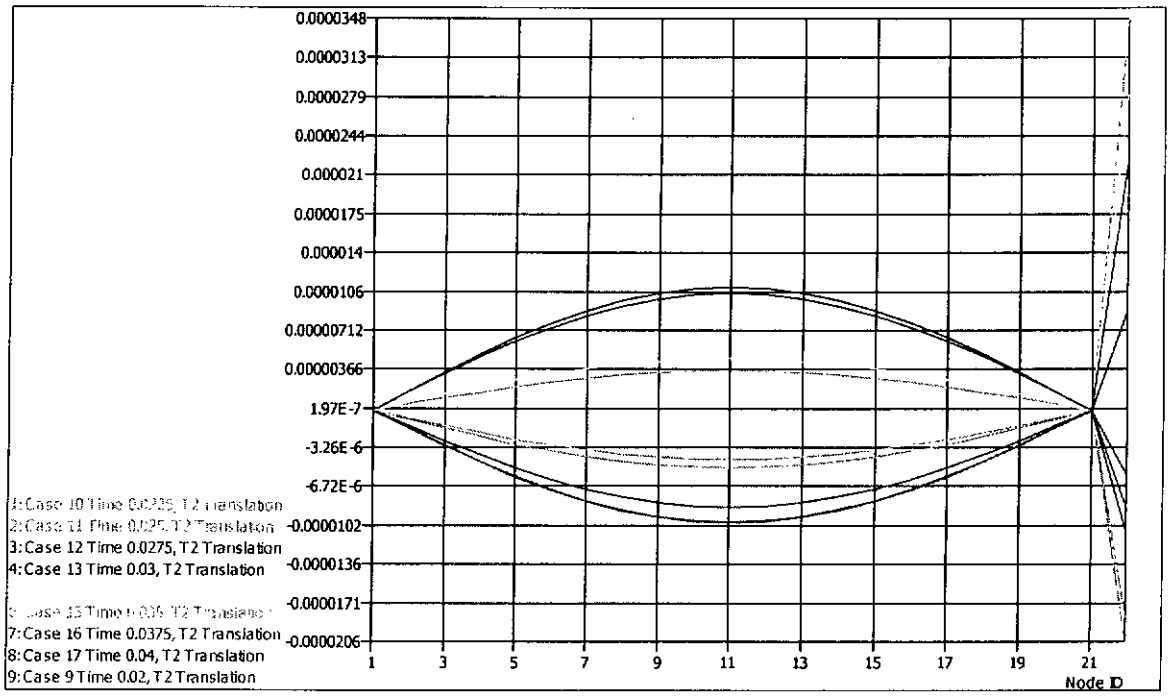

Figure 5.1.3. When the vibration absorber at node 11 (mid-point of the beam)

When the vibration absorber at node 11 (mid-point of the beam) the maximum vibration amplitude of the beam was 0.0109 mm, which is only about one third of that of the vibrating beam without dynamic absorber. In addition, we can see that the vibration amplitude of the vibration absorber is about 0.0348 mm, which is very high when compare to the vibration amplitude of the beam, and it tells us that when the absorber is attached on the anti-node of the object, the transmissibility will be high.

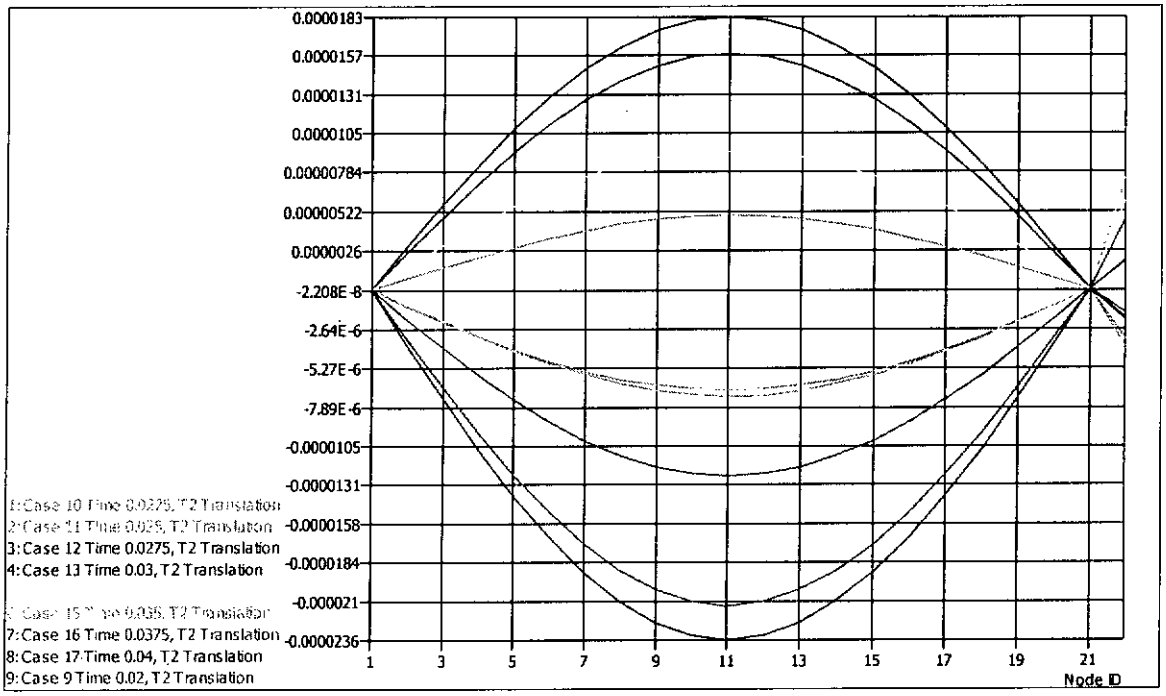

Figure5.1.4. When the vibration absorber at node 3 (near one of ends of the beam)

When the vibration absorber attached on position node 3 (near one of the ends of the beam) the maximum vibration amplitude of the beam was 0.0222mm, which is a little bit higher than the amplitude of the beam attached the dynamic absorber at mid-point (ant-node of the vibrating mode). In addition, we can see that the vibration amplitude of the vibration absorber is only about 0.00784mm, which is very small when compare with the vibration amplitude of the beam, and it tells us that when the absorber is attached on to a point other than the anti-node of the object, the transmissibility will be smaller.

The simulations shows that if the Dynamic Vibration absorber has the resonant frequency close to the forcing frequency, the amplitude of the vibration of the beam will be reduced and some of the vibration will be transmitted to the vibration absorber.
Also, the location of the DVA affects the transmissibility where higher transmissibility will be obtained at the point near the anti-node of the beam.

Appendix III – Computer simulations of vibration suppression of beams with dynamic absorber by a self-written Matlab program

File name:
tang42.m
F=2500 r=0.2

Original natural freq of the beam (rad/s)
37.9 105.2 208.7 394.

Absorber at the 3rd node of the beam
Forcing freq = absorbing freq = 37.9 Applied at 1st degree of freedom (translational force at node 1)

		Natural frequencies	Steady-state amplitude	Force transmitted	freq range
1.052	Translation	1052	-0.0105	2.78E+03	9.7
0.6529		652.9	-0.0048		
0.3949		394.9	-0.0096		
0.2093		209.3	0.0046		
0.1067		106.7	0		
0.0427		42.7	0.0025		
0.033		33	0.0872		
1.0618	Rotation	1061.8	-0.0102	-2.06E+03	15.2
0.6686		668.6	-0.0047		
0.4032		403.2	-0.0099		
0.2098		209.8	0.0038		
0.1057		105.7	-0.0033		
0.0451		45.1	0		
0.0299		29.9	-0.0234		

Absorber at the 3rd node of the beam
Forcing freq = absorbing freq = 71.55 Applied at 1st degree of freedom (translational force at node 1)

		Natural frequencies	Steady-state amplitude	Force transmitted	freq range
1.0522	Translation	1052.2	0.0115	-7.61E+03	44.1
0.6529		652.9	0.0079		
0.3951		395.1	0.0165		
0.2114		211.4	-0.0053		
0.0362		36.2	0		
0.0688		68.8	-0.0052		
0.1129		112.9	-0.0578		
1.0898	Rotation	1089.8	0.0044	-455.4989	41.6
0.706		706	0.0045		
0.4191		419.1	0.0115		
0.2118		211.8	0.0003		
0.0655		65.5	0.0081		
0.1071		107.1	0		
0.0336		33.6	0.0107		

Absorber at the 3rd node of the beam

Forcing freq = absorbing freq = 105.2 Applied at 1st degree of freedom (translational force at node 1)

		Natural frequencies	Steady-state amplitude	Force transmitted	freq range
1.0523	Translation	1052.3	0.0007	-3.56E+03	44.4
0.3954		395.4	0.0021		
0.653		653	0.0048		
0.2158		215.8	-0.0003		
0.0364		36.4	0		
0.0855		85.5	-0.0019		
0.1299		129.9	-0.0113		
1.1439	Rotation	1143.9	-0.0175	2.46E+03	30.3
0.7545		754.5	-0.0027		
0.434		434	0.0058		
0.2138		213.8	0.0187		
0.0792		79.2	0.0253		
0.0342		34.2	0		
0.1095		109.5	0.0079		

Absorber at the 3rd node of the beam

Forcing freq = absorbing freq = 156.95 Applied at 1st degree of freedom (translational force at node 1)

		Natural frequencies	Steady-state amplitude	Force transmitted	freq range
1.0528	Translation	1052.8	-0.0069	-1.12E+04	71.5
0.6531		653.1	0.0025		
0.3965		396.5	0.0078		
0.2337		233.7	0.0041		
0.0365		36.5	0		
0.1641		164.1	-0.0049		
0.0926		92.6	-0.0149		
1.291	Rotation	1291	0.0009	-4.80E+03	102.4
0.8173		817.3	0.0016		
0.4489		448.9	0.002		
0.216		216	-0.0021		
0.0885		88.5	-0.0024		
0.1136		113.6	0		
0.0344		34.4	0.0001		

Absorber at the 3rd node of the beam

Forcing freq = absorbing freq = 208.7 Applied at 1st degree of freedom (translational force at node 1)

		Natural frequencies	Steady-state amplitude	Force transmitted	freq range
1.0534	Translation	1053.4	0.0028	3.77E+03	91
0.6532		653.2	-0.0001		
0.3987		398.7	-0.0015		
0.2729		272.9	-0.0022		
0.1819		181.9	0		
0.0365		36.5	0.0016		
0.0945		94.5	0.0029		

1.5032	Rotation	1503.2	-0.0061	-3.28E+04	100.5
0.8523		852.3	0.0052		
0.4568		456.8	0.008		
0.2173		217.3	-0.0019		
0.0919		91.9	-0.0063		
0.0344		34.4	0		
0.1168		116.8	0.0009		

Absorber at the 3rd node of the beam
Forcing freq = absorbing freq = 301.75 Applied at 1st degree of freedom (translational force at node 1)

		Natural frequencies	Steady-state amplitude	Force transmitted	freq range
1.0551	Translation	1055.1	0.0006	1.45E+03	164.5
0.6537		653.7	0.0005		
0.4173		417.3	-0.0002		
0.355		355	-0.0012		
0.1905		190.5	0		
0.0366		36.6	0.0008		
0.0955		95.5	0.0006		
1.9659	Rotation	1965.9	0.000974	4.08E+03	244.8
0.8784		878.4	-0.0001809		
0.4633		463.3	-0.0004818		
0.2185		218.5	-0.0004693		
0.094		94	0.0003319		
0.0345		34.5	0		
0.1199		119.9	-0.0000615		

Absorber at the 3rd node of the beam
Forcing freq = absorbing freq = 394.8 Applied at 1st degree of freedom (translational force at node 1)

		Natural frequencies	Steady-state amplitude	Force transmitted	freq range
1.0579	Translation	1057.9	0.001	-1.90E+03	115.8
0.6551		655.1	-0.0028		
0.3817		381.7	-0.0002		
0.1928		192.8	0.0028		
0.0958		95.8	0		
0.0366		36.6	-0.0022		
0.4975		497.5	-0.0008		
2.4711	Rotation	2471.1	0.0004194	2.88E+03	246.9
0.8883		888.3	0.0001768		
0.466		466	-0.0002048		
0.2191		219.1	-0.0005638		
0.0948		94.8	0.0001658		
0.0345		34.5	0		
0.1214		121.4	-0.0000315		

Absorber at the 3rd node of the beam
Forcing freq = absorbing freq = 723.4 Applied at 1st degree of freedom (translational force at node 1)

		Natural frequencies	Steady-state amplitude	Force transmitted	freq range
1.0975	Translation	1097.5	0.0001192	1.11E+03	211.1
0.8603		860.3	-0.0000351		
0.6492		649.2	-0.0000548		
0.3883		388.3	-0.0001362		
0.1947		194.7	0		
0.0962		96.2	-0.0003087		
0.0366		36.6	0.0000511		
4.3487	Rotation	4348.7	0.0000946	-911.0601	429
0.8979		897.9	-0.0003266		
0.4689		468.9	0.000012		
0.2196		219.6	-0.000235		
0.0345		34.5	0.0000236		
0.0954		95.4	0		
0.123		123	-0.0000043		

Appendix IV - Experimental data of suppression of forced vibration of a plate using a dynamic vibration absorber

Resonant frequency of cantilever plate (2nd Mode) = 300Hz
Resonant frequency of cantilever plate (1st Mode) = 50Hz
Forcing frequency = 300Hz
Input Signal Amplitude = 0.5Vpp and 2.0Vpp

	Vpp = 0.5				Vpp = 2			
	Amplitued (mU)				Amplitued (mU)			
	Blank Cantilever	Absorber on:			Blank Cantil	Absorber on:		
Measured Position		Hole 1	Hole 2	Hole 6		Hole 1	Hole 2	Hole 6
1	20.1	0.901	0.634	1.89	79.9	3.58	2.43	7.67
2	15.2	0.881	0.585	1.37	62.5	3.52	2.31	5.67
3	10.9	0.817	0.552	1	44	3.28	2.18	4.19
4	5.72	0.659	0.523	0.541	24.3	2.54	2.08	2.28
5	0.908	0.407	0.502	0.2	4.73	1.7	2.01	0.797
6	3.03	0.098	0.462	0.248	13.2	0.341	1.88	0.906
7	6.95	0.206	0.398	0.569	28	0.946	1.54	2.36
8	10.1	0.591	0.258	0.82	40.9	2.39	1.06	3.5
9	13.3	0.932	0.088	1.09	52.2	3.76	0.418	4.48
10	15.2	1.2	0.08	1.27	61.3	4.73	0.186	5.22
11	16.8	1.43	0.236	1.38	67	5.69	0.861	5.69
12	17.1	1.6	0.35	1.42	69.1	6.35	1.35	5.86
13	17.2	1.67	0.46	1.39	68.3	6.67	1.75	5.72
14	16.3	1.63	0.493	1.3	65.3	6.57	1.89	5.34
15	14.9	1.51	0.488	1.18	58.5	6.03	1.87	4.84
16	12.9	1.33	0.446	1.07	50.9	5.32	1.73	4.41
17	10.6	1.1	0.388	1.02	42.4	4.51	1.51	4.24
18	8.4	0.844	0.3	0.982	32.4	3.33	1.16	4.01
19	5.54	0.601	0.215	0.815	22.7	2.4	0.819	3.27
20	3.29	0.35	0.136	0.531	13.4	1.49	0.487	2.72
21	1.7	0.182	0.074	0.299	7.53	0.731	2.56	1.37
A1		1.85	1.42	4.74		2.9	5.98	17.9
A2		1.72	1.13	2.98		6.84	4.04	11.9

Resonant frequency of cantilever plate (2nd Mode) = 300Hz
Resonant frequency of cantilever plate (1st Mode) = 50Hz
Resonant frequency of dynamic absorber used = 250Hz
Forcing frequency = 250Hz
Input Signal Amplitude = 2.5Vpp

Amplitude of the signal at 250 Hz (mU)

	Absorber Position							
Measuring Position	Blank Plate	Hole 1	Hole 2	Hole 3	Hole 4	Hole 5	Hole 6	Hole 7
1	27.50	5.20	4.51	6.27	32.70	45.40	1.99	7.78
2	21.70	5.30	4.42	5.81	26.30	32.20	1.45	5.85
3	17.00	5.30	4.40	5.48	21.40	24.40	0.96	4.63
4	11.40	4.83	4.39	5.07	16.20	13.30	0.23	3.00
5	6.63	4.06	4.47	4.82	11.90	4.48	0.03	1.86
6	2.65	3.07	4.39	4.67	7.51	2.69	0.32	0.42
7	2.70	1.86	4.01	4.60	4.18	11.30	0.89	0.86
8	6.35	0.31	3.32	4.71	1.10	17.90	1.35	1.88
9	9.32	0.62	2.37	4.85	0.97	24.70	1.64	2.83
10	12.00	2.10	1.46	4.60	2.10	29.40	1.93	3.46
11	14.00	3.39	0.26	4.10	2.02	34.10	2.14	3.98
12	15.40	4.44	0.64	3.35	1.32	37.10	2.33	4.31
13	15.90	5.25	1.69	2.42	1.16	39.00	2.42	4.42
14	15.80	5.78	2.31	1.14	1.17	39.60	2.55	4.24
15	14.90	5.90	2.86	0.48	1.44	39.00	2.64	3.87
16	13.30	5.62	3.00	0.05	1.50	35.10	2.80	3.03
17	11.30	4.99	2.79	0.25	1.40	30.80	2.87	2.30
18	8.62	4.02	2.39	0.41	1.15	23.30	2.93	1.51
19	5.49	2.87	1.81	0.36	0.90	16.20	2.56	0.81
20	3.72	1.44	1.06	0.15	0.58	10.10	1.55	0.63
21	1.92	0.87	0.59	0.12	0.27	5.25	0.98	0.50
A1		8.99	7.93	10.10	9.56	57.30	10.50	5.13
A2		12.50	12.30	18.20	42.30	48.30	25.20	22.00

References

1 R.G. Jacquot, Suppression of Random Vibration In Plates Using Vibration Absorbers, Journal of Sound and Vibration, 4, 585-596, 2001

2 R.E.D Bishop and D.C. Johnson, The Mechanics of Vibration, 1960

3 J.T. Wissenberger, Vibration beam with a concentrated spring, mass and dashpot, Journal of Applied Mechanics, 35, 327-332, 1968

4 R.G. Jacquot, The response of a system when modified by attachment of an additional sub-system, Journal of Sound and Vibration, 49, 345-351, 1976

5 W.O. Wong, K.T. Chan and T.P. Leung, Identification of antinodes and zero-surface-strain contours of flexural vibration with time-averaged speckle pattern shearing interferometry, Applied Optics, 106, 3776-3784, 1997

6 W.O. Wong and K.T. Chan, Quantitative Vibration Amplitude Measurement with Time-average Digital Speckle Pattern Interferometry, Optics and Laser Technology, 30, 317-324, 1998

7 J. P. Den Hartog, Mechanical Vibrations (4th edition) Mc Graw-Hill, New York, 1956

8 C. Harris, C. Crede, Shock and Vibration Handbook (vol. 1), Mc Graw-Hill, New York, 1961

9 T. H. Rockwell, Investigation of Structure-Borne Active Vibration Dampers, Journal of Acoustical Society America, Vol. 38, 623-8, 1965

10 J.Q. Sun, M.R. Jolly and M.A. Norris, Passive, adaptive vibration absorbers – a survey, Transactions of ASME 17, 234-242, 1995

11 G.B. Warburton, Optimum absorber parameters for various combinations of response and excitation parameters, Earthquake Engineering and Structural Dynamics, 10, 381-401, 1982

12 G.B. Warburton and E.O. Ayorinde, Optimum absorber parameters for simple systems, 1980, Earthquake Engineering and Structural Dynamics, 8, 197-217, 1980

13 Y.Z. Wang and S.H. Cheng, The optimal design of dynamic absorber in the time domain and the frequency domain, Applied Acoustics, 28, 67-78, 1989

14 H. Nishimura, K. Yoshida and T. Shimogo, Optimal dynamic vibration absorber for multi-degree-of-freedom systems, JSME International Journal, 32, 373-379, 1989

15 L. Kitis, W.D. Pilkey and B.P. Wang, Optimal frequency response shaping by appendant structures, Journal of sound and vibration, 95 (2), 161-175, 1984

16 C.A. Bavastri, J.J. Espindola and P.H. Tixeira, Hybrid algorithm to compute the optimal parameters of a system of viscoelastic vibration reduction over a frequency range, Proceeding of the MOVIC'98, Zurich, Switzerland, 1998

17 J.J. Espindola and C.A. Bavastri, Reduction of vibrations in complex structures with viscoelastic neutralizers: a generalized approach and a physical realization, Proceedings of the ASME Design Engineering Technical Conferences, Sacramento, CA, U.S.A., 1997

18 C.R. Fuller and R.J. Silcox, Active structural acoustic control, Journal of the Acoustical Society of America, 91, 519, 1992

19 C.R. Fuller, J.P. Maillard, M. Mercadal and A.H. Von Flotow, Control of aircraft interior noise using globally detuned vibration absorbers, Proceedings of the First CEAS/AIAA Aeroacoustics Conference, Munich, 615-624, 1995

20 K. Nagya and L. Li, Control of sound noise radiated from a plate using dynamic absorber under the optimization by neural network, Journal of Sound and Vibration, 208(2) 289-298, 1997

21 C.R. Fuller and F.J. Fahy, Characteristics of wave propagation and energy distribution in cylindrical elastic shell, Journal of sound and vibration, 81, 501-518, 1982

22 C.R. Fuller, Monopole excitation of vibrations in infinite cylindrical elastic shell field with fluid, Journal of Sound and Vibration, 96, 101-110, 1984

23 C.R. Fuller, Mechanisms of transmission and control of low-frequency sound in aircraft interior, AIAA Paper, 850-879, 1985

24 I.E. Waterman, H. Kaptein, D. Sarin and S.L. Fokker, Activities in cabin noise control for propeller aircaft, SEA Technical Paper Series, 830736(1983)1-6.

25 Z.H. Sun , Y. Dai & J.C. Sun, Vibration and sound radiation of aircraft panel equipped with dynamic vibration absorbers, J. Northwestern Polytechnic University, 11, 470-475, 1993

26 Z.H. Sun, J.C. Sun, C. Wang & Y. Dai, Dynamic Vibration Absorbers used for increasing the noise Transmission Loss of aircraft Panels, Applied Acoustics, 4(48), 311-321, 1996

27 O.J. Lokberg., ESPI-the ultimate holographic tool for vibration analysis, J. Acoust Soc Am, 75, 1783-1791, 1984

28 R.L. Powell and K.A. Stetson, Interferometric Vibration Analysis by Wavefront Reconstruction, Journal of Optical Society of America, 55, 1593-98, 1963

29 A. Macovski, S.D. Ramsey and L.F. Shaefer, Time-lapse Interferometry And Contouring Using Television Systems, Applied Optics, 10, 2722-2727, 1971

30 J. Daniel Inman, Engineering Vibration, Prentice Hall International Editions, 1994

31 J. Ormondroyd and J.P. Den Hartog, Trans ASME, 50, A9, 1928

32 S.S. Rao, Mechanical Vibrations, Fourth Edition, Pearson Education Inc., 2003

33 Jr. W. William, P. Stephen Timoshenko, H. Donovan Young, Vibration Problems in Engineering, Fifth edition, A Wiley-interscience Publication, 1989

34 L. Meirovitch, Principles and techniques of vibrations, Prentice-Hall Inc., 1997

35 O.C. Zienkiewicz, Finite elements and approximation, New York Wiley, 1983

36 R. Tirupathi Chandrupatla and D. Ashoh Belegundu, Introduction to finite elements in engineering, Prentice-Hall Inc., 1991

37 M. Cyril Haris, Shock Vibration Handbook 3rd edition, 1988